CHAPTER 1

Introduction

1.1 GEOMORPHOLOGICAL AND PALAEOENVIRONMENTAL BACKGROUND TO THE STUDY

The high Drakensberg and eastern Lesotho highlands have received much interest and debate on their Quaternary environmental history. Considerable geomorphological work has been undertaken on periglacial and possible glacial landforms found in the eastern Lesotho highlands. However, the origin of several of these landforms remains controversial and differences in opinion concerning their original process mechanisms and associated climatic implications remains unresolved. The high Drakensberg is one of the few remaining places where uncertainty prevails regarding the occurrence of Quaternary glaciation.

A host of publications advocate for Quaternary glaciation in southern Africa (e.g. Sparrow, 1967a, 1967b; Marker and Whittington, 1971; Harper, 1969; Dyer and Marker, 1979; Borchert and Sänger, 1981; Sänger 1988; Hanvey and Lewis, 1990; Marker, 1991; Lewis, 1996; Hall, 1994; Grab, 1996a; Lewis and Illgner, 2001; Mills and Grab, 2005). Yet, Meadows (1988) argues that although many geomorphological features have been analysed in eastern Lesotho, these are associated with periglacial conditions and that there is no evidence suggesting that southern Africa was glaciated during the Quaternary. Observations on ‘cirque-shaped hollows’ located at altitudes above 2900 m a.s.l. led to the first suggestions for Quaternary glaciation in southern Africa (Sparrow, 1967a, 1967b; Harper, 1969; Marker and Whittington, 1971). Yet, 75% of the 577 hollows plotted in the highlands of Lesotho are located on the warmer north-facing slopes (Dyer and Marker, 1979; Marker, 1991), which begs to question the feasibility of a glacial origin as these north-facing slopes are exposed to maximum insolation (Grab, 2000a) and late-lying snow patches predominantly occur on south-facing slopes (Mulder and Grab, 2002). There is also a distinct lack of field evidence from these ‘cirques’, as no glacial erosional or depositional features have been identified, thus further questioning the origin of these hollows (Grab, 1994a, 1996a). The occurrence of the north-facing hollows has been attributed to a combination of lithological and climatological factors (Grab and Hall, 1996). It has been suggested that ground seepage at sites which are lithologically favourable, would enhance weathering and subsequent transport of material (Grab and Hall, 1996). Small apparent cirques, moraines and outwash fans have been identified in the higher parts of the Western Cape Mountains, suggesting a Pleistocene glaciation according to Sänger (1988). It has however been challenged that the steep valley heads owe their origin to structural conditions and the outwash fans provide no evidence for glacial outwash (Boelhouwers and Meiklejohn, 2002).

Evidence for the origin of steep east-facing riverheads ‘cutbacks’ along the Drakensberg escarpment has also been attributed to glacial erosion (Hall, 1994; Grab, 1996a). Debris ridges emanating from steep, high altitude (>3200 m a.s.l.) south-facing exposures of cutbacks on the eastern flank of the Great Escarpment apparently support the hypothesis of localised plateau, niche and cirque glaciation on higher summits during the Late Pleistocene (Hall, 1994; Grab, 1996a). It has also been suggested that these debris ridges formed as a result of debris flows, initiated from the melting of ice (Hall, 1994). The evidence for this was from rounded clasts of fluvial origin, with block sizes >2 m in diameter having been mobilized (Hall, 1994). However, in response to this, Sumner (1995) suggested that basalt clasts tend to be predominantly rounded in shape, whilst debris flows could also have been initiated by a warmer, moister climate, with high intensity rainfall events, which would have intensified weathering. Grab (1996a) also postulated that the higher reaches of the plateau summits and escarpment edge, sidewalls and rock niches were eroded by glacial ice during the Last Glacial Maximum (LGM) (21 000 to 15 000 yrs BP). A hypothesis of glacial dumping over the escarpment sidewalls to produce the moraine-like ridges has been suggested (Grab, 1996a); yet detailed sedimentological investigations of these deposits are still required to verify a glacial origin.

Similar Late Quaternary landforms in the Eastern Cape Province contain striated clasts and have apparently been classified as glacial moraine, despite the relatively low altitude of *ca.* 2100 m a.s.l (Lewis and Illgner, 2001). It has been proposed that such glaciation may be the result of an extensive snow-blow area, suggesting that the Equilibrium Line Altitude (ELA) reflects the temperature-precipitation-wind ELA and that temperatures were probably at least 10°C below those at present (Lewis and Illgner, 2001).

Climatic work includes that by Harper (1969), who calculated that a 9°C temperature lowering was necessary to produce the older periglacial features and a 5°C lowering to produce the younger features in eastern Lesotho. However, others have suggested that temperatures were reduced by approximately 5ºC to 6ºC during the LGM in southern Africa (Partridge *et al.*, 1990, 1999; Talma and Vogel, 1992; Stute and Talma, 1997; Holmgren *et al.,* 2003). Precipitation is a major factor controlling the occurrence of Quaternary glaciation in the Drakensberg. During the winter months, the passage of cold fronts may deliver snowfalls to the high Drakensberg (Grab, 1999a). It is believed that there was a high frequency of cold front events during the LGM, and that present snow patch distribution may provide a guide to snow accumulation sites at that time (Mulder and Grab, 2002). The greater frequency of cold fronts is based on the view that Antarctic polar fronts would have been displaced further north (Howard, 1985), thus increasing winter precipitation as a result of increased snowfalls (Van Zinderen Bakker, 1982; Marker, 1991; Grab, 1996a). However, the lack of conclusive evidence for an increase in the amount of cold fronts is contradictory to other proxy information (Boelhouwers and Meiklejohn, 2002).

There is no recorded evidence of modern permafrost in the Drakensberg (Boelhouwers, 1994; Grab, 1998). However, evidence for the occurrence of permafrost during one of the Pleistocene periods at various localities in Lesotho has been presented through the identification of fossil permafrost horizons (Fitzpatrick, 1978). In addition, the occurrence of large relict sorted circles on high (*ca.* 3400 m a.s.l.) plateau interfluves in the Drakensberg is apparently indicative of Late Quaternary permafrost and would not support the contention of widespread summit glaciation during the same period (Grab, 2002). These relict patterns may either represent areas that have not been glaciated, or areas preserved beneath cold-based ice, similar to that reported by Rea *et al.*, (1998). In contrast, Sumner (2003, 2004a, b) proposes that there is no direct evidence for permafrost in this area. It has also been suggested that although it is possible for marginal glaciation, periglacial and permafrost conditions to have coexisted in the Drakensberg, no work so far resolves that these three environments did indeed coexist (Sumner, 2004c).

Although a considerable amount of work has been undertaken in Lesotho in order to determine the likely climate during the Late Pleistocene, no conclusive evidence for Quaternary glaciation has yet been found. Over 30 years ago, Butzer (1973) suggested that too many interpretations based on periglacial and glacial processes had been founded on high latitude preconceptions. This in turn led to vague and sometimes erroneous identification of features and processes. Twenty years later this problem still existed, which led Hall (1992) to call for greater rigour in southern African periglacial studies. However, a further ten years on, Boelhouwers and Meiklejohn (2002) reiterated that "considerable effort is required to improve the status and scientific image of high altitude southern African geomorphology" (p53). It is thus important that an in-depth study account for the as yet understudied features such as debris deposits, which occur in the higher parts of the Drakensberg.

1.2 REGIONAL SETTING

Lesotho is a small land-locked country of approximately 30,300 km^2 and is enclosed within South Africa (Nixon, 1973; Sene *et al.*, 1998; Kakonge, 2002; Eckert, 2002). It is occupied by the Drakensberg Mountains along its eastern border, whilst the flat plains of the Free State occur to the west (Spence, 1968; Calles and Kulander, 1996). The mountains cover 58% of Lesotho and their slopes are usually too steep and the soils too shallow to permit cultivation (Smit, 1967). Its geographic coordinates range from approximately 28º40'S, 27°E to 29º30'S, 29°20'E (Figure 1.1). Lesotho was originally known as Basutoland, however was renamed the Kingdom of Lesotho in 1966 upon independence from the United Kingdom (Spence, 1968). The access to Sani Pass (2874 m a.s.l.), where much of the research takes place, is only possible through the use of a 4X4 vehicle (Figures 1.1 and 1.2).

Lesotho can be divided into four geographic zones (Figure 1.3). These include the lowlands, which form a narrow strip with South Africa and range in elevation from 1500 m a.s.l. to 1800 m a.s.l, the foothills which range from 2000 m a.s.l. to 2500 m a.s.l, the Senqu River valley which is a major grassland area, and the mountain region, which ranges from 2500 m a.s.l. to 3482 m a.s.l. at Thabana Ntlenyana (Smit, 1967;

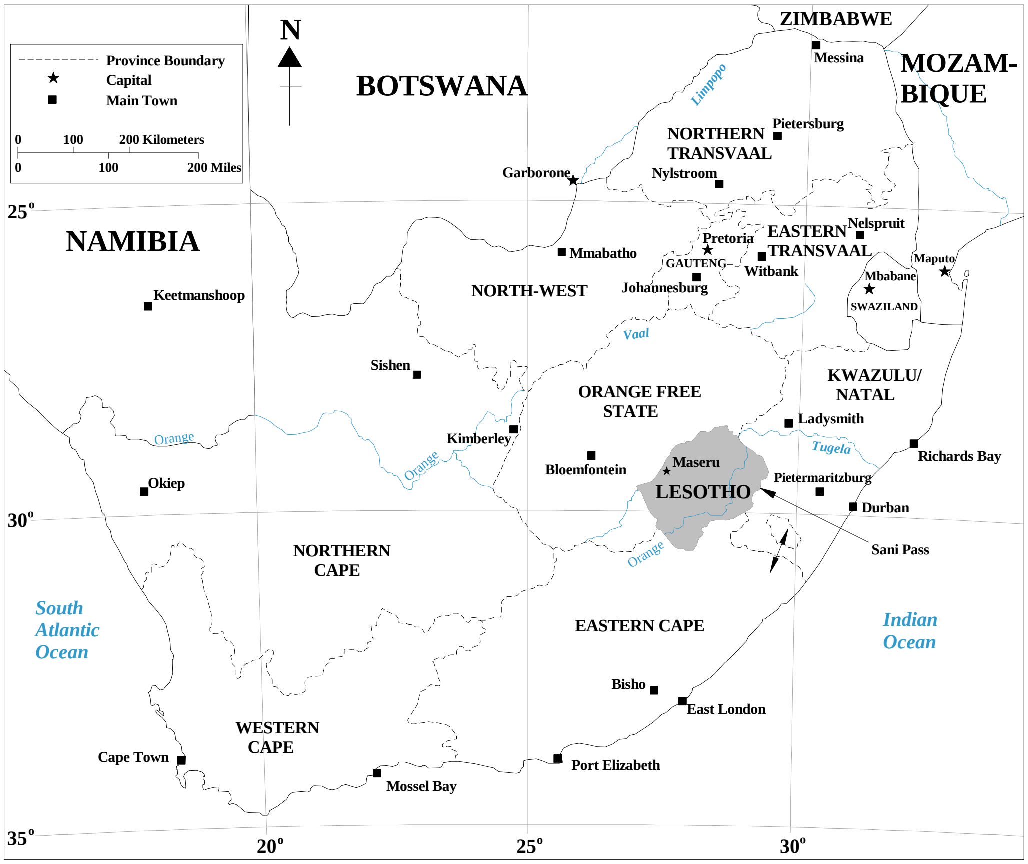

Figure 1.1 Map of South Africa indicating the land-locked position of Lesotho (after UT library, 1995. Source: US Central Intelligence Agency).

Figure 1.2 The road up Sani Pass (arrow indicates road) (photo by S. Mills).

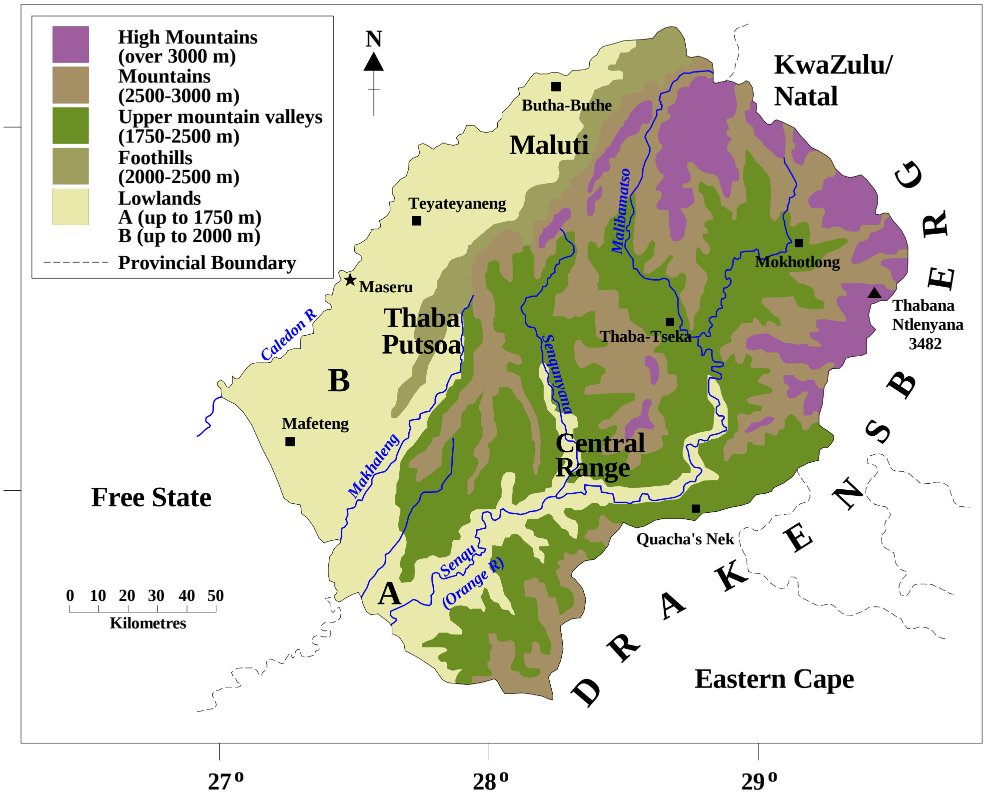

Figure 1.3 The geographic regions of Lesotho (after Marake *et al.*, 1998. Original source: Cartographic Unit, University of Natal).

Marake *et al.*, 1998). The Drakensberg escarpment forms a natural border between South Africa and Lesotho, whilst the Maluti Mountains form a second mountain range and separate the north-western part of the highlands from the lowlands to the west (Figure 1.3) (Sene *et al.*, 1998). The lowest altitudinal position in Lesotho is at the junction of the Orange and Makhaleng Rivers at 1400 m a.s.l (Marake *et al.*, 1998). All streams and rivers rising in the highland region ultimately join the Orange River, which flows into South Africa across the south-western border of Lesotho (Sene *et al.*, 1998). The Orange River has a catchment area of 953 200 km^2 and is the largest basin in southern Africa (Goudie, 2005).

The Lesotho climate can be categorised as semi-arid to sub-humid and continental, given the warm moist summers and cold dry winters (Marake *et al.*, 1998; Mosenene, 1999). The higher peaks (>3000 m a.s.l.) receive enough snow to cover the ground for several months during some winters; however the lowlands typify a warmer and drier climate. The mean annual rainfall for the country is approximately 780 mm and varies between 500 mm in the south-western lowlands to 1600 mm in the northern lowlands and eastern highlands (Sene *et al.,* 1998). Approximately 80% of the annual precipitation falls during summer (October to April), with a pronounced dry season in winter (Calles and Kulander, 1996). The mean annual temperature ranges from 7°C in the highlands (Schulze, 1979) to more than 16°C in the southern lowlands (Marake *et al.*, 1998).

The majority of Lesotho's population (60%) relies on agriculture for employment (Mosenene, 1999). Livestock and crops dominate the sector, however there is biomass disequilibrium on both rangeland and cropping areas as a result of the heavy burden from increasing human and livestock numbers (Mosenene, 1999). By 2002, only 1 km^2 of arable land was available per 325 people (Eckert, 2002). It is the poor management of increased numbers of livestock, together with topographic, soil and rainfall factors, which are responsible for accelerated soil erosion and severe land degradation (Strömquist, 1991; Mosenene, 1999). There are two main types of soil in Lesotho; namely the Mollisols which are fairly deep and are moderately fertile, and the Alfisols, which generally have a coarse top layer with fine clay underneath. The clay causes a hard pan that reduces rainfall infiltration and thus makes these soils highly erodible (Mosenene, 1999).

1.3 STUDY AREA

Having surveyed the high Drakensberg region, several slope deposits were discovered on south-facing slopes along the southeastern Drakensberg escarpment, yet their geomorphic origin has thus far been unknown. It is believed that these deposits may provide valuable information on former geomorphological processes and associated past climates in the high Drakensberg. Four sites were identified for investigation and six sedimentary features analysed. The study sites are located on plateau slopes, immediately to the west of the high Drakensberg escarpment in eastern Lesotho (Figure 1.4). Three sites host linear deposits and these have only been identified thus far along three mountain ranges (Tsatsa-La-Mangaung, Sekhokong and Leqooa ranges). The Sekhokong mountain range hosts several linear deposits, however two were chosen in the case of this study based on their varying morphologies and close proximity to one another. The Tsatsa-La-Mangaung range has been surveyed in detail and the deposit identified is the only one along this mountain range, which is why it

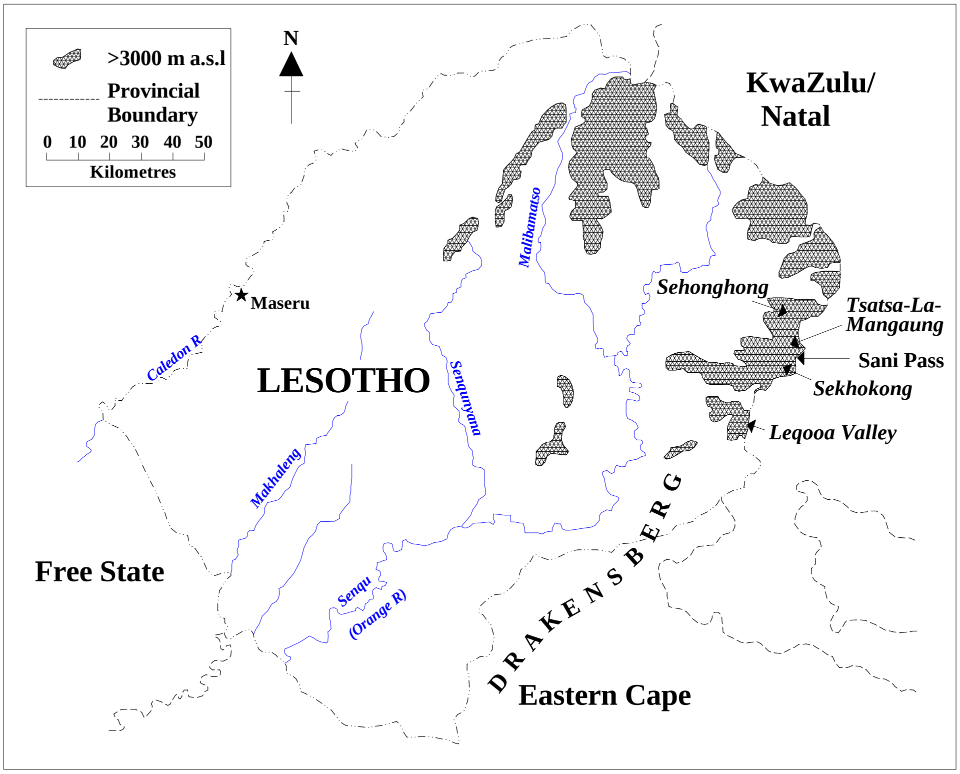

Figure 1.4 Location map for the Tsatsa-La-Mangaung, Sekhokong, Leqooa Valley and Sehonghong sites (base Map from Marake *et al.*, 1998. Original source: Cartographic Unit, University of Natal).

was selected for this research. The Leqooa site was selected because two deposits occur within a few hundred metres of each other which appears to be unique in this area. Lastly, a fourth site was chosen where colluvial mantles follow the Sehonghong River, so that a comparison could be made between the sedimentary characteristics of these mantles and the linear deposits.

The Sehonghong site is located between 29º29’30”S, 29º15’38”E and 29º29’38”S, 29º16’34”E, along the Sehonghong river where deep valley deposits greater than 8 m in depth have been exposed through fluvial incision. This site encompasses approximately 2 km along the Sehonghong River. The Tsatsa-La-Mangaung site is located at 29º33’35”S and 29º17’39”E and is approximately 2 km west of the Great Escarpment, on the south-facing aspect of the Tsatsa-La-Mangaung mountain range, which reaches an altitude of 3275 m a.s.l. (Figure 1.4). The Sekhokong site is located along the Sekhokong range which reaches an altitude of 3244 m a.s.l., where two deposits are investigated. These are located at 29º36’51”S, 29º14’51”E and

29º36’29”S, 29º13’52”E. These deposits are both situated on south-facing slopes, within 2 km of each other and within 4 km of the Great Escarpment. The Leqooa site is located at 29º44’35”S and 29º06’57”E, on a south-facing slope of the Leqooa range, which reaches an altitude of 3431 m a.s.l., and where two ridges, 350 m apart, occur approximately 1 km from the Great Escarpment.

Access to the sites was difficult and was only possible on foot or on horse back. The Tsatsa-La-Mangaung site was the most accessible as it was only 1 ½ hours walk from Sani Top, however the Sekhokong site was approximately 3 hours walk, the Sehonghong site one days walk and the Leqooa valley two days walk. Horses were hired for the Leqooa valley and the Sehonghong sites, in order to help carry equipment and samples. There were a few logistical problems with sample analysis and thin section production; however these were mostly overcome by transporting sediment samples to Royal Holloway, University of London in the UK, where the appropriate facilities permitted the necessary analysis to be undertaken.

1.4 AIMS AND HYPOTHESES

This research investigates recently discovered sedimentary deposits on high altitude (>3100 m a.s.l.) south-facing plateau slopes, located immediately (1 km to 4 km) to the west of the Great Escarpment, and valley deposits on a south- and north-facing slope which have been exposed through fluvial incision. The objective of this research is to ascertain the likely geomorphic processes that produced the deposits. On the basis of these findings, the study evaluates the feasibility for Quaternary glaciation in southern Africa. There are a number of specific aims which this PhD project wishes to achieve in fulfilling the objective discussed above:

1. To identify and compare the morphology of the various slope deposits found along the Tsatsa-La-Mangaung, Sekhokong and Leqooa mountain ranges, and those along the Sehonghong River valley of eastern Lesotho.
2. To analyse the sedimentology and micromorphology of the deposits and in so doing, provide some understanding of the past geomorphic processes that operated at the sites.

3. To undertake a multi-faceted methodological approach to evaluate the feasibility for past Quaternary glaciation in the high Drakensberg (e.g. by applying palaeoclimatic extrapolations and glacier reconstruction).

The slope deposits must be considered in the context of the various climatic conditions required for their formation. Four hypotheses are considered with regards to climate and deposition, whilst a further hypothesis will be considered with regards to erosion:

1. The deposits are a result of contemporary mild and wet climatic conditions producing one or more features, such as debris flows, debris avalanches, mud flows and landslides.
2. The deposits are a result of past cold (periglacial) climatic conditions producing one or more features such as rock glaciers, solifluction lobes, pronival ramparts, debris flows and mass wasting.
3. The deposits are a result of glacial climatic conditions, producing features of glacial origin (e.g. moraines).
4. The Sehonghong feature is a result of fluvial deposition.
5. The features are remnants of eroded slope material, in which the original slope material has been incised to produce the remnants.

1.5 THESIS STRUCTURE

The thesis is organised into chapters in order to best address the aims and hypotheses set out in section 1.4. This chapter (introduction) is followed by chapter 2 (a review of the relevant literature), which provides an understanding of the possible processes taking place in the study area and their associated landforms. Chapter 3 provides a description of the environmental and geomorphic setting of the area. The research methodology is described in Chapter 4 and presents an outline of the main laboratory techniques used, and a justification for the use of these techniques. Chapters 5, 6, 7 and 8 present the results for the Tsatsa-La-Mangaung, Sekhokong, Leqooa Valley and Sehonghong Sites, whilst Chapter 9 discusses these results and assigns a process origin to each individual feature. Chapter 10 deals with the reconstruction of the palaeoclimate at the four sites during the LGM in order to ascertain the likelihood for the presence of small cirque/niche glaciers and the part they played in the formation of the features described. The extent to which the aims and objectives of the research are met is assessed in the concluding part of the thesis (Chapter 11).

CHAPTER 2

Literature Review

2.1 PROCESS ORIGINS

2.1.1 Introduction

This chapter comprises of three sections. The first section gives a description of the different types of slope deposits considered in the aims and hypotheses in Chapter 1 (section 1.4), and their relevance to the South African context. The selection of the hypotheses with regards to the process origins of the debris deposits found in the Drakensberg is based on their morphological and sedimentological characteristics and encompasses a broad range of mass movement, periglacial, nival, glacial and fluvial processes. These various geomorphological features of a mountain environment are presented in Figure 2.1 and their individual characteristics will be described for comparative purposes in later chapters. Each geomorphological feature will also be discussed in terms if its relevance to the southern African literature (Table 2.1). Section 2 discusses the various problems regarding the identification of the features described in section 1, based on their morphological similarities and combined processes. This section also discusses the problems encountered when using techniques such as clast orientation and particle shape. Finally, section 3 examines the palaeo-climate during the LGM in the Southern Hemisphere, so as to relate past climates to the likely climatic conditions in the high Drakensberg during this time. This section will only focus on the Late Pleistocene as there is not enough evidence at present to support geomorphic activity in the Drakensberg during the Middle Pleistocene. It is however suggested that future work beyond this PhD should possibly investigate this, given that evidence suggests that places such as Patagonia and Tasmania suffered less extensive glaciations during the LGM (Colhoun and Fitzsimons, 1990; Coronato *et al.*, 2004).

2.1.2 Mass movement

2.1.2.1 Slope form

Slope form is an important component of mass movement as it affects the processes which occur on the hillslope. However it is these hillslope processes which also shape the landscape. Slopes are usually a product of a variety of processes which interact in

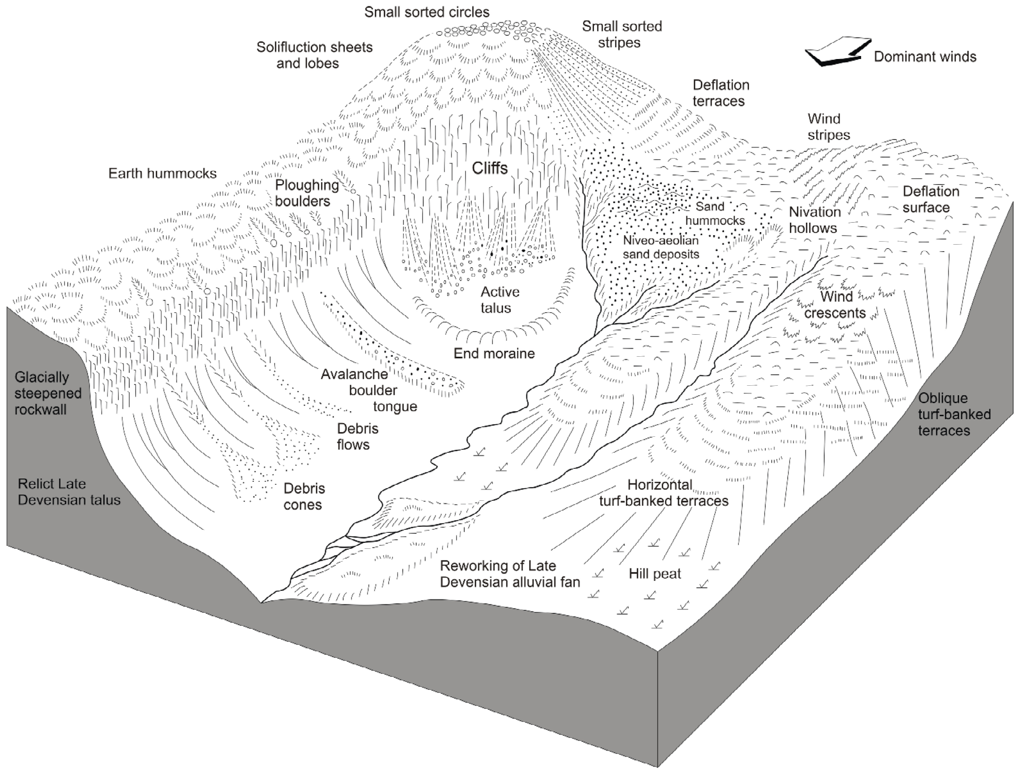

Figure 2.1 An example of active periglacial features on British mountains (after Ballantyne 1987a).

time and space; therefore they form sequences of units which display different characteristics (Dikau *et al.*, 2004). The nine-unit landsurface model proposed by Dalrymple *et al.* (1968) (Figure 2.2) treats the hillslope system as a three-dimensional complex, which extends from the drainage divide to the centre of the channel bed, and from the groundsurface to the uppermost boundary of weathered rock (Selby, 1993). In most cases slope form comprises an upslope convexity, which leads down to a rectilinear main slope and ends in a basal concavity (Summerfield, 1991). It is unusual to find all nine units occurring on any one slope profile, neither do they always occur in the order shown in Figure 2.2, and individual units may occur more than once in a single profile (Selby, 1993).

2.1.2.2 Mass movement processes

Mass movement is the downward and outward movement of slope material under the influence of gravity, without the direct aid of a transporting medium such as water, ice or air (Summerfield, 1991; Selby, 1993; Dikau, 2004a). Most mass movement classifications are based on morphology, mechanism, type of material and rate of

Table 2.1 A list of the literature for southern African high mountain environments, for each process mechanism presented in this research.

Processes and landforms	Publications
Debris flows/avalanches	Hanvey *et al.* (1986), Lewis and Hanvey (1988), Illgner (1995), Lewis (1996), Boelhouwers *et al.* (1998, 1999), Grab (1999b), Sumner and Meiklejohn (2000).
Landslides	King (1982), Paige-Green (1985), Garland and Olivier (1993), Sumner (1993, 1994), Sumner and Meiklejohn (2000), Bijker (2002), Hardwick (in prep).
Mudflows/mudslides	Boelhouwers *et al.* (1996).
Solifluction lobes and processes	Harper (1969), Linton (1969), Marker and Whittington (1971), Hastenrath and Wilkinson (1973), Nicol (1973), Fitzpatrick (1978), Dardis and Granger (1986), Lewis (1987, 1988a, 1988b 1996), Lewis and Hanvey (1988), Boelhouwers (1991, 1994, 1998), Marker (1992), Grab (1997a, 1999b, 2000b), Boelhouwers *et al.* (2002), Kück and Lewis (2002), Boelhouwers and Sumner (2003), Sumner (2003).
Rock glaciers	Marker (1986), Lewis and Hanvey (1993), Lewis (1994a).
Pronival ramparts	Marker (1990), Lewis (1994a, 1994b).
Glacial moraines	Borchert and Sänger (1981), Sänger (1988), Lewis (1996), Lewis and Illgner (2001), Mills and Grab (2005).
Fluvial deposits	Butzer and Helgren (1972), Moon and Partridge (1993), Dollar and Rowntree (1995), Hattingh (1996), Lewis and Illgner (1998), Rowntree (2000), Lewis (2005).

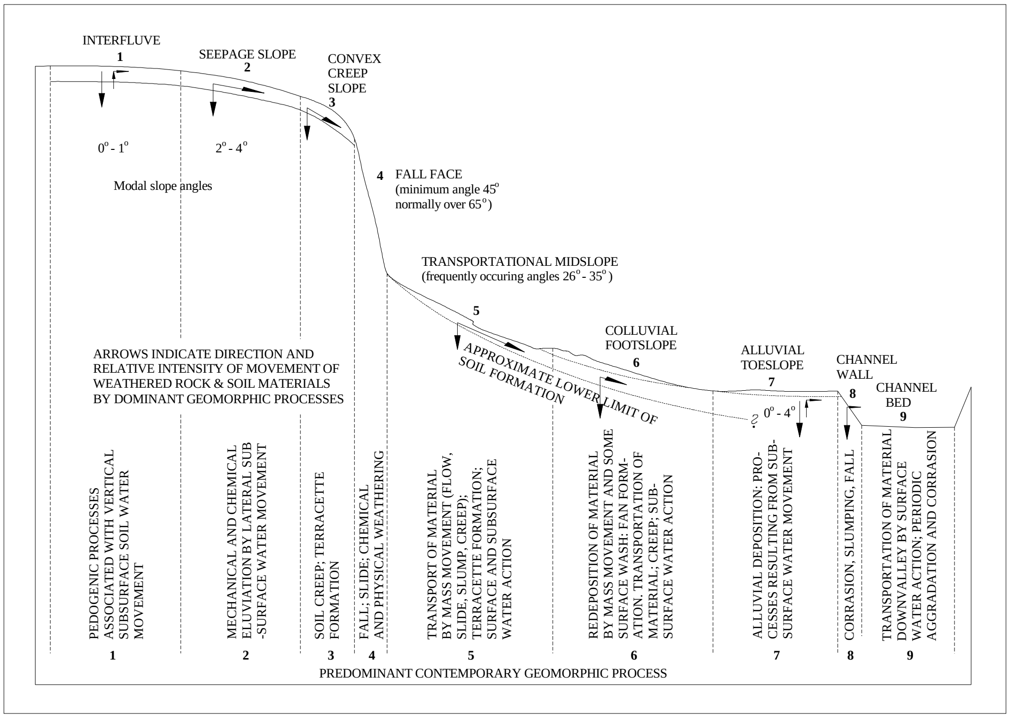

Figure 2.2 A theoretical slope profile containing a comprehensive range of slope units related to particular types of slope processes (after Dalrymple *et al.,* 1968).

movement (Dikau, 2004a). Classifications of the various processes of mass movement are invaluable; however in reality most mass movements involve a combination of processes (Summerfield, 1991). Table 2.2 indicates the classification of mass movement types, however only the ones relevant to this research will be discussed.

2.1.2.2.1 Debris flows

The definition of a debris flow is a rapid mass movement of a mixture of wet rock and soil, which has the consistency of wet concrete (Lewin and Warburton, 1994). This mixture of solid and fluid materials forms a wave that moves steadily through a channel with superimposed, smaller waves travelling at velocities higher than those of the debris flow itself (Johnson and Rodine, 1984) (Figure 2.3). Debris flows occur in virtually any mountain environment and will depend upon factors such as relief, climate and lithology (French, 1996; Boelhouwers *et al.,* 1998). They are generally most likely to occur on slopes steeper than 25º (Nieuwenhuizen & Van Steijn, 1990; Lewin and Warburton, 1994; Boelhouwers *et al.*, 2000; Iverson, 2004), however they have also mobilised from slopes greater than 39° in California (Bailey and Rice,

Table 2.2 Classification and characteristics of the major types of mass movement (after Summerfield, 1991).

PRIMARY MECHAMNISM		MASS MOVEMENT TYPE	MATERIALS IN MOTION	MOISTURE CONTENT	TYPE OF STRAIN AND NATURE OF MOVEMENT	RATE OF MOVEMENT
LATERAL COMPONENT PREDOMINANT	Creep	Rock creep	Rock (especially readily deformable types such as shales and clays)	Low	Slow plastic deformation of rock, or soil producing a variety of forms including cambering, valley bulging and outcrop bedding curvature	Very slow to extremely slow
		Continuous creep	Soil	Low		
	Flow	Dry flow	Sand or silt	Very low	Funnelled flow down steep slopes of non-cohesive sediments	Rapid to extremely rapid
		Solifluction	Soil	High	Widespread flow of saturated soil over low to moderate angle slopes	Very slow to extremely slow
		Gelifluction	Soil	High	Widespread flow of seasonally saturated soil over permanently frozen subsoil	Very slow to extremely slow
		Mud flow	>80% clay-sized	Extremely high	Confined elongated flow	Slow
		Slow earthflow	>80% clay-sized	Low	Confined elongated flow	Slow
		Rapid earthflow	Soil containing sensitive clays	Very high	Rapid collapse and lateral spreading of soil following disturbance, often by an initial slide	Very rapid
		Debris flow	Mixture of fine and coarse debris (20-80% of particles coarser than sand-sized)	High	Flow usually focused into pre-existing drainage lines	Very rapid
		Debris (rock) avalanche (sturzstrom)	Rock debris, in some cases with ice and snow	Low	Catastrophic low friction movement of up to several kilometres, usually precipitated by a major rock fall and capable of overriding significant topographic features	Extremely rapid
		Snow avalanche	Snow and ice, in some cases with rock debris	Low	Catastrophic low friction movement precipitated by fall or slide	Extremely rapid
		Slush avalanche	Water-saturated snow	Extremely high	Flow along existing drainage lines	Very rapid
	Slide – *Translational*	Rock slide	Unfractured rock mass	Low	Shallow slide approximately parallel to ground surface of coherent rock mass along single fracture	Very slow to extremely rapid
		Rock block slide	Fractured rock	Low	Slide approximately parallel to ground surface of fractured rock	Moderate
		Debris/ earth slide	Rock debris or soil	Low to moderate	Shallow slide of deformed masses of soil	Very slow to rapid
		Debris/ earth block slide	Rock debris or soil	Low to moderate	Shallow slide of largely undeformed masses of soil	Slow
	Slide – Rota-tional	Rock slump	Rock	Low	Rotational movement along concave failure plane	Extremely slow to moderate
		Debris/ earth slump	Rock debris or soil	Moderate	Rotational movement along concave failure plane	Slow
	Heave	Soil creep	Soil	Low	Widespread incremental downslope movement of soil or rock particles	Extremely slow
		Talus creep	Rock debris	Low		
VERTICAL COMPONENT PRPMINANT	Fall	Rock fall	Detached rock joint blocks	Low	Fall of individual clocks from vertical faces	Extremely rapid
		Debris/ earth fall (topple)	Detached cohesive units of soil	Low	Toppling of cohesive units of soil from near-vertical faces such as river banks	Very rapid
	Subside-nce	Cavity collapse	Rock or soil	Low	Collapse of rock or soil into underground cavities such as limestone caves or lava tubes	Very rapid
		Settlement	Soil	Low	Lowering of surface due to ground compaction usually resulting from withdrawal of ground water	Slow

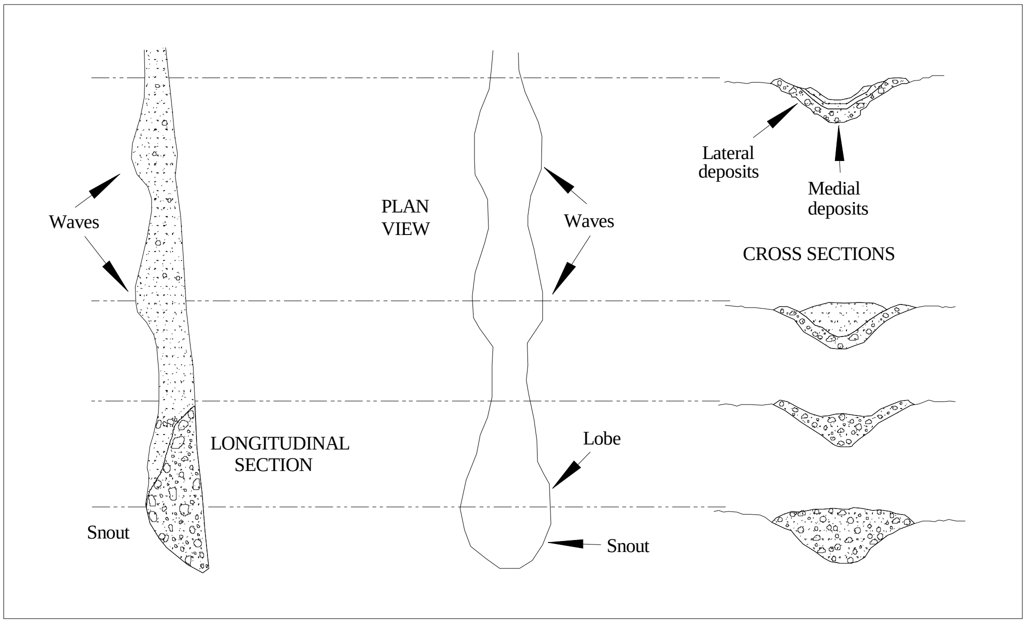

Figure 2.3 Idealised representations of a debris flow arm, showing waves and deposits formed by successive waves of debris (after Johnson and Rodine, 1984).

1969), from slopes steeper than 17° in Virginia (Williams and Guy, 1973), between 42° and 48° for 80% of the debris flows observed on Hawaii (Wentworth, 1943) and from slopes steeper than 30° in several areas in the western United States (Johnson and Rodine, 1984). Debris flows occur where there is abundant source material which can be mobilised by the addition of water (Selby, 1993). These conditions typically exist on hillslopes with colluvial soils and saprolites, and especially in hollows where there are thick colluvial infills (Selby, 1993).

Debris flows usually consist of an erosional scar and two major depositional features including lateral levees and bouldery frontal lobes (Rapp and Nyberg, 1981; Johnson and Rodine, 1984). In terms of their sedimentology, they usually consist of large, coarse material embedded in a fine-grained matrix (Dikau, 2004a), Typical debris flow particle characteristics tend to contain poorly sorted material (Costa, 1984; Owen, 1991, 1994; Phillips and Davies, 1991), a wide grain size distribution from clay to large boulders (Phillips and Davies, 1991; Coussot and Meunier, 1996) and <5% clay (Dikau, 2004a). Clay is important in the mobility of debris flows as its ability to fill pore spaces between debris allows a build up of pore pressure required to enhance the mobility of a debris flow (Johnson and Rodine, 1984; Costa, 1984).

However, an even distribution of particle sizes may also be effective in filling up pore spaces, which reduces the importance of clay (Boelhouwers *et al.*, 1998). Coarse materials dominate the flow heads in debris flows as a result of dispersive shear pressures, pushing the largest fragments most efficiently (Takahashi, 1978, 1991; Johnson and Rodine, 1984).

Debris flow fabrics tend to show variability in both orientation and imbrication, with orientations that range from parallel to transverse or oblique to flow direction (Lawson, 1979; Mills, 1984, 1991; Smith, 1986; Van Steijn and Coutard, 1989; Gale and Hoare, 1991; Nieuwenhuizen and Van Steijn, 1990; Owen, 1991; Benn, 1994a) (Table 2.3). It is also suggested that debris flow fabrics may be disorganised and reflect short travel distances or high strength and high viscosity flows (Nemec and Steel, 1984). Preferred parallel or transverse orientation may result from strongly sheared laminar flow (Lewis *et al.*, 1980), whilst transverse orientations may also result from turbulent flow with a significant tractional component (Lowe, 1982). As the water content of the debris flow increases, more clasts become aligned parallel to flow direction (Lawson, 1979). Further work includes that by Innes (1983), who reported that the fabric of the debris flow lobe had no preferred orientation, whilst the fabric in the debris flow levees displayed orientation patterns. It has been reported that clast dip within debris flows ranges between 9° to 42° (Innes, 1983) and is generally <40° (Boelhouwers *et al.*, 1998). It has also been suggested that imbrication in debris flows may reflect the abundance of matrix and that clast-rich debris flows would show stronger imbrication (Bertran *et al.*, 1997).

Angular clasts are typical of the sedimentary properties of debris flows (Owen, 1991; Phillips and Davies, 1991) (Table 2.4). The presence of angular clasts within debris flow lobes has also been described by Illgner (1995) in the Cape Province, South Africa. Debris flow work undertaken in the southern Alps in New Zealand has identified 72% of angular to very angular clasts, whilst 0% of clasts fall within the rounded to very rounded categories (de Scally and Owens, 2005). In addition, work undertaken in Death Valley, California, indicates that debris flow clasts fall predominantly in the angular to subangular categories (46-69%) (Blair, 1999). It is suggested that the difference in clast roundness between the Southern Alps and Death

Table 2.3 Summary for clast-fabric data for specific landforms (ND = No data).

	Fabric	Dip	Isotropy	Elongation
Debris flow/avalanche	Parallel, transverse or oblique to flow direction [1, 2, 3,4,5,6,7,8,9]. Flow lobes show no preferred orientation, however levees display preferred orientation [10]. Weakly developed fabrics [11].	High, uphill (9º to 42º) [2]. Mostly <40º [11]. Better imbrication in clast rich flows [12].	0.100-0.450 [1, 2].	0.210-0.740 [1, 2].
Mudflow/mudslide	No preferred orientation. Strong fabrics may develop periodically [13, 14].	ND	ND	ND
Landslide	Parallel or transverse to movement [15].	ND	ND	ND
Pronival rampart	No preferred orientation [16, 17]. Oblique to ridge crest [18, 19].	Downslope [19].	ND	ND
Rock glacier	Preferred downslope orientation [20, 21]. Weak fabrics [22].	< 30º [23]. Upslope [22].	ND	ND
Solifluction lobe	Strong fabrics in the direction of the local slope [24] Fabrics aligned in the direction of gelifluction movement [25, 26]. High fabric variability [27]. Transverse orientation in frontal lobe [28]. Random orientation in frontal lobe [29].	10º to 20º in gelifluction deposits [24, 30, 31].	0.044-0.165 [9].	0.167-0.671 [9].
Lodgement till	Strong preferred orientation in the direction of ice flow [32, 33, 34].	Low up glacier dips [32].	0.114 [35].	0.491 [35].
Subglacial melt-out till / basal ice	Clasts aligned parallel to direction of strain, although transverse fabrics may occur due to compressive flow [36, 33, 34].	Steeply dipping clasts [37].	0.097 [35]. 0.047 [1]. 0.038 [38].	0.597 [39]. 0.903 [1]. 0.795 [38].
Deformation till	Well-developed fabrics in the direction of tectonic transport, usually similar to the ice flow direction [34].	High dips [34].	0.127 [35]. 0.070-0.115 [31, 39].	0.501 [35]. 0.470-0.672 [31, 39].
Supraglacial melt-out till	Poorly developed [22, 34]. Parallel to direction of local ice flow or pattern of strain within the basal ice layer [33].	Few steeply dipping clasts (>40º), strong mode in the class <10º [37].	0.161 [38]. 0.037 [1]. 0.209 [35].	0.652 [38]. 0.82 [1]. 0.428 [35].
Flow till	Strong preferred orientation [40]. Weak down-valley fabrics [41]. Variation throughout deposit [34].	ND	0.122 [35]. 0.231 [1].	0.436 [35]. 0.455 [1].
Sublimation till	Strong in the direction of ice flow [34].	ND	ND	ND
Fluvial deposit	In the direction of flow[42]. Parallel to flow[43].	Upstream dips [42, 44].	ND	ND

[1]. Lawson, 1979. [2]. Mills, 1984. [3]. Mills, 1991. [4]. Smith, 1986. [5]. Van Steijn and Coutard, 1989. [6]. Gale and Hoare, 1991. [7]. Nieuwenhuizen and Van Steijn, 1990. [8]. Owen, 1991. [9]. Benn, 1994a. [10]. Innes, 1983. [11]. Boelhouwers *et al.*, 1998. [12]. Bertran *et al.*, 1997. [13]. Lindsay, 1968. [14]. Binda and Van Eden, 1972. [15]. Hewitt, 1999. [16]. Washburn, 1979. [17]. Pérez, 1988. [18]. Shakesby *et al.*, 1999. [19]. Harris, 1986. [20]. Giardino and Vitek, 1985. [21]. Harrison and Anderson, 2001. [22]. Nicolas, 1994. [23]. Vere and Matthews, 1985. [24]. Nelson, 1985. [25]. Harris, 1981a. [26]. Harris, 1987. [27]. Millar, 2005. [28]. Benedict, 1976. [29]. Bertan *et al.*, 1997. [30]. Harris and Wright, 1980. [31]. Elliot and Worsley, 1999. [32]. Sharp, 1984. [33]. Hicock, *et al.*,1996. [34]. Bennett and Glasser, 1996. [35]. Bennett *et al.*, 1999. [36]. Boulton, 1970. [37]. Dowdeswell and Sharp, 1986. [38]. Ham and Mickelson, 1994. [39]. Benn, 1995. [40]. Lowe and Walker, 1994. [41]. Owen, 1994. [42]. Colhoun, 2004. [43]. Bridge, 2003. [44]. Ward, 2004.

Table 2.4 A summary of the characteristics of particle shape for the various process origins. (ND = No Data).

Landform	Particle Roundness	Particle Shape	C_{40} index
Debris flow	Angular clasts [1, 2, 3]. Very angular to angular [4]. Angular to subangular [5].	Platy [6].	36 [4].
Debris avalanche	Angular with subrounded edges [7]. Angular [8]. Rounded [9]. Subrounded to well rounded [10].	ND	ND
Mudflow/mudslide	Angular clasts [11].	ND	ND
Landslide	Angular [12]. Very angular to angular [13].	ND	ND
Pronival rampart	Very angular to angular [14, 15, 16, 17, 18, 19, 20].	Slabby [21].	~ 38 to 69 [22].
Rock glacier	Angular to subrounded [22, 23]. Angular to subangular [24]. Angular [25].	Blocky [25, 26, 27, 25]. Platy [29]. Platy to bladed [22].	40 to 66 [22]. ~20 [23].
Solifluction lobe	Angular [30, 31, 32].	Platy [30].	ND
Moraine -Supraglacial	Angular [1, 33, 34, 35, 36].	Platy and elongate [35, 37]. Bladed [38]	>60 [34].
- Subglacial	Subrounded [37]. Rounded [36]. Subangular to subrounded [35].	Compact [34].	<16 [34].
Fluvial sediments	Rounded [39, 40]. Subrounded [41].	Prolate/elongate [42].	ND

[1]. Owen, 1991. [2]. Phillips and Davies, 1991. [3]. Illgner, 1995. [4]. de Scally and Owens, 2005. [5]. Blair, 1999. [6]. Johnson and Rodine, 1984. [7]. Schneider and Fisher, 1998. [8]. Schneider *et al.*, 1999. [9]. Crandell, 1969. [10]. Holmes, 1965. [11]. Corominas, 1995. [12]. Heim, 1932. [13]. Hewitt, 1999. [14]. Washburn, 1979. [15]. Shakesby, 2004. [16]. Shakesby *et al.*, 1995. [17]. Shakesby *et al.*, 1999. [18]. Harris, 1986. [19]. Tinkler and Pengelly, 1994. [20]. Fukui, 2003. [21]. Ballantyne and Kirkbride, 1986. [22]. Harrison and Anderson, 2001. [23]. Vere and Matthews, 1985. [24]. Humlum, 1998a. [25]. Giardino and Vitek, 1988. [26]. Wahrhaftig and Cox, 1959. [27]. Evin, 1987. [28]. Chueca, 1992. [29]. Ikeda and Matsuoka, 2006. [30]. Grab, 2000b. [31]. Eyles and Paul, 1983. [32]. Washburn, 1973. [33]. Owen, 1994. [34]. Benn and Ballantyne, 1993. [35]. Benn and Evans, 1998. [36]. Bennett and Glasser, 1996. [37]. Knight, 2004. [38]. Dowdeswell, 1982. [39]. Lewin and Brewer, 2002. [40]. Bridge, 2003. [41]. McEwen and Matthews, 1998. [42]. Howard, 1992.

Valley is due to the very short transport distances in the case of the Southern Alps (de Scally and Owens, 2005).

The majority of work undertaken on the micromorphology of debris flows has focussed on cohesive debris flows which contain significant amounts of silt and clay (Van Vliet-Lanoë, 1985a; Bertran, 1993; Bertran and Texier, 1994). These contain a homogeneous fine-grained matrix, a porphyric coarse vs fine (*c/f*) relative distribution and an undifferentiated or crystallitic b-fabric (Bertran and Texier, 1999). Voids are typically poorly interconnected, irregular to rounded vesicules (Bertran and Texier, 1999) and debris flows which occur in periglacial environments tend to display silt cappings disrupted and scattered within the matrix of the flow (Van Vliet-Lanoë, 1985a).

Further work on the micromorphology of debris flows describes a common occurrence of clay balls within a silty clay matrix, and grains exhibit no apparent orientation (Menzies and Zaniewski, 2003). Subhorizontal bands of higher packing density clay are also observed within these debris flows (Menzies and Zaniewski, 2003). Tile structures may be a result of debris flow processes and occur as a result of a pulsed movement of fine-grained silts and clays associated with porewater diffusion and subsequent brittle disruption (Menzies and Zaniewski, 2003). This leads to brecciation of the banded units of clays and silt during consolidation and dewatering (Menzies and Zaniewski, 2003). These tiled structures represent arrangements of gravels, silt cappings and coats, laminated silt intercalations and various brecciated structures (Bertran, 1993; Bertran and Texier, 1999; Bertran *et al.*, 1995). Marbled matrix sediments also appear to be indicative of debris flows and these occur possibly as a result of intense mixing during flow transport (Menzies and Zaniewski, 2003). A further characteristic of sediment flows is that in thin section, they are characterised by near horizontal laminations of undulating sand and silt layers (Lachniet *et al.*, 2001). Rounded coarse clasts are preferentially aligned with their a-axis along laminations or are imbricated upslope (Lachniet *et al.*, 2001). It is suggested that laminations form under ductile deformation during sediment flow (Lachniet *et al.*, 1999).

Rotational features are also evident in debris flows whereby rounded clasts may have a matrix of coatings around grains (Bertran, 1993). In some cases, this may be a result of the translocation of fine particles due to an intense washing down of sediment following the melting of snow and soil ice, which is generally associated with gelifluction (Harris and Ellis, 1980; Van Vliet-Lanoë, 1985b). The rotation of clasts allows silts to progressively accumulate around them (Bertran, 1993). A simple shear produces the rotation of particles and leads to the development of a preferred orientation of a-axes.

In southern Africa, debris flows occur in the KwaZulu Natal Drakensberg and in the Eastern and Western Cape mountains (Boelhouwers *et al.*, 1998, 1999; Lewis, 1996). A debris flow deposit has been described by Hanvey *et al.* (1986) near Rhodes in the Eastern Cape and it was suggested that this debris deposit was related to the existence of a former snowbody and formed under Quaternary periglacial conditions. The presence of a snowpatch was suggested based on the sedimentary characteristics of the debris deposit, which indicated increased water content, which may have been due to the melting of a snowpatch. Boelhouwers *et al.* (1998) investigated the morphology and sedimentology of a recent debris flow in the Western Cape Mountains, which is used to help recognise relict debris flow deposits. Debris flow deposits in the Cederberg Mountains of the Western Cape have also been described by Boelhouwers *et al.* (1999). These deposits are open work (the fine matrix has been washed out after deposition), have developed terminal lobes and levees and are lacking in vegetation due to an absence of matrix material (Boelhouwers *et al.*, 1999). In the Eastern Cape, debris flows are extensive even at low altitudes (Lewis, 1996), and debris flow lobes have been described at 1 800 m a.s.l. (Lewis and Hanvey, 1988). Further work from the Cape Province describes debris flow deposits studied in the Bushmans River Valley, which have been attributed to heavy rainfall events under contemporary climatic conditions (Illgner, 1995). Debris flow descriptions from the Drakensberg are rare, however Grab (1999b) ascribed slope deposits at Njesuthi (3090 m a.s.l. to 3160 m a.s.l.) as being of debris flow origin. It has also been suggested that debris flow occurrence in the Drakensberg is associated with lithology, and these predominantly occur in shales (Sumner and Meiklejohn, 2000).

2.1.2.2.2 Debris avalanches

Debris avalanches are rapid gravitational movements of wet or dry rock debris occurring on steep slopes (Blikra and Nemec, 1998) and typically have a triangular morphology in plan view (Guadagno *et al.*, 2005). They may also spread into thin sheets and fan out on flat surface areas (Campbell, 1989). They can only move rapidly on steep slopes as a result of the large friction angle of granular masses (Coussot and Meunier, 1996) and are most powerful in areas with sparse vegetation cover (Becht, 1995). The initiation of debris avalanches can be a factor of slope angle, the apex angle of the source area with a triangular shape, the height of the natural and artificial scarps and the thickness of the supply material (Guadagno *et al.*, 2005). Threshold slope angles of between 25º to 30º have been reported for debris avalanches in New Guinea (Selby, 1982).

Debris avalanches can occur with small amounts of volume of debris and then increase in volume as they move downslope. They may then be channelled into narrow gullies where they evolve into debris flows (Guadagno *et al.*, 2005). The role of water within debris avalanches is minor because grains dilate and the ratio of water to air is small (Pierson and Costa, 1987; Coussot and Meunier, 1996). Debris avalanches contain a wide range of particle sizes, the clay fraction is negligible (Coussot and Meunier, 1996) and material is poorly sorted (Coussot and Meunier, 1996; Schneider and Fisher, 1998). These may begin as slides consisting of large masses of rock but then rapidly break up to form flows as the material is pulverised in transit (Summerfield, 1991). The description of particle shape within debris avalanches is scarce; however Schneider and Fisher (1998) describe particle shape from a large volcanic debris avalanche from the Cantal Volcano in France where clasts are angular with subrounded edges (Table 2.4). Further work by Schneider *et al.*, (1999) on the internal fabric of a debris avalanche in the Swiss Alps describes the presence of angular clasts, which indicates that the behaviour of the debris avalanche is not characterised by strong interactions between clasts. Rounded clasts within a debris avalanche were described by Crandell (1969), however this was attributed to the large distance travelled. Subrounded to well rounded clasts have also been described by Holmes (1965), however this roundness was attributed to older resedimented material rather than that which was freshly fragmented.

No descriptions of debris avalanches have been found in South Africa; however these may have been described as debris flows, given that debris flows and debris avalanches can be very difficult to differentiate from one another (Palmer *et al.,* 1991; Smith and Lowe, 1991). The possibility of the occurrence of former debris avalanches has however been described by Grab (1999b), based on steep gradients and talus build-up in some areas of the Drakensberg.

2.1.2.2.3 Landslides

Landslides are described as discrete mass movement features with distinct boundaries and usually undergo significantly high rates of movement (Crozier, 2004). Precipitation is well known as one of the major landslide triggers (Van Asch *et al.,* 1999) and these are commonly the result of major storms or areas conducive to erosion as a result of climatic regimes (Selby, 1993). There are several morphological features associated with landslides (Figure 2.4). The first is the distinctive slide scar (Rapp and Nyberg, 1981; Crozier, 2004). The displaced mass may then travel downslope, leaving a transport track, ending in a colluvial accumulation zone (Crozier, 2004). The length-width ratio of landslides is typically 10:1 (Selby, 1993). In addition to the length-width ratio, attempts have been made to use the ratio between the depth and length of landslides as a means of interpreting the processes which gave rise to the landforms (Selby, 1993) (Table 2.5).

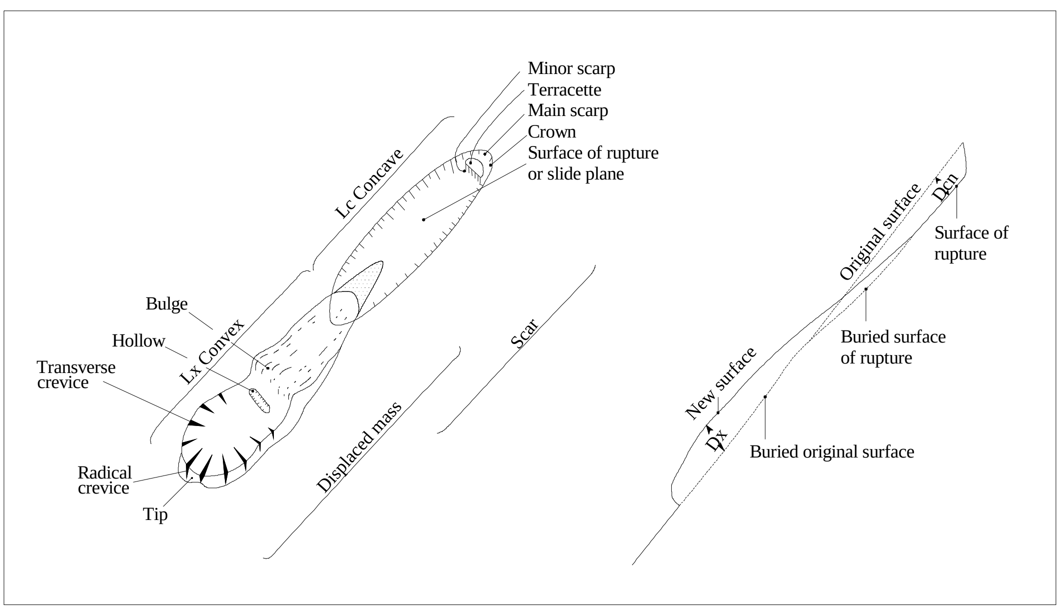

Figure 2.4 The terminology of a landslide (after Crozier, 1973).

Table 2.5 Typical depth/length (D/L) ratios and limiting (threshold) slope inclinations for landslides in soils (after Selby, 1993).

Landslide type	D/L (%)	Lower limit (°)
Debris slides, Avalanches	5-10	22-38
Slumps	15-30	8-16
Flows	0.5-3.0	3-20

Hillslope orientation appears to play a role in landslide occurrence, with 48% of all landslides occurring on equator-facing slopes and less than 10% on pole-facing slopes (Salter *et al.,* 1981). This has been further reinforced by Crozier *et al.* (1980), who attributed the cause to greater insolation, with consequential wetting and drying cycles and greater soil cracking, higher infiltration and higher pore-water pressures (Selby, 1993). In contrast, very uneven landslide distribution is observed in the Du Toit's Kloof area in the Western Cape, South Africa, with 78% of landslides investigated occurring on south-facing slopes, which is attributed to slope asymmetry (Boelhouwers *et al.,* 1998).

Landslides are generally fine grained and contain a significant clay fraction, which ensures cohesion of material (Giardino and Vick, 1987; Barsch, 1996; Coussot and Meunier, 1996; Krainer and Mostler, 2000). Clast orientation within catastrophic landslides has been described as more or less parallel or transverse to movement (Hewitt, 1999) (Table 2.3). Work on the shape of particles within landslides is limited; however Heim (1932) describes the shape of particles within catastrophic landslides as angular (Table 2.4). Further work undertaken in the Karakoram Himalaya describes the presence of angular to very angular clasts within catastrophic landslides, with over 70% of clasts falling within the very angular to angular categories of clast roundness (Hewitt, 1999).

The main micromorphological features which typify debris slides are the occurrence of branching slickensided slip planes, brecciated structures composed of sedimentary clasts in a homogenised matrix, the deformation of former bedding in the form of folds, and stretching or boudinage (Hutchinson, 1970; Brunsden, 1984; Harris and Lewkowicz, 1993). Thin sections in clay rich earth slides reveal a heterogeneous material characterised by sedimentary clasts scattered in a dense matrix which has an open porphyric *c/f* related distribution with areas containing angular to sub-rounded sedimentary clasts (Bertran and Texier, 1999). The b-fabric ranges from undifferentiated or crystallitic, to striated in sheared bands (Bertran and Texier, 1999). Fissures related to post depositional wetting and drying are common (Bertran and Texier, 1999). Coatings do not form in earth slides where the orientation of clasts is weak, due to limited movement (Bertran, 1993).

Several papers have examined the occurrence of landslides in southern Africa (e.g. Paige-Green, 1985; Garland and Olivier, 1993; Sumner, 1994). Durban frequently suffers from landslides and it has been found that housing development and construction work have contributed towards most slope failures (Garland and Olivier, 1993). A landslide susceptibility map of South Africa has been developed by Garland and Olivier (1993) and the Drakensberg occurs in the '*highly susceptible to instability*' class (Figure 2.5).

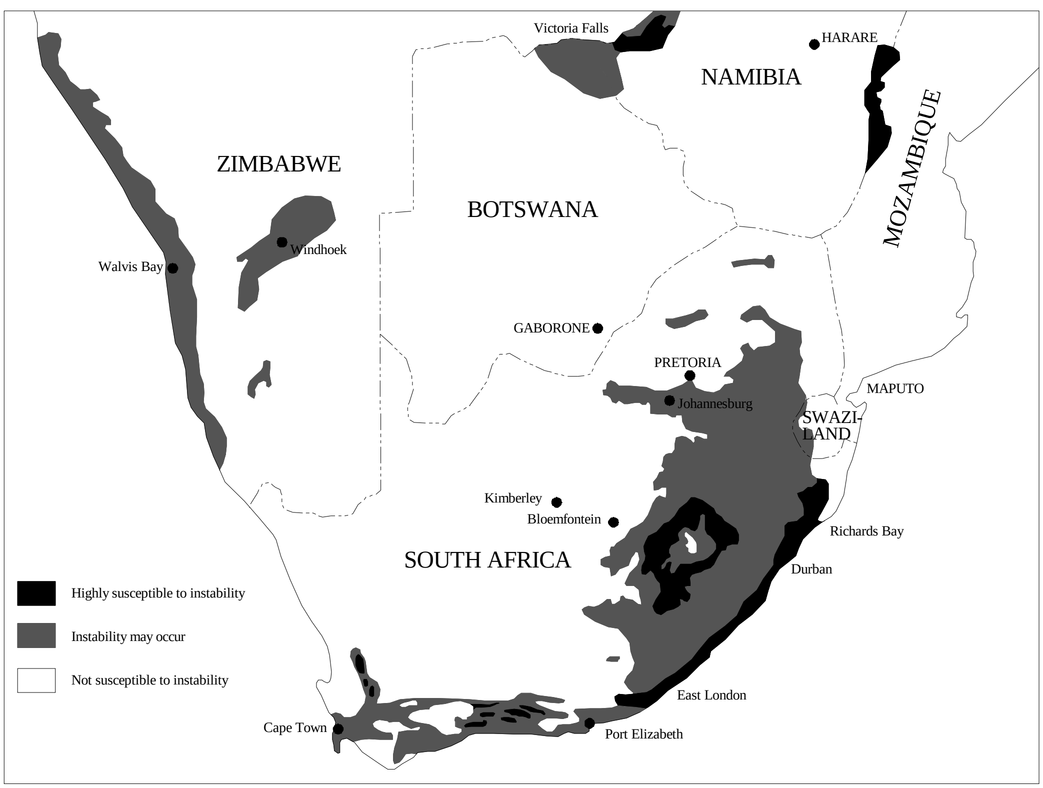

Figure 2.5 Landslide susceptibility in South Africa (after Paige-Green, 1985).

Very little is known on the nature and distribution of landslides in the Drakensberg and southern Africa, however in the little Berg, these features are commonly associated with slopes which occur on sandstone (Sumner, 1994). Sumner and Meiklejohn (2000) further reinforce the importance of lithology in the distribution of landslides. In addition, oversteepended slopes, high pore water pressure and deep bedrock weathering have also been suggested as contributing to landslide failures and they may also be triggered by rockfalls (Sumner, 1993). Translational landslides are most common, incorporating soil and slope debris, whilst large landslides that incorporate bedrock are less common under present conditions (Sumner and Meiklejohn, 2000). There are no data available on the event frequency-magnitude for the Drakensberg region, therefore the significance of past and present landslide occurrence is not known (Sumner and Meiklejohn, 2000). However, recent work which is unpublished on landslide modelling in the Drakensberg includes that by Bijker (2002) and Hardwick (in prep).

2.1.2.2.4 Mudflows/mudslides

Mudflows may occur as wet mudflows, wet sand flows and dry sand flows (Schrott *et al.*, 1996; Dikau, 2004a). The morphology of alpine mudflows is typical to that of debris flows with a slide scar at the top, an erosional gully, block levees and a bouldery front lobe or front fan of finer material (Rapp and Nyberg, 1981; Brunsden, 1984; Dikau, 2004a) (Figure 2.6). Mudslides consist of failure scars, disturbed slumps and rotational slips (Brunsden, 1984). Mudflow lobes usually consists of two parts, namely an upper, flatter area with an angle between 1º and 5°, and a convex curved distal toe with an angle that may range between 10º and 25º (Brunsden, 1984). This area of accumulation usually has an irregular surface with steps formed by overlapping lobes at the head, arcuate ridges in lower areas and a complex microrelief (Brunsden, 1984). The longitudinal profile of a mudflow in the Buzau Subcarpathians had a gradient of 7º to 12º with some steeper portions (40º) (Balteanu, 1976). Recent work on mudslides in the eastern Pyrenees indicates that the average slope angle of mudslides is 26º, decreasing at the toe to 17º (Corominas, 1995).

Mudflows and mudslides tend to occur in saturated clays (Brunsden, 1984) and therefore contain a higher proportion of fine material (Rapp and Nyberg, 1981; Corominas, 1995). Most mudslide material includes silt and sand, and may also

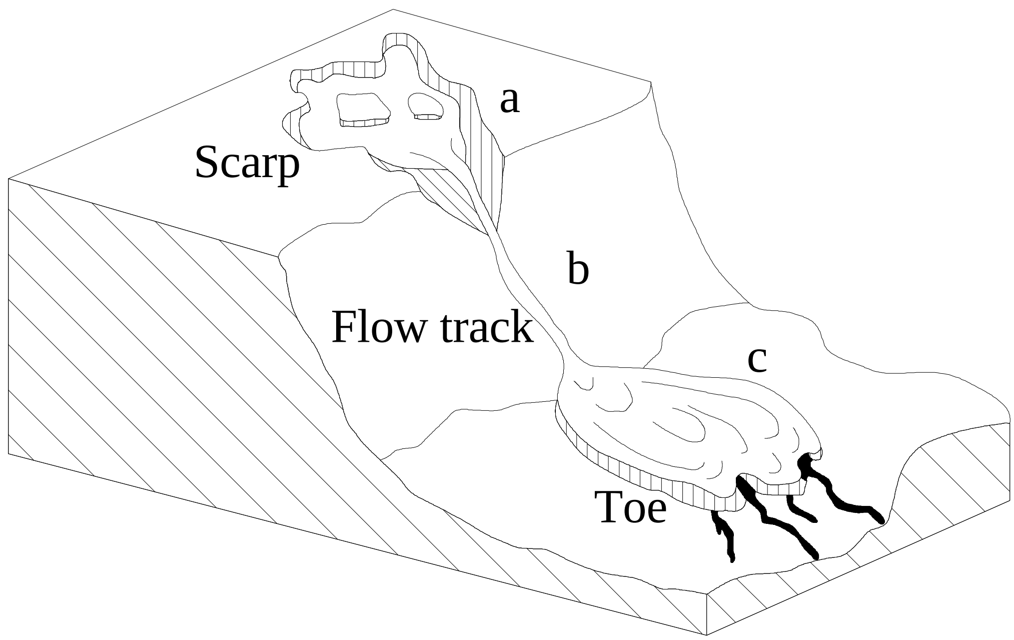

Figure 2.6 Diagram showing typical features of a small mudflow (a = zone of initiation, b = zone of channel erosion, c = zone of accumulation) (after Schrott *et al.*, 1996).

consist of fine sands and silts overlying and moving on clays (Brunsden, 1984). The clay content of mudslides often exceeds 50% (Brunsden, 1984) and has been recorded to increase with depth (Corominas, 1995). Mudflows also significantly lack coarse-grained material (Dikau, 2004a) and tend to lack any preferred orientation as a result of turbulent flow within a mudflow (Binda and Van Eden, 1972) (Table 2.3). In some cases, strong fabrics may develop in mudflows due to Jeffery rotation (suggested by Jeffrey, 1922) during laminar flow, yet these are uncommon and periodic in nature (Lindsay, 1968). Fabric ultimately reverts back to a random state, and further changes may occur once the mudflow has ended and final settling of the clasts takes place (Lindsay, 1968). The description of particle shape within mudflows is also relatively scarce; however Corominas (1995) describes clasts found within the lateral ridges of a mudflow deposit as angular (Table 2.4).

There has been little work undertaken on mudslides and mudflows in South Africa, however Boelhouwers *et al.* (1996) suggested that mudflows near Cape Town were partly the result of wildfire, which caused a water repellent layer, inhibiting infiltration and leading to greatly enhanced runoff.

2.1.2.2.5 Rock avalanches

Rock avalanches are also known as rockfall avalanche, rockslide avalanche and Sturzström (Angeli *et al.,* 1996). These usually consist of a high volume of dry rock material, are created by large falls and slides and move at high velocities over long distances (Hsü, 1975). Rock avalanches may develop in two ways. Either by the fall or slide of a rock body, which looses its cohesion during movement and turns into dry debris and thus develops into a debris avalanche, or by the sudden mobilization of a debris deposit because of the fall of an overhanging rock mass or by seismic shocks (Dikau, 2004b). Rock avalanches are slope failures of large masses of rock (>500 000m^3) (Ballantyne, 2003), which is far greater in volume than the deposits being investigated in this research, and will therefore not be considered as a hypothesis for the formation of the deposits.

2.1.2.2.6 Solifluction deposits

Landforms that result from solifluction processes include solifluction sheets and lobes (French, 1996). The original meaning of solifluction was the process of slow flowing water-saturated waste from higher to lower ground (Andersson, 1906), which is not restricted to cold climates, and therefore the term gelifluction referred to the slow soil flow associated with thawing ground (Washburn, 1979; Harris, 1981a; French, 1988). More recently, studies have revealed that slow mass movements in cold regions include several processes and do not necessarily require saturation (Matsuoka, 2001). Nowadays, solifluction represents the collective term for slow mass wasting, associated with freezing (Ballantyne and Harris, 1994; French, 1996; Matsuoka, 2004), whilst the saturated soil movement associated with ground thawing is designated as gelifluction (Washburn, 1979; Matsuoka, 2001).

Solifluction lobes tend to occur in alpine regions where soil movement is localised and surface conditions (vegetation, material and topography) are variable, whereas sheets dominate polar slopes which experience more uniform movement and where surface conditions are homogeneous (Harris, 1981a; Matsuoka, 2001, 2004). Solifluction lobes are tongue-shaped accumulations of material (Harris 1981a; Matsuoka, 2001) and their fronts are usually bulging, with the riser of one lobe commonly overlapping the tread of another (Benedict, 1976). Solifluction sheets and lobes are usually between 2 m and 50 m in width or length, and up to 1m in height

(Harris, 1981a; Matsuoka, 2001, 2004; Matsuoka *et al.*, 2005). The height of solifluction lobes reflects the maximum depth of soil movement (Matsuoka, 2001, 2004). Small lobes of about 0.2 m in height mainly occur near slope-crest locations, where the regolith is thin and only responds to diurnal freeze-thaw action (Matsuoka, 2001).

Solifluction lobes commonly display a stepped, tread-like slope which may range in angle from 3° to 5° upwards to 35° (Benedict, 1976; Bertran *et al.*, 1995; French, 1996). In addition, it has been suggested that solifluction lobes occur on slopes of between 5º and 23º (Hugenholtz and Lewkowicz, 2002). They may be absent on steeper gradients as a result of rapid moisture drainage or the inability to maintain their fronts (Benedict, 1976). It is suggested that turf-banked solifluction lobes may collapse as they pass from a moderate slope, onto a 25º to 29º slope (Price, 1969). Solifluction sheets may exhibit treads of up to 300 m wide with low angles commonly between 3° and 10° or treads of less than 100 m wide with angles up to 31º where valleys are incised (Harrison, 2002). Solifluction data from mid-latitude to tropical mountain environments reveal that lobes occur on slopes with angles ranging between 5° to 29° and the lobe risers may reach a maximum of 4 m in height (Matsuoka, 2001).

Sorted solifluction lobes tend to have a surface concentration of boulders which are underlain by fine soil (Ballantyne and Harris, 1994; Grab, 2000b), whilst non-sorted lobes contain small clasts which are embedded in a fine-grained matrix (Harris, 1981a; Ballantyne and Harris, 1994). Stratification develops by the movement of stone-banked solifluction sheets and lobes (Francou, 1988, 1990; Bertran *et al.*, 1993). Solifluction lobes contain a matrix-rich layer, which ranges from 7 cm to 10 cm, and represents the depth of freezing (Bertran *et al.*, 1995). The proportion of particles >2mm within solifluction lobes ranges from 10% to 80% (Bertran *et al.*, 1995). However, silts can accumulate on top of the buried matrix-rich layers and give rise to silty pans in well-drained areas and openwork layers often show vertical gradings of either an upward or downward coarsening of pebbles (Bertran *et al.*, 1995). Sediment characteristics from a solifluction lobe in northern Norway suggests that clay-sized sediment contributes <20% of the total size fraction, which means that the lobe is more granular than clayey (Elliot and Worsley, 1999). The thickness of active solifluction lobes does not exceed the thickness of the seasonally thawed surface layer and modern examples of active layer thicknesses range from 0.3 m to 2 m (Hinkel and Outcalt, 1994; Romanovsky and Osterkamp, 1995). There are no examples of modern solifluction features in permafrost areas which exceed 2 m to 3 m in thickness (Humlum, 1998a).

Solifluction lobe sediments described from the Yukon Territory, Canada are poorly sorted and are primarily composed of sand (49%), with secondary fractions of gravel (26%) and silts (26%), with very little clay (1%) and bimodal grain size distributions (Kinnard and Lewkowicz, 2006). Almost all solifluction lobes contain at least one buried organic soil horizon (Benedict, 1976), which was also observed at the solifluction lobes in the Yukon Territory, where a 3 cm to 15 cm thick organic horizon was present in all lobes (Kinnard and Lewkowicz, 2006). Sorting in solifluction lobes is variable given that gelifluction encourages textural homogeneity, whereas frost creep encourages wide variations in soil texture within short distances (Benedict, 1970). However, fossil solifluction landforms tend to show a certain amount of sorting as a result of frost creep and sorting processes once gelifluction has ceased (Benedict, 1976).

It has been documented that the a-axis of elongate clasts conforms closely to the direction of flow for solifluction landforms (Lundqvist, 1949) (Table 2.3). Subsequent work by Nelson (1985) established that solifluction deposit fabrics have strong modes aligned with the direction of the local slope and dip into the slope. Similarly, work by Harris (1981a, 1987) concluded that larger clasts in gelifluction deposits tend to become oriented with the longer axis parallel to the direction of gelifluction movement and show low-angled dips. The strength of downslope orientation is highly variable, possibly reflecting various styles of strain, vertical velocity gradients and amounts of downslope movements (Benn and Evans, 1998). Transverse clast orientation in solifluction deposits have also been recorded near the lobe fronts, where movement is slowed down (Benedict, 1976), however random orientations at lobe fronts have also been described by Bertran *et al.* (1997). Clast dip within gelifluction deposits tends to be low angled (Harris, 1981a, 1987), where angles vary between 10° and 20º (Harris and Wright, 1980; Nelson, 1985; Elliot and Worsley, 1999). In contrast, clast imbrication within a solifluction lobe in La Cumbre in the Bolivian Andes has been described as well-developed (Bertran *et al.,* 1997).

Although work on the description of particle shape within solifluction lobes is limited, Grab (2000b) describes the occurrence of angular, platy clasts within a stone-banked solifluction lobe in the high Drakensberg (Table 2.4). Eyles and Paul (1983) ascribe angular clasts within solifluction deposits as a result of freeze-thaw weathering of exposed bedrock. Earlier work also describes the presence of angular clasts within solifluction deposits (Washburn, 1973), however it is suggested that this is a consequence of mechanical weathering processes independent of downslope movement, as neither frost creep nor gelifluction are capable of causing significant changes in the angularity of stones (Benedict, 1976).

Micromorphological features within solifluction deposits include platy structures, which develop due to the growth of ice lenses (Van Vliet-Lanoë, 1976; Bertran *et al.,* 1995; Bertran and Texier, 1999). Elluviation features are very important within solifluction lobes, in which downslope gradients of elluviation usually develop (Bertran *et al.,* 1995). When ice lensing interferes with accumulation, silts are incorporated in the whole matrix and where freezing is shallow, these silts and clays form microlaminated coatings on voids (Bertran and Texier, 1999). Coatings are related to the shape of clasts and coatings around grains tend to occur on rounded and subrounded clasts, whereas less rounded clasts tend to only be capped on their surface (Bertran and Texier, 1999). The amount of silt coatings also tends to increase downslope in solifluction lobes due to increased elluviation and decreased velocity (Bertran and Texier, 1999). It is suggested that the downward translocation of fines is responsible for the development of such coatings (Harris and Ellis, 1980; Harris, 1981b). Clasts near the soil surface undergo a rotation, with translocated silts progressively wrapping around them. Grains then move downslope by translocation, with silts accumulating on their upper surface (Bertran, 1993). The rate of particle motion during flow depends on its shape and the amount of displacement (Ildefonse *et al.,* 1992; Jesek *et al.,* 1996), as opposed to the speed of movement (Bertran and Texier, 1999). Rounded clasts tend to be embedded in silt, whilst flatter clasts tend to only be capped on their upper surface (Bertran and Texier, 1999).

Solifluction landforms have been identified at high altitudes in southern Africa by several authors (e.g. Linton, 1969; Nicol, 1973; Dardis and Granger, 1986; Lewis, 1987, 1988a, 1988b; Lewis and Hanvey, 1988; Boelhouwers, 1991, 1994, 1998; Marker, 1992; Grab, 1997a, 2000b). Many of these deposits are believed to have originated under climates of lower temperature and enhanced snowfall (Marker, 1992). A variety of solifluction deposits in the mountains of Lesotho and the Eastern Cape are currently active (Hastenrath and Wilkinson, 1973; Dardis and Granger, 1986; Lewis, 1988a, 1988b, 1996; Kück and Lewis, 2002) and the altitudinal distribution of these active periglacial features in Lesotho is between 1900 m a.s.l. and 3300 m a.s.l (Hastenrath and Wilkinson, 1973; Dardis and Granger, 1986; Lewis 1988a; Boelhouwers, 1994). Active stone- and turf-banked lobes have also been reported from the Hex River Mountains in the Western Cape (Boelhouwers, 1998). Longitudinal solifluction lobes have been identified in the Drakensberg by Marker (1992), where deposits consisting of a lobate form and matrix supported boulders have been emplaced by slow flow. Turf- and stone-banked lobes above 3000 m a.s.l in the Lesotho highlands have also been identified by Boelhouwers (1991, 1994, 1998) and Grab (1997a, 2000b). These stone-banked lobes appear to be restricted to the colder slopes, rich in talus and where vegetation is or was sparse in the past (Grab, 1997a). Small-scale turf-banked lobes and stone-banked lobes have also been described from the Drakensberg by Dardis and Granger (1986), however vegetation growth on the solifluction lobe fronts indicates that these features are inactive (Boelhouwers, 1991). This is further reinforced by Grab (2000b), who suggests that only above 3200 m a.s.l. do small lobes appear to be active.

2.1.2.2.7 Mass wasting deposits and the periglacial environment in the Drakensberg

In periglacial environments, mass wasting may be divided into the gradual displacement of slope sediments due to repeated freezing and thawing and more localised rapid slope failures that occur intermittently during thaw of the active layer or underlying permafrost (Ballantyne and Harris, 1994). Slow processes of mass wasting include frost creep, solifluction and gelifluction (Ballantyne and Harris, 1994; French, 1996), whilst more rapid processes include debris flows/avalanches and mudflows. Mass wasting occurs in all climatic regions, however is most abundant in periglacial environments due to the large quantities of water, in particular soil water released by the melting of ground ice during the spring and summer thaw (Ballantyne and Harris 1994; French, 1996). The flattening of landscape and smoothing of slopes is thought to be typical of many periglacial regions and is generally attributed to mass wasting (Ballantyne and Harris, 1994; French, 1996).

Sediment that has been transported across and deposited on slopes as a result of mass movement processes and soil wash is termed colluvium (Summerfield, 1991; Blikra and Nemec, 1998; Goudie, 2004). It is composed of poorly sorted mixtures of gravel, sand, silt and clay-sized particles and accumulates on the lower hillslopes (Fairbridge, 1968; Watson *et al.,* 1984). Colluvium can be many metres thick (Crozier *et al.,* 1990), is frequently derived from the erosion of weathered bedrock and deposited on low-angled slopes, and it can be distinguished from fluvially deposited material, which is well sorted and bedded (Watson *et al.,* 1984; Goudie, 2004).

The term periglacial was originally used with regards to non-glaciated but frost-affected regions adjacent to the Pleistocene ice sheets (Lozinski, 1912), however this definition was later altered to encompass areas where mean temperatures are below 0ºC and mean annual precipitation is below 1500 mm, regardless of the proximity to glaciers (Thorn, 1992). More recently, French (1996) has defined the periglacial domain as areas where the mean annual air temperature is less than 3ºC, however based on what constitutes a periglacial region, it is believed that no region in South Africa is truly periglacial in nature (Sumner and Meiklejohn, 2000). The periglacial domain can be further subdivided into environments where frost action dominates (mean annual temperature less than -2ºC) and those where frost-action processes occur but do not necessarily dominate (mean annual air temperature between -2ºC and +3ºC) (French, 1996).

The Lesotho highlands are classified as marginal or sub-periglacial environments as a result of limited frost activity (Boelhouwers, 1991; Hanvey and Marker, 1992; Boelhouwers and Meiklejohn, 2002). Above 2800 m a.s.l. there are a range of ground-ice related landforms which exist and are active during surficial soil freezing in winter (Sumner, 2003). Depositional features which relate to past periglacial conditions include patterned ground (Harper, 1969; Hastenrath and Wilkinson, 1973; Boelhouwers, 1991, 1994; Hanvey and Marker, 1992; Grab, 1996b, 1997a, 2000a, 2002; Sumner, 2000a), solifluction lobes (Boelhouwers, 1991; Grab, 2000a), gelifluction sheets and lobes (Marker and Whittington, 1971; Boelhouwers, 1994), and blockstreams and blockfields (Hastenrath and Wilkinson, 1973; Boelhouwers, 1994; Grab, 1999b, 2000a; Grab *et al.,* 1999; Sumner and Meiklejohn, 2000; Boelhouwers *et al.,* 2002; Boelhouwers and Sumner, 2003).

Periglacial mass wasting landforms predominantly occur on south- and southwest-facing slopes in the High Drakensberg and are absent on north-facing slopes (Grab, 1999b). Periglacial mass wasting has been an important component in the overall evolution of south-facing slopes (Grab, 1999b). South-facing slopes have been characterised by seasonal ground freeze, whilst north-facing slopes have been subject to diurnal freeze (Grab, 1999b). The basaltic chemical weathering mantles would have covered many slopes following a long period of warm climates in the Tertiary in the Lesotho highlands (Partridge and Maud, 1987; Boelhouwers, 1999). This would have provided an ideal substrate within a frost-susceptible matrix at the onset of Quaternary periglacial conditions for frost heave and solifluction (Boelhouwers, 1999). Such processes would result in the concentration of blocks at the surface and where sufficiently steep gradients occur, permit their subsequent downslope transport by slow periglacial mass wasting (Boelhouwers, 1999).

Evidence for mass wasting in the High Drakensberg also takes the form of angular boulders and gravel transported by solifluction processes, which accumulate as colluvial deposits in the valley bottoms (Harper, 1969). ‘Head’ deposits have also been described from the Little Caledon Valley in the Orange Free State (Nicol, 1973). These deposits tend to terminate in lobes, exhibit mild stratification and are suggested to have formed as a result of solifluction processes, based on the a-axis of stones displaying a preferred orientation in the direction of slope (Nicol, 1973). Active gelifluction terraces have been recorded in the Sani Pass area at altitudes between 2990 m a.s.l. and 3109 m a.s.l. (Marker and Whittington, 1971; Fitzpatrick, 1978). These have bulging fronts which seldom exceed a metre in height (Lewis, 1996). Additional gelifluction terraces have been described from Champagne Castle at altitudes exceeding 3000 m a.s.l (Dardis and Granger, 1986). Further ‘head’ deposits are described from the southern Cape Province (Linton, 1969). These deposits contain rubble drift, which includes large clasts, rounded by weathering, and are associated with the LGM (Linton, 1969). Active terracettes also occur between 2750 m a.s.l. and 2880 m a.s.l. in the Eastern Cape Drakensberg, and are associated with needle ice formation (Kück and Lewis, 2002). It is suggested that the terracettes form over a narrow altitudinal range, which is the result of higher temperatures at lower altitudes, whilst at higher altitudes the regolith cover is thinner and slope angles are greater (Kück and Lewis, 2002).

Soil frost is a regular occurrence in the Drakensberg in winter and gives rise to sorted patterns which degrade in summer, probably due to rainwash and livestock trampling (Sumner, 2003). Although it has been suggested that ground-ice activity in winter is limited to the upper 20 cm (Sumner, 2003), the greatest recorded depth of frost penetration is 50 cm (Grab, 2004). Periglacial conditions are suggested for the LGM, based on geomorphic evidence such as blockstreams (Boelhouwers, 1994; Boelhouwers *et al.*, 2002) and evidence for former permafrost has been suggested for elevations as low as 2280 m a.s.l. (Fitzpatrick, 1978; Lewis, 1996). Active and relict periglacial landforms have been studied near Thabana Ntlenyana, (3482 m a.s.l.) (Grab, 1994b, 2002; Sumner, 2000a; Boelhouwers *et al.*, 2002) and mean annual air temperatures at summit altitudes are estimated to be around 3ºC to 4ºC at present (Grab, 2002). It has been suggested that in order for large (143.5 cm in diameter) patterned ground to develop, the MAAT would have to be less than -1ºC, and that the occurrence of permafrost was thus limited to above 3400 m a.s.l. during the LGM (Grab, 2002).

Differences in north- and south-facing slopes have been illustrated by Boelhouwers *et al.* (2002), who describe north-facing slopes as having a thin debris covering of less than 1 m in thickness, whilst south-facing slopes contain a thicker debris mantle. Boelhouwers *et al.* (2002) describe an exposure in one catchment as a uniform, coarse, clast-supported diamict at least 4 m thick, whilst an exposure from another catchment is 15 m to 20 m thick and is composed of a massive, unstratified, granular loam, with the occasional thin layer of small stones which are restricted to the upper 40 cm. In another catchment about 300 m upstream, they describe a 3 m thick exposure, with the presence of a 1.6 m thick clast-supported diamict, underlain by a 1.5 m thick uniform granular loam (Boelhouwers *et al.*, 2002). The concentration of blocky material in the upper sections of the exposures is attributed to scarp recession as a result of mechanical weathering and mass wasting during colder Pleistocene periods (Boelhouwers and Sumner, 2003). The thick debris mantles are similar to *in-situ* chemical weathering profiles found in nearby road sections and suggest the mobilization of a pre-existing regolith (Boelhouwers *et al.*, 2002).

The main phase of mass wasting and frost creep in the Drakensberg probably took place during the LGM, however in order to permit 1 m to 2 m deep frost penetration, snow cover must be largely absent (Boelhouwers *et al.*, 2002), as this would provide an insulating cover (Sumner, 2004d). It is suggested that the slope materials became largely stabilised in the Early Holocene (Boelhouwers *et al.*, 2002) and that the thicker debris mantles on the south-facing slopes are a result of the longer and wider south-facing slopes and also the more advanced bedrock weathering on these slopes (Boelhouwers *et al.*, 1999). For significant segregation ice to develop, sufficient moisture must have been available at the time of freeze-up in autumn. Furthermore, sufficient water supply is a necessity for failure under high pore water conditions (Boelhouwers *et al.*, 1999), which contradicts the absence of snow cover during periglacial conditions. However, Boelhouwers *et al.* (1999) explain this by suggesting that during present-day conditions, summer precipitation generates seasonal wetlands whereby the drainage to these wetlands continues during the autumn, even during reduced precipitation. This would suggest that precipitation patterns during the LGM were not significantly different than at present (Boelhouwers *et al.*, 1999).

2.1.3 Rock glaciers

Rock glaciers are lobate or tongue-like bodies of angular boulders that resemble a small glacier, generally have ridges and furrows on their surface, and commonly have a steep snout (Washburn, 1979; Barsch, 1996; Haeberli, 2000). Rock glacier fronts have typical gradients of 35º to 45º and may range from 15 m to 75 m in height (Gordon and Ballantyne, 2006). However, ice typically constitutes 50% to 90% of the volume of rock glaciers (Barsch, 1996), therefore once the ice has melted to form relict rock glaciers, these may have a much more subdued topography than their active counterparts with reduced frontal gradients (Humlum, 1998a; Hughes *et al.*, 2003).

The term rock glacier was subdivided into a threefold classification by Wahrhaftig and Cox (1959), based on the length to breadth ratio and their topographic position. Lobate rock glaciers are single or multiple ridges extending out from the bases of talus slopes or talus aprons and are characteristically as wide, as or wider than, they are long, which is clearly not the case for the linear slope deposits. Tongue-shaped rock glaciers are commonly longer than they are broad, and they may be fed from three sides or extend downvalley from cirques (Wahrhaftig and Cox, 1959). Spatulate rock glaciers widen abruptly near their fronts to form rounded bulges at their lower ends (Wahrhaftig and Cox, 1959). Rock glaciers are very variable and may reach dimensions of about 1 km long and a few hundred metres in width (Whalley, 2004). Small rock glaciers have been described by Humlum (1998a) and measure 50 m to 150 m in length, 20 m to 200 m in width and 15 m to 20 m in thickness. These smaller dimensions are similar to those for rock glaciers in other regions of the world (e.g. Humlum, 1982, 1984, 1988, 1996; Vere and Matthews, 1985).

Most rock glaciers are composed of a clast supported, bouldery debris mantle over a much more massive core of poorly sorted sediment (Nicolas, 1994). Bouldery rock glaciers contain open-work boulders as large as 10 m in diameter (Matsuoka *et al.*, 2005), whereas pebbly rock glaciers have a gravelly active layer filled with fine grained material and surficial clasts, which range from pebbles to small boulders (>1 m in diameter) (Matsuoka, 2005). Active rock glaciers possess a three-layer structure, a 1 m to 3 m thick top layer consisting of large rock fragments, covering a deforming ice-rich permafrozen core, below which consists a unit of rock fragments deposited at the active rock glacier terminus, which is subsequently overrun by the uppermost two units (Haeberli, 1985; Barsch, 1996; Humlum, 1996, 1998b). The debris layer may be up to a few metres thick and composed of two horizons. The uppermost horizon consists of a very coarse-grained surface layer with angular clasts which generally range in size from about 0.5 m to 1.5 m. (Wahrhaftig and Cox, 1959; Giardino and Vick, 1987; Krainer and Mostler, 2000; Berger *et al.*, 2004). The separation of boulders and fines is partly due to downwashing and principally due to the frost heave of boulders (Barsch, 1996). The finer-grained layer is composed of a till-like mixture of frozen silt, sand and gravel sized particles that form a matrix within which larger fragments are embedded (Wahrhaftig and Cox, 1959; Giardino and Vick, 1987; Krainer and Mostler, 2000; Berger *et al.*, 2004). In general, the material in this layer consists of approximately 60% sand and 30% silt (Barsch *et al.,* 1979). The grain size of the surface layer may vary considerably, for example results from a rock glacier in Austria indicate that grain size distribution ranges from very coarse-grained to finer grained, with the presence of large blocks up to several metres in diameter (Berger *et al.,* 2004). This surface layer was 1.2 m in thickness, below which a horizon composed of silty sand and sandy silt with embedded boulders was present. Sorting within rock glaciers is reported to be poor to very poor (Vere and Matthews, 1985; Haeberli, 1985; Evin, 1987; Krainer and Mostler, 2000; Berger *et al.,* 2004) and kurtosis has been described as platykurtic (Vere and Matthews, 1985).

Relict rock glaciers also contain the two layered system of coarse boulders underlain by finer-grained material at the front and side slopes (Barsch, 1996). The internal structure of a relict rock glacier has been described from southwest Poland, where five lithological units to about 5 m in depth were distinguished as alternating units of diamict and sand (Zurawek, 2002). The diamict units consisted of coarse clasts within a loamy matrix, where clasts as long as 30 cm were common and the largest block was 85 cm in length in the first unit, whilst the largest block in the third unit was 20 cm long. The sand units were separated from the diamict units by a distinct plane and the sand generally became finer towards the top of the unit. In addition, a relict rock glacier has been described from the Faeroe Islands as comprising a diamict containing large (1 m to 4 m) rock fragments as well as smaller particles (Humlum, 1998a).

There are few reported cases of clast fabric orientation within rock glaciers. However, Harrison and Anderson (2001) measured clast fabric within a late Devensian rock glacier in North Wales and found that clasts had a pronounced preferred orientation with the a-axes dipping steeply into the landform (Table 2.3). It is suggested that these were most likely to have been formed by the compressive shearing of debris (Harrison and Anderson (2001). Clast orientation measured from a rock glacier in Norway varies between no preferred orientation on the ridge crest sites to orientations at right angles to the ridges (Vere and Matthews, 1985). Similarly, Nicolas (1994) describes weak fabrics within rock glaciers from the La Sal Mountains in Utah. Earlier work by Giardino and Vitek (1985) also proposed that fabric measured from ridges and furrows within a rock glacier showed parallel alignment with surface lineation. Clast dip tends to be <30º from a rock glacier in Jotunheimen (Vere and Matthews, 1985). Clasts have also been recorded as having an upslope imbrication by Nicolas (1994).

Rock glaciers mainly develop in lithology producing blocky debris, and are infrequent on slopes composed of platy debris with finer materials (Wahrhaftig and Cox, 1959; Evin, 1987; Giardino and Vitek, 1988; Chueca, 1992). However, pebbly rock glaciers have been reported from slopes dominated by platy debris (Ikeda and Matsuoka, 2006) (Table 2.4). Particle shape within a late Devensian rock glacier in the Nantlle Valley, north Wales, indicates that the rock glacier contains shapes that range from very platy to platy and very bladed to bladed (Harrison and Anderson, 2001). Material obtained from a relict rock glacier in North Wales ranges from angular to subrounded, which demonstrates the complex nature of depositional processes supplying material to the site of rock glacier formation (Harrison and Anderson, 2001). In addition, Humlum (1998a) describes the presence of angular to subangular clasts within a relict rock glacier in the Faeroe Islands.

In South Africa, Lewis and Hanvey (1993) identified the remains of what was interpreted to be a rock glacier at 1800 m a.s.l. near Barkley Pass and Elliot. Organic material sampled from what is believed to be a rock glacier in the Bottelnek area of the east Cape Drakensberg yielded a radiocarbon date of 21 000 ± 400 yrs BP, suggesting that the rock glacier was active around this time (Lewis and Hanvey, 1993). This feature was interpreted as a relict rock glacier based on its morphology, stratigraphy, particle size, clast characteristics and morphology of quartz grains (Lewis, 1994a). There was a clear distinction between coarse debris overlying fine debris, which is typical of rock glaciers (Lewis, 1994a). Rock glaciers form in areas of discontinuous permafrost where the MAAT is approximately -2ºC (Haeberli, 1985; Whalley and Martin, 1992). In order for such temperatures to occur at 1800 m a.s.l., a temperature drop of 17ºC would be necessary during the LGM for the Eastern Cape, however no other southern African proxy data confirm such a drop (Grab, 2000a). It has therefore been suggested that this so called rock glacier may owe its origins to solifluction processes (Grab, 2000a).

Features similar to small rock glaciers, however termed 'screes' have also been described in South Africa by Marker (1986) in the Amatola Mountains at approximately 2000 m a.s.l. The screes occur on south-facing slopes in association with nivation niches that receive little winter insolation. The majority of the scree tongues (70%) are less than 100 m in length. Features which extend over 150 m in length occur on the Elandsberg and Tafelberg slopes where rainfall exceeds 450 mm per annum (Marker, 1986). Over 75% of these screes are south-facing and Marker (1986) suggests that these represent a cold period, when frost action would have been intensified. However, more recent observations in this area indicate that screes occur on several other aspects, which are determined by geological and topographical factors (Sumner and de Villiers, 2002), and thus cannot be ascribed to the effects of nivation as previously suggested by Marker (1986). In addition, the screes do not preferentially lie in hollows, and are also present on rectilinear slope segments or on spurs (Sumner and de Villiers, 2002). It is suggested that these screes are remnants of relatively continuous scree slopes which have subsequently been infilled by matrix (Sumner and de Villiers, 2002).

2.1.4 Pronival ramparts

The term ‘pronival rampart’ has been used to describe ridges composed of mostly coarse material usually found at or near the foot of a talus slope, which formed as a result of the accumulation of debris along the margins of a perennial snowbank (Washburn, 1979; Ballantyne, 1987b; Lowe and Walker, 1997). Pronival ramparts usually form parallel to the mountain slopes (Linder and Marks, 1985) and may range from as little as 1 m to 2 m in height (Dawson, 1990), to as much as 30 m in thickness and 55 m in height from the crest to the foot of the distal slope (Sissons, 1976; André, 1985). It is suggested that on relatively steep slopes, pronival ramparts tend to have short proximal slopes and long distal slopes (Ballantyne and Kirkbride, 1986; Shakesby, 2004). Maximum distal slope angles are generally reported to be steeper than 34º (Ballantyne and Kirkbride, 1986). Earlier work suggests that distal and proximal slopes should be symmetrical (Behre, 1933; Harris, 1986), and Shakesby *et al.* (1995) have reinforced this and suggested that active ramparts vary in terms of their cross-sectional form.

Pronival ramparts consist of coarse, clastic, poorly sorted sediments, with an absence of fines even at depth (Washburn, 1979; Linder and Marks, 1985; Ballantyne and Kirkbride, 1986; Hall and Meiklejohn, 1997). However, in some cases the coarse sediment may be embedded in a matrix of fines (Shakesby *et al.,* 1995). It is suggested that the absence of fines within pronival ramparts is owing to a lack of momentum to bounce, slide or roll across the snow (Washburn, 1979), and that any fines present would appear to be the products of granular disintegration of exposed clasts (Ballantyne and Kirkbride, 1986). In addition, such clasts demonstrate a much greater roundness than those in the adjoining subsurface layer (Ballantyne and Kirkbride, 1986). Further evidence for the presence of fine particles found within pronival ramparts comes from Pérez (1988), who described a pronival rampart from Lassen Peak, California. It was established that large angular blocks were common on the proximal inner face of the rampart which had been recently deposited, however there was a high sand and silt content in the distal face of the rampart, which was vegetated and inactive (Pérez, 1988). The presence of finer material is also described form the Japanese Alps by Fukui (2003). The pronival rampart contains a subsurface layer consisting of non-sorted, angular clasts within a sandy matrix which contains 85% sand and 15% silt and clay (Fukui, 2003). It is therefore suggested that both coarse and fine grained particles may be present in pronival ramparts.

Clasts in pronival ramparts are reported to lack a preferred orientation (Washburn, 1979; Pérez, 1988) (Table 2.3). More recently however, Shakesby *et al.* (1999) observed an oblique alignment of particles to the ridge crest of a pronival rampart, whilst Harris (1986) observed weakly developed orientations perpendicular to the ridge crest, with downslope dips. Clasts within pronival ramparts tend to range from very angular to subangular, however the majority of clasts tend to fall within the very angular and angular categories (Washburn, 1979; Harris, 1986; Tinkler and Pengelly, 1994; Shakesby, 2004; Shakesby *et al.,* 1995, 1999) (Table 2.4). Particle shape analysis at a pronival rampart in the Romsdalsalpane in southern Norway revealed that each site had an angular modal class and <6% of clasts were subrounded (Shakesby *et al.,* 1995). Clast roundness from within a rampart was compared to that on a snowbed, and clasts on the snowbed were statistically more angular than those on the rampart itself, which indicates that supranival transport is not the only source of debris supply and that subnival processes may also be taking place (Shakesby *et al.* 1995). Further work on particle shape at pronival ramparts in southern Norway suggests that in this case, the modal class for the clasts measured was in the very angular category, however there were also a significant number of subangular clasts

(2% to 32%) and a small number of subrounded clasts (2% to 6%) (Shakesby *et al.*, 1999).

Work undertaken on pronival ramparts in southern Africa is scarce, however Marker (1990) identified three so-called pronival ramparts at Golden Gate in the Orange Free State. These ramparts are situated at between 2155 m a.s.l. and 2316 m a.s.l. They consist of angular clasts, which are attributed to frost shattering from a cliff, which were subsequently transported across a snow patch and deposited as pronival ramparts (Marker, 1990). The view that the angular nature of the clasts represents frost shattering has however been severely criticised (Hall, 1991; 1992). It is stressed that angular clasts can result from thermal fatigue, wetting and drying, salt weathering, hydration shattering or biological weathering (Hall, 1992).

Similarly, a debris ridge in the East Cape Drakensberg has been interpreted as a pronival rampart on the basis of morphological and sedimentological investigations (Lewis, 1994b). Lewis (1994b) suggests that the rampart provides evidence of former perennial snowbeds and discontinuous permafrost in this area at 2000 m a.s.l. and higher. However, according to Shakesby (1997), permafrost is not viewed as a requirement for rampart formation. Thus, suggestions that the Killmore ridge in South Africa is a pronival rampart have misleading implications for the palaeo-climate of southern Africa. It has more recently been suggested that this rampart is in fact a glacial moraine (Lewis pers. comm.); however its true origin remains speculative.

2.1.5 Glacial moraines and tills

2.1.5.1 Glacial moraine types

Moraines are landforms which are created by the deposition or deformation of sediment by glacier ice (Knight, 2004). Most moraines that occur in mountain environments are ice-marginal in origin (Johnson and Menzies, 1996). The character of moraines depends on glacial dynamics, which includes mass balance and the nature and style of deglaciation (Johnson and Menzies, 1996). Four types of moraines have been identified by Benn and Evans (1998); 1) glaciotectonic landforms, 2) push and squeeze moraines, 3) dump moraines and 4) latero-frontal fans and ramps.

Glaciotectonics involves structural deformations of the upper horizon of the lithosphere as a result of stress exerted by glaciers (Van der Wateren, 2002). Glaciotectonic moraine ridges are defined as those in which glacio-tectonized pretectonic and syntectonic sediments constitute >25% of the unit area of the moraine (Benn and Evans, 1998). These landforms may be composed of pre-Quaternary bedrock, pre-existing Quaternary sediments or contemporary sediment (Andrews, 1980). The most common type of glacitectonic landforms are composite ridges and thrust block moraines (Benn and Evans, 1998). These have been termed push moraines by some researchers (Boulton, 1986; Etzelmüller *et al.,* 1996; Bennet, 2001; Van der Wateren, 2002). Composite ridges comprise arcuate suites of subparallel ridges and intervening depressions in plan form, conforming to the general shape of the glacier margin (Benn and Evans, 1998).

Push moraines are small ridges, usually less than 10 m in height, produced by minor glacier advances (often annual) (Benn and Evans, 1998), and may attain 100 m in height (Summerfield, 1991). Small push moraines may be formed by seasonal bulldozing of sediment at the margin of a glacier that varies seasonally and larger push moraines may form from several seasonal advances, or by a substantial advance of the glacier (Knight, 2004). Push moraines usually display an asymmetric cross-section with gentle proximal and steep distal slopes (Van der Meer, 1997a). Push moraines are composed of a diverse range of sediments (Bennet, 2001) and can consist of subglacial till, mass movement deposits, water-sorted sediments or large boulders, depending on the nature of the sediment available (Benn and Evans, 1998; Van der Wateren, 2002). Push moraines tend to form in unlithified or weakly lithified sediments, which include tills, fluvial and glaciofluvial sands and gravels, chalk, sandstone and clay (Van der Wateren, 2002). Morphologically, push moraines tend to have asymmetric cross-profiles with gentle ice-proximal and steep ice-distal slopes (Van der Meer, 1997a; Benn and Evans, 1998).

Four types of push moraines were identified by Sharp (1984) (Figure 2.7), of which the most common type is the ‘type A moraine’. These have proximal slopes of deformation till recording glacier overriding. ‘Type B moraines’ also have an ice core and a surface covering of resedimented debris on the proximal zone. ‘Type C moraines’ are superimposed on type A cores and are formed wherever debris bands

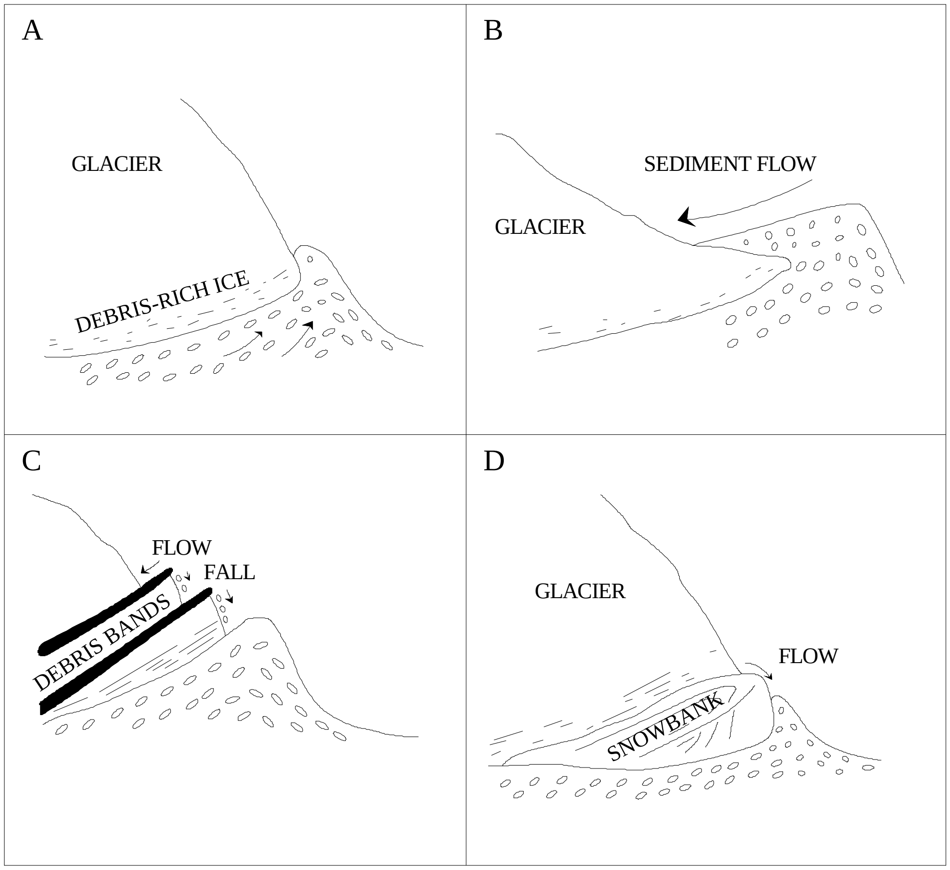

Figure 2.7 Annual moraine ridge formation based upon examples at Skálafellsjökull, Iceland (after Sharp, 1984).

crop out of the ice surface. Debris flows are common as the ice melts out. 'Type D moraines' are produced where marginal snowbanks are pushed forward and overridden by the glacier. The snowbank may be incorporated into the moraine where debris from the glacier falls over it and is deposited on the pushed ridge. The snowbank will later melt and initiate debris flows (Sharp, 1984; Benn and Evans, 1998).

The sedimentology of push moraines consists of tills and debris, accumulated at the glacier snout during the summer, which is then pushed when the glacier re-advances the following winter (Van der Wateren, 2002). Push moraines may also include basal tills and glacifluvial outwash from previous more extensive advances (Van der Wateren, 2002). Fabric analysis of moraines includes work by Sharp (1984), who produced a model for clast a-axis fabrics of push moraines (Figure 2.8). Work

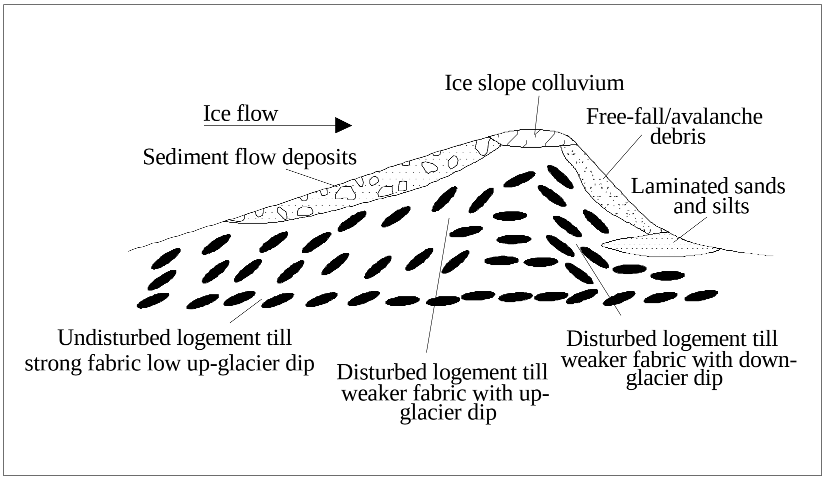

Figure 2.8 Idealised model of clast fabric and facies variation within a seasonal push moraine (after Sharp, 1984).

undertaken by Rabassa *et al.* (1979) on the sedimentology of push moraines in Argentina indicates the presence of angular to rounded clasts and fine material in some samples. It is suggested that the more rounded clasts and finer material reflects the pushing effect of the advancing glacier, whereas the more angular clasts suggest material brought onto the moraine by gravitational processes (Rabassa *et al.,* 1979).

Dump moraines are formed by material accumulating at the surface of a glacier, which is transported to the glacier margin and then dumped where the glacier ends (Benn and Evans, 1998; Knight, 2004). Lateral moraines (Small, 1983) form a continuum around the former valley glacier margin (Johnson and Menzies, 1996) and comprise of frost-shattered debris which has fallen onto the edge of a glacier from the adjacent valley walls, above and below the ice (Summerfield, 1991; Knight, 2004) (Figure 2.9). Such features may be morphologically distinct, displaying narrow ridges with steep slopes, and their character will depend on glacial dynamics including mass balance and the style and nature of deglaciation (Johnson and Menzies, 1996). Steep valley sides and weathering produce talus material consisting of predominantly large angular boulders, which are subsequently deposited at the foot of the slope and incorporated into the moraines as they build up (Winkler and Nesje, 1999). Supraglacial debris may slide, roll, flow and fall from the glacier margins and be deposited as ice-contact scree (Benn and Evans, 1998). The debris is then incorporated into the glacier by snow and ice burial in the accumulation area

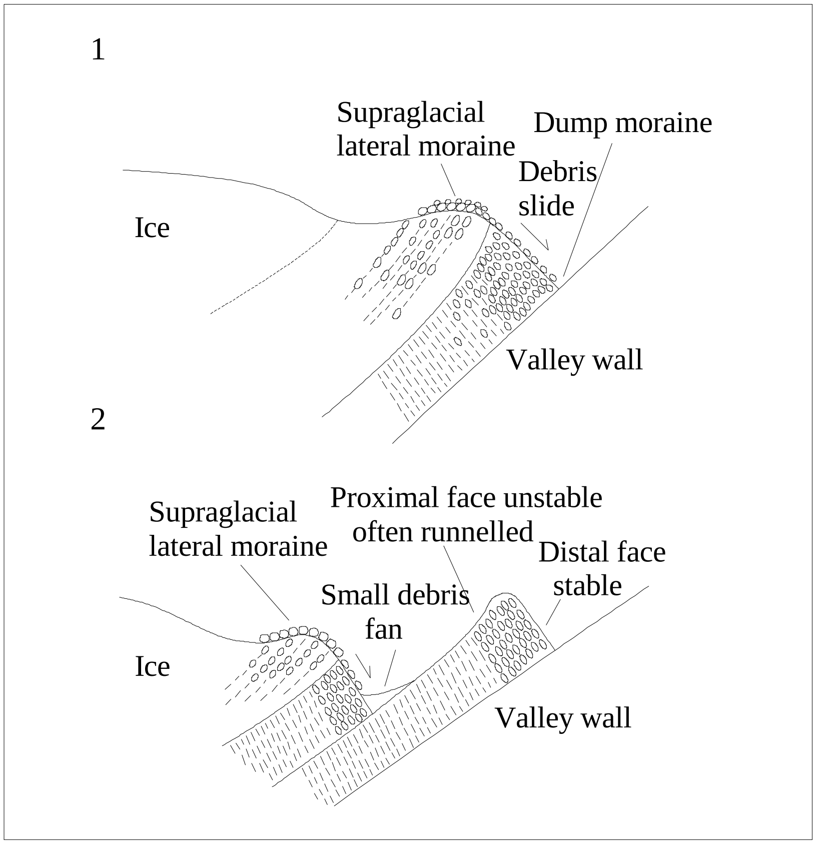

Figure 2.9 Lateral moraine formation by dumping of supraglacial debris (after Small, 1987).

(Huddart, 2004). The debris may be predominantly passively transported rockfall material which suffers little modification, retaining its primary parent material characteristics which tend to be coarse, angular clasts with little matrix (Benn and Evans, 1998). However, actively transported debris may also take place and result in matrix-rich debris in some dump moraines (Small, 1983; Benn and Evans, 1998; Huddart, 2004). Work by Raab and Völkel (2003) on lateral moraines in southern Germany has measured clast orientations parallel to the former glacier flow direction, whilst clast orientation within a lateral moraine in Norway is in the direction of the local moraine slope (Vere and Matthews, 1985).

Latero-frontal fans and ramps form as a result of deposition by debris flows and glacifluvial processes around stationary glacier margins (Benn and Evans, 1998). They consist of coalescent debris fans which descend from the glacier snout (Owen and Derbyshire, 1989). Whilst their outer slopes have shallower gradients than latero-frontal dump moraines, their inner slopes are steep, producing a pronounced asymmetric cross-profile (Benn and Evans, 1998). The sedimentology of glacifluvial sediments is dominated by massive, often bouldery, diamicts with inversely graded beds up to tens of metres thick and dipping away from the glacier snout (Benn and Evans, 1998; Whiteman, 2002). This is typical of water-laid glacifluvial processes where there is an absence of fines (Summerfield, 1991).

2.1.5.2 Tills

Various till types exist and their properties may be affected by their transport processes. The transport paths include passive transport and active transport (Benn and Evans, 1998) (Figure 2.10). When debris does not come into contact with the glacier bed, the term passive transport is employed (Bennett and Glasser, 1996; Benn and Evans, 1998). Debris falls onto the surface of the glacier by rockfall, avalanching and mass movement and becomes buried by fresh accumulations of snow above the equilibrium line, or stays on the surface of the glacier below the equilibrium line until it reaches the snout (Summerfield, 1991; Bennett and Glasser, 1996; Hambrey and Lawson, 2000). Supraglacial debris is likely to be most abundant in valley and cirque glaciers and may retain its primary characteristics as it is unaltered by glacier transport (Summerfield, 1991). Such debris is thus typically angular, coarse and contains a small proportion of fines (Owen, 1994; Bennett and Glasser, 1996; Benn and Evans, 1998). According to Boulton (1976), supraglacially derived debris has a silt-clay content of below 15% owing to the lack of a tractive phase. The angular nature of supraglacial debris suggests little modification of the clasts during flow and reflects fracture during weathering and transport onto the glacier (Owen, 1991, 1994; Benn and Ballantyne, 1993; Benn and Evans, 1998) (Table 2.4). Supraglacial clasts also tend to be platy and elongate (Benn and Ballantyne, 1993), whilst Dowdeswell (1982) suggests that supraglacial debris tends to contain a high percentage of bladed shapes (Table 2.4).

Englacial transport may take place in the glacier accumulation area and then be transported by glacier flow to the ablation area where it melts out to form part of a lateral moraine (Benn and Evans, 1998). Debris can be abraded and fractured whilst held in the englacial zone, which would reduce particle size characteristics (Hambrey, 1976). It can also be reworked and transported by englacial streams, which can result in significant debris modification, particularly if there is a copious supply of debris

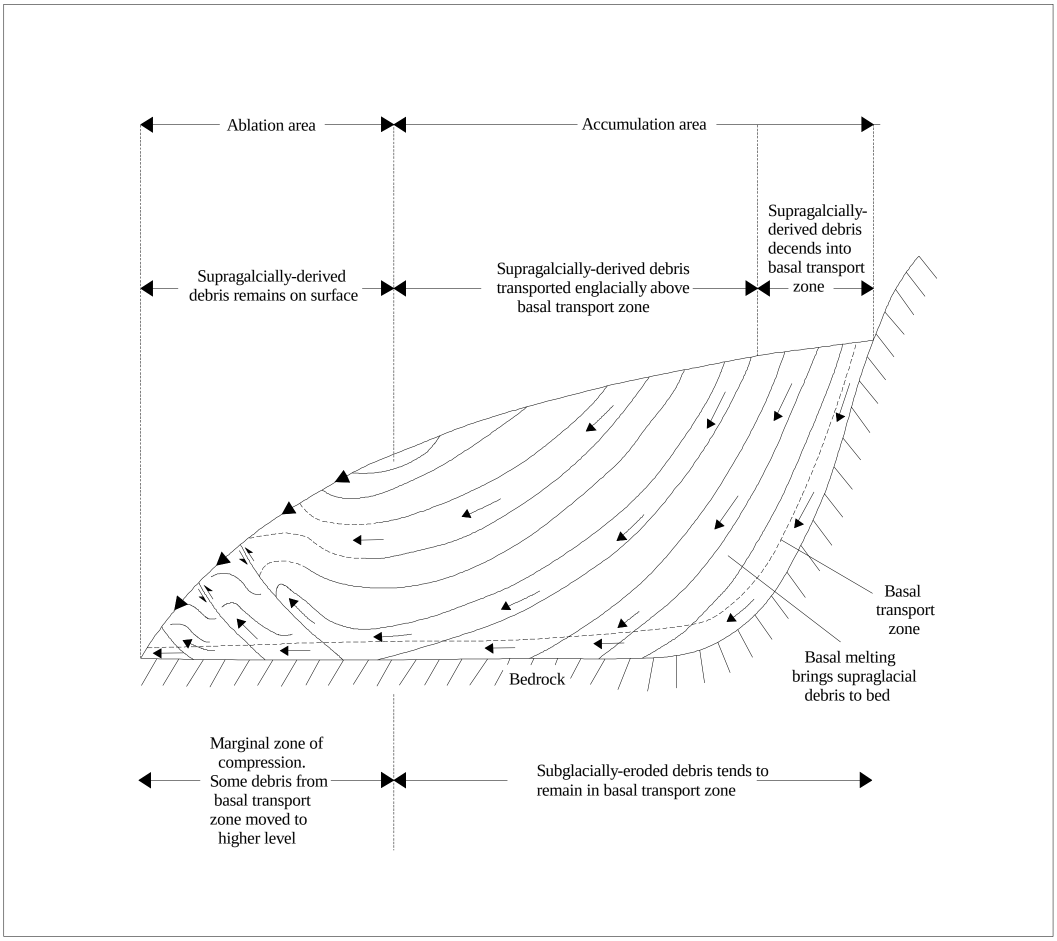

Figure 2.10 The transport pathways of debris through a valley glacier (after Bennett and Glasser, 1996).

and a well developed internal and superficial drainage network (Kirkbride and Spedding, 1996). Englacial transport may take place in the suspension zone of the glacier, which is close to the bed but not in contact with it (Boulton, 1978; Boulton and Eyles, 1979; Eyles, 1983). Debris in the suspension zone does not generally undergo abrasion, however this zone may contain debris that has been elevated from the glacier bed and may therefore reflect shape characteristics and grain size distributions from episodes of active transport (Benn and Evans, 1998).

Active transport involves the movement of debris along the base of the glacier (Summerfield, 1991; Benn and Evans, 1998). Debris may be derived from the bed by subglacial erosion or indirectly from debris which falls onto the glacier surface and makes its way to the bed (Bennett and Glasser, 1996; Kirkbride, 2002). This debris may remain at the base of the glacier until it is deposited, or it may be elevated to the surface by upward flow or by thrusting associated with glacier compression (Bennett and Glasser, 1996). Basal transport alters the shape and size of particles, with grain-size distributions of basally transported debris usually being bimodal or multi-modal (Bennett and Glasser, 1996; Benn and Evans, 1998). These distributions reflect the effects of crushing and abrasion (Haldorsen, 1981). Crushing involves the breakage of two inter-locking grains and abrasion involves two grains sliding past each other, producing fine-grained fragments (Benn and Evans, 1998). Clast shape tends to be compact and blocky in subglacial till (Benn and Ballantyne, 1994) and particles tend to have intermediate clast roundness characteristics and fall within subangular and subrounded classes (Benn and Evans, 1998; Knight, 2004) (Table 2.4). This is indicative of actively transported sediment where supraglacial streams and englacial conduits commonly entrain debris from the ice walls of channels, which becomes rounded with stronger equant forms (Kirkbride, 2002). Fluvial sediments both on and within glaciers, therefore tend to contain clasts superficially resembling traction-zone debris, but with a conspicuous absence of striations (Kirkbride, 2002). There is a tendency for clast roundness to increase downslope within moraines (Matthews and Petch, 1982), which is due to an increasing proportion of actively transported debris in the moraines closer to the former glacier centre-line (Benn and Ballantyne, 1994).

Glacial till which is deposited by the glacier retains its transport characteristics and may be deposited in four ways (Bennett and Glasser, 1998):

1. Lodgement - this occurs when a clast at the glacier bed ceases to move as its frictional resistance exceeds that imposed by the overlying ice.
2. Melt-out - this regards the direct release of debris by melting.
3. Sublimation - this occurs when vaporisation of the ice causes the direct release of debris.
4. Subglacial deformation - this involves the incorporation of sediment into a deforming layer beneath the glacier.

These processes combine to produce six types of till: (1) Lodgement till, (2) subglacial till, (3) deformation till, (4) supraglacial melt-out (moraine) till, (5) flow till and (6) sublimation till (Bennett and Glasser, 1996), which are summarised in Tables 2.6 and 2.7 which further describes gravity flow tills.

Considerable work has been undertaken on the micromorphology of subglacially deformed sediments (Van der Meer, 1987, 1993, 1997b; Menzies and Maltman, 1992; Menzies *et al.*, 1997; Menzies, 1998). These microstructures include discrete shears, kink bands, brecciation, galaxy or turbate structures (orientation of clasts around a core stone), casing of fine-grained material around a clast (halo), pressure shadows, crushed quartz grains, plasma fabrics, deformation of laminations and faults and folds (Lachniet *et al.*, 2001). Rotation structures consist of a nucleus, composed of a grain or a stiff matrix, surrounded by finer grains, which spiral the nucleus (Van der Meer, 1997b). The size of these rotation structures is usually in the order of a few millimetres to 1 cm; therefore detection depends on the availability of an appropriate diamict (Van der Meer, 1997b). The rotation structures indicate that these form under rotational shear during ductile deformation (Hatcher, 1990; Van der Meer, 1993; Menzies *et al.*, 1997), whilst the discrete shear lines indicate brittle deformation, which may be associated with low pore-water pressures and may form after deposition (Lachniet *et al.*, 2001; Menzies and Zaniewski, 2003).

In comparison to the volume of research on subglacial tills, there is relatively little work on the micromorphology of supraglacial tills (Van der Meer, Pers Comm., 2004). However, Dreimanis (1988) suggests that gravitational and flow processes are likely to play an important role in the characteristics of supraglacial tills and these are likely to be less overconsolidated than subglacial sediments.

The identification of Quaternary moraines in southern Africa includes work by Borchert and Sänger (1981), Sänger (1988), Lewis (1996), Lewis and Illgner (2001) and Mills and Grab (2005). It has been suggested that the Western Cape Mountains were characterised by some plateau, cirque and valley glaciers during the Pleistocene, and moraines have been identified in the pediment zone of these Mountains (Borchert and Sänger, 1981; Sänger, 1988). Although clasts within these moraines lack striations, this has been explained by the nature of the material, in which striations would not be preserved (Sänger, 1988). More recently however, it has been suggested that these moraines are in fact erosional remnants of bedrock (Boelhouwers and

Table 2.6 Summary of the main sedimentary characteristics of the main types of till (after Bennett and Glasser, 1996).

	Lodgement till	Subglacial melt-out till	Deformation till	Supraglacial melt-out (moraine) till	Flow till	Sublimation till
Particle shape	Clasts show characteristics typical of basal transport: rounded edges, spherical form, and striated and faceted faces. Large clasts may have a bullet-shaped appearance.	Clasts show characteristics typical of basal transport, being rounded, spherical, striated and faceted. These characteristics are less pronounced than those of lodgement till.	Dominated by the sedimentary characteristics of the sediment which is being deformed, although basal debris may also be present.	Usually dominated by sediment typical of high-level transport, but subglacially transported particles may also be present. The majority of clasts are not normally striated or faceted.	Broad range of characteristics, but dominated by particles which are angular and have a non-spherical form. The majority of clasts are not striated or faceted.	Clasts typical of basal transport, being rounded, spherical, striated and faceted.
Particle size	The particle size distribution is typical of basal debris transport, being either bimodal or multimodal.	The particle size distribution is typical of basal debris transport, being either bimodal or multimodal. Sediment sorting associated with dewatering and sediment flow may be present.	Diverse range of particle sizes reflecting that found in the original sediment. Rafts of the original sediment may be present, causing marked spatial variability.	The size distribution is typically coarse and unimodal. Some size sorting may occur locally where meltwater reworking has occurred.	The size distribution is normally coarse and unimodal, although locally individual flow packages may be well sorted.	The particle size distribution is typical of basal debris transport, being either bimodal or multimodal.
Particle fabric	Lodgement tills have strong particle fabrics in which elongated particles are aligned closely with the direction of local ice flow.	Fabric may be strong in the direction of ice flow, although it may show a greater range of orientation than typical of lodgement till.	Strong particle fabric in the direction of shear; this may not always be parallel to the ice flow direction. High-angle clasts and chaotic patterns of clast orientation are also common.	Clast fabric is unrelated to ice flow, is generally poorly developed and is spatially highly variable.	Variable pebble fabric; individual flow packages may have a strong fabric, reflecting the former palaeoslope down which flow occurred.	Strong in the direction of ice flow, although it may show a greater range in orientation than a typical lodgement till.
Particle packing	Typical dense and well-consolidated sediments.	The sediment may be well packed and consolidated, although this is usually less marked than in a lodgement till.	Densely packed and consolidated.	Poorly consolidated, with a low bulk density.	Poorly consolidated with a low bulk density.	Typically has a low bulk density and is loose and friable.
Particle lithology	Clast lithology is dominated by local rock types.	Clast lithology may show an inverse superposition.	Diverse range of lithologies reflecting that present within the original sediments.	Clast lithology is usually very variable, and may include far-travelled erratics.	Variable, but may include far-travelled erratics.	Clast lithology may show an inverse superposition.
Structure	Massive structureless sediments, with well-developed shear planes and foliation. Sheared or brecciated clasts (smudges) may be present. Boulder clusters or pavements may occur within the sediment, along with evidence for ploughing of clasts.	Usually massive but if it has been subject to flow it may contain folds and flow structures. Crude stratification is sometimes present. The sediment does not show evidence of shearing and overriding during formation.	Fold, thrust and fault structures may be present if the level of shear homogenisation is low. Rafts of undeformed sediment may be included. Smudges (brecciated clasts) may also be present.	Crude bedding may occur but generally it is massive and structureless.	Individual flow packages may sometimes be visible. Crude sorting, basal layers of tractional clasts, may be visible in some flow packages. Sorted sand and silt layers may be common, associated with reworking by meltwater. Individual flow packages may have erosional bases. Small folds may also be present.	The deposit is usually stratified and may preserve englacial fold structures.

Table 2.7 Criteria for the identification of gravity flow till (after Dreimanis, 1988).

Criterion	Gravity flow till
Position and sequence in relation to other glaciogenic sediments	Most commonly it is the uppermost glacial sediment in a non-aquatic facies association. Associated also locally with subglacial tills, where cavities were present under glacier ice, or where the glacier had over-ridden the ice-marginal flow till. May be interbedded or interdigitated with glaciofluvial, glaciolacustricne or glaciomarine sediments, particularly away from its original source at the glacier ice.
Basal contact	Variable; seldom planar over longer distances. The flows may fill shallow channels or depressions. The contact may be either concordant, or erosional, with sole marks parallel to the local direction of sediment flow. Loading structures may be present at the basal contact of waterlain flow till and the underlying soft sediment.
Surface expression, landforms	Associated with most ice marginal landforms. Also as a thin surface layer on many direct glacial landforms.
Thickness	Very variable. Individual flows are usually a few decimetres to metres thick, but the may locally stack up to many metres, particularly in proglacial ice marginal moraines and some lateral moraines.
Structure, folding, faulting	The structure depends upon the type of flow and associated other mass movements, the water content and the position in the flow. Either massive, or displaying a variety of flow structures, such as: (a) overturned folds with flat-lying isoclinical anticlines, (b) slump folds or flow lobes with their base usually sloping downflow, (c) roll-up structures, (d) stretched-out silt and sand clasts (e) intraformationally sheared lenses of sediments incorporated from substratum, with their upper downflow end attenuated, if consisting of fine-grained material, or banana shaped.
Grain size composition	Usually a diamict with polymodal particle size distribution. It is texturally similar to that primary till to which it is related, but with a greater variability in grain size composition, owing to washing out of, or enrichment in, fines or incorporation of soft substratum sediments during the flow. Some particle size redistribution takes place during the flow. The grain size composition depends greatly upon the type of flow, and the position or zone in it. Sorting, inverse or normal grading may develop in some zones of flows, and parts of clasts may sink to the base of flow.
Lithology of clasts and matrix	The lithologic composition is generally the same as that of the source material of flow till – a primary till or glacial debris, plus some substratum material incorporated during the flowage. Material of distant derivation dominates in flow tills derived from supraglacial and englacial debris, but dominance of local material indicates derivation from basal debris. Soft sediment clasts derived from the substratum, or from sediment interbeds in multiple flows, are common.
Clast shapes and their surface marks	If present, soft sediment clasts are either rounded or deformed by shear or dewatering. The more resistant rock clasts are in the same shape as they were in the source material when resedimented by the flowage. Therefore, the relative abundance of glacially abraded subangular to subrounded clasts versus completely angular clasts in flow tills of mountain glaciers will indicate the approximate participation of basal debris versus supraglacial debris in the formation of the flow till. Some rounded water-reworked clasts, without striations, may derive in flow tills from melt-water stream deposits.
Fabrics: macro-fabric (orientation of clasts) or micro-fabric (orientation of particles in the matrix)	Variable and depending greatly upon the type of flow and the position in the flow. It may range from randomly oriented to strong fabric, in thin flow tills. Fabric maxima are either parallel or transverse to the local flow direction, unrelated to glacial movement; the a-b planes are either subparallel to the base of flow, or they dip upflow. Fabric maxima may also differ laterally on short distances.
Consolidation, permeability, density	Primarily normally consolidated and relatively permeable. If clayey, may become over-consolidated owing to postdepositional desiccation. Density lower than in primary tills.

Meiklejohn, 2002). So called evidence for Quaternary glaciation in the Eastern Cape has been provided by Lewis and Illgner (2001), who describe moraine ridges with the presence of striated clasts, which formed when temperatures were 17ºC below present. However, other southern African proxy data fail to confirm such a large drop in palaeo- temperature. In contrast, Shakesby (pers. comm.) suggests that moraine-like deposits occur in close proximity to the Killmore rampart described by Lewis (1994b). More recent work on moraines located in the Lesotho highlands (a portion of this research) has shown that moraine-like features formed as a result of niche/cirque glaciation (Mills and Grab, 2005). These features appear to have formed under a climate where temperatures were between 6ºC and 7ºC colder than at present, which is more in-line with proxy data for South Africa (Heaton *et al.,* 1986; Talma and Vogel, 1992; Partridge *et al.,* 1999; Tyson and Partridge, 2000; Grab and Simpson, 2000; Holmgren *et al.,* 2003).

2.1.6 Fluvial deposits

The possibility that the Sehonghong deposits are of fluvial origin has been addressed in section 1.4, therefore fluvial sedimentation and resulting deposits will be discussed in this section. The floodplain is considered to be the relatively flat area of land that stretches from the banks of the river to the base of the valley walls, which is inundated during seasonal floods (Bridge, 2003; Marriott, 2004). Floodplains are formed by lateral accretion from the formation of bars, by movement of relatively coarse bedload and vertical accretion, which occurs through the deposition of finer material during overbank flow (Marriott, 2004). Most sediment deposition occurs during floods, when flow velocity, bed shear stress and sediment transport rates are large (Bridge, 2004).

The thickness of floodplain sediment, deposited by major seasonal floods, averages between millimetres and decimetres (Wolman and Leopold, 1957; Farrell, 1987; Ten Brinke *et al.,* 1998; Perez-Arlucea and Smith, 1999; Walling, 1999; Bridge, 2003). Alluvium is the predominant contributor to the sediment comprising the floodplain, with minor contributions from aeolian and colluvial sediments (Marriott, 2004). Alluvium is the term used for the sediments that are deposited by flowing water, which takes place both inbank and overbank as velocity decreases locally (Bridge, 2004; Nanson and Gibling, 2004). Alluvial sediment originates from the weathering of rock on land, which is then transported downslope by mass wasting, overland flow and floodplain flow and is deposited in areas where water flow decelerates (Bridge, 2004). The floodplain is formed from a combination of within-channel and overbank deposits (Knighton, 1998) and deposits are mainly sands, silts and clays (Bridge, 2004). The distribution and grain-size characteristics of overbank deposits depends on relative channel position, composition of the suspended load, the topography of the floodplain and vegetation cover (Walling *et al.,* 1993; Knighton, 1998).

A depositional terrace is a former floodplain that has been incised by the river and differs from an active floodplain by being too far above the river channel for overbank flows (Summerfield, 1991; Harden, 2004). These terraces may be metres to kilometres wide, and flank the valley sides or follow the present course of the river for thousands of kilometres (Lowe and Walker, 1997; Harden, 2004). Levees are ridges which lie parallel to the river channel and may rise to a height of several metres above the level of the floodplain (Summerfield, 1991). Relict fluvial terraces are a reflection of changing climatic conditions (Lowe and Walker, 1997). Many of the terraces in contemporary landscapes are Pleistocene and Holocene in age and record changes in river regimes as a result of variations in climate and geomorphic processes during glacial and interglacial periods (Harden, 2004). Relatively low incision rates occur during colder periods as a result of high stream sediment loads, therefore terraces form during warmer periods, when sediment availability is reduced and higher incision rates are possible (Lowe and Walker, 1997; Hanson *et al.,* 2006).

Clasts within fluvial deposits tend to be imbricated and point downstream (Harden, 2004) (Table 2.3). Orientations parallel to the current have been described by Krumbein (1940, 1942) and Schlee (1957). Grains which are not spherical tend to be oriented in different ways during transport on the bed immediately prior to deposition (Bridge, 2003). Ellipsoidal or rod-shaped particles tend to be oriented with their long-axes parallel to flow on plane beds and disk and tabular-shaped particles tend to dip upstream (Bridge, 2003). Upstream imbrication occurs as a result of flow movement (Ward, 2004) and is usually indicative of gravel deposited from traction (Ballantyne and Harris, 1994).

Clast roundness in fluvial deposits occurs as a result of abrasion (Lewin and Brewer, 2002) and collisions between grains as they are transported, particularly near the river bed (Bridge, 2003). These collisions induce grinding, crushing, breakage, impact and rubbing, which chip and fracture particles (Kuenen, 1956; Schumm and Stevens, 1973). The potential for each mechanism varies according to particle lithology, potential fracture surfaces and the extent to which clasts have been weathered (Lewin and Brewer, 2002). Clast rounding initially tends to occur rapidly, but then slows down, due to lower abrasion rates of sand grains (Bridge, 2003). Clast shape in river conglomerates have been described by Howard (1992), where river sediments contain between 46% and 53% spheres, 26% to 33% discs (platy), 16% to 17% rods (elongate) and 4% to 5% bladed clasts. Prolate (rod-shaped/elongate) clasts are known to be characteristic of river gravels (Howard, 1992). Subrounded clasts are indicative of fluvial transport (McEwen and Matthews, 1998) (Table 2.4).

Floodplains are normally subject to pedogenesis, and thus soil horizons are usually present in alluvium (McCarthy and Plint, 1999; Bridge, 2004). This enables the use of micromorphology in identifying palaeosols through specific micromorphological features which reflect specific pedological features operating under particular environmental conditions (McCarthy and Plint, 1999). These features may include illuviated clay, precipitation of soluble salts and pedoturbation (Netterberg, 1980; Kemp, 1985, 1989; McCarthy and Plint, 1999).

Considerable work has been carried out on the pattern of river terraces within the Vaal and Orange River drainage basins (Rowntree, 2000), and it has been suggested that drainage adjustment has been a factor of climate change and tectonic activity (Moon and Partridge, 1993). A significant proportion of work has been undertaken on fluvial terraces in the Eastern Cape (e.g. Dollar and Rowntree, 1995; Hattingh, 1996; Lewis and Illgner, 1998; Lewis, 2005). Work on river terraces in the Sundays River valley have been described as being of Pliocene age (Hattingh, 1996), whilst Butzer and Helgren (1972) have investigated alluvial deposits near Loerie, within the Gamtoos River catchment and have suggested that the environmental balance has not been stable during Holocene times. Terraces near Grahamstown have been ascribed to deposits accumulating from bedload deposition and having exceeded the rate of pedogenesis (Lewis and Illgner, 1998). Four climatic phases have been described in the Eastern Cape Drakensberg during the LGM, where considerable climatic fluctuations took place (Coetzee, 1967), however these are not evidenced in the fluvial deposits described by Lewis (2005). During the arid glacial periods, the development of colluvium was increased, which acted as an important source of sediment for the rivers (Rowntree, 2000).

2.2 PROBLEMS ASSOCIATED WITH THE IDENTIFICATION OF A PROCESS ORIGIN FOR THE DEPOSITS

2.2.1 Similarities between deposits

The problem in determining a process origin for the deposits is that all the processes considered have common characteristics. Debris slides, avalanches and flows are not always distinguishable from each other (Selby, 1993). The difference between these features is based upon the degree of soil deformation and the water content of the sliding mass (Selby, 1993). Debris avalanches may begin as slides, consisting of large masses of rock which then rapidly break up to form flows as the material is pulverised in transit and if sufficient water is available (Summerfield, 1991; Selby, 1993).

Slope failure in mountain environments is both a significant paraglacial erosion process and an important delivery mechanism, by which debris is transferred from valley and cirque walls to glaciers (Benn and Evans, 1998; Arsenault and Meigs, 2005). The term paraglacial is defined as non-glacial processes that are directly conditioned by glaciation (Church and Ryder, 1972). If water released during ice-melt is not easily displaced, then glacial debris may become liquefied and flow (Whiteman, 2002). Glacier ice typically steepens towards its margins, which provides locations for a wide variety of mass movements, of which flow is the dominant process (Whiteman, 2002). Although flow processes may cause resedimentation, the debris is accumulated by glacier activity and transported and deposited through glacial processes, and it is thus unlikely that debris flow mechanisms alone can transport the same debris to the same place, without the assistance of glacial processes (Whiteman, 2002).

It has been reported that rock glaciers may be derived from lateral moraines, (e.g. Messerli and Zurbuchen, 1968; Vere and Matthews, 1985). Yet to compound the problem, it has been suggested that a lateral moraine (in its latero-terminal section) may have contained remnants of glacier ice, which in turn became isolated by retreat of the glacier snout (Vere and Matthews, 1985). Sedimentological analyses suggest that subglacial sources account for a proportion of the rock glacier material, which in turn suggests that rock glacier composition may be viewed as a sediment continuum, reflecting both supraglacial and subglacial sources, depending on local conditions (Vere and Matthews, 1985). In addition, features in the Canadian Arctic have been referred to as rock glacierised moraines (Dyke *et al.*, 1982; Dyke, 1990; Evans, 1993). It is suggested that such features form when ice-cored moraines develop into rock glaciers, as the protected ice core begins to flow internally as a result of the stress that the debris imposes (Messerli and Zurbuchen, 1968; Vere and Matthews, 1985). It has also been suggested that rock glaciers may form as a result of landsliding or rocksliding (Vick, 1987; Whalley and Martin, 1992). This may occur when material falls onto a glacier and modifies its behaviour, or when the fallen debris produces a feature that morphologically resembles a rock glacier (Whalley and Martin, 1992; Whalley and Azizi, 2003).

Whilst landsliding may not be responsible for the rock glaciers in their present form, they may have been the primary mechanism in generating the debris necessary for the initiation of creep in frozen moraine deposits (Vick, 1987; Whalley and Martin, 1992). It may be difficult to distinguish between large boulder deposits and rock glaciers, given their similarity in size, thickness and microrelief (Shroder, 1987). These morphological similarities suggest a genetic continuum between certain kinds of rock glaciers and some landslide-generated boulder deposits (Shroder, 1987). Pronival ramparts have also been described as embryonic talus rock glaciers, based on the similarity between pronival ramparts and small but active talus rock glaciers (Barsch, 1996). The difference between the two features may be somewhat arbitrary (Ballantyne and Kirkbride, 1986).

There is also considerable controversy concerning the origin of ice within rock glaciers. Some authors claim a non-glacial (periglacial) origin for rock glaciers, whilst others argue that many rock glaciers contain a significant core of glacial ice (Humlum, 2000). A number of researchers suggest that the deforming ice within a rock glacier consists of glacier ice (Potter, 1972; Whalley and Martin, 1992; Whalley *et al.*, 1995; Clark *et al.*, 1996; Humlum, 1996), whilst others favour a non-glacial origin (i.e. permafrost) for the ice (Barsch, 1988, 1996; Haeberli, 1985, 1989;

Haeberli and Vonder Mühll, 1996). The presence of ice-cored moraines, which occur in proximity to rock glaciers and even grade into rock glaciers has been described for sites in western Greenland (Humlum, 2000). Rock glaciers have been described as transitional forms because glacial or periglacial processes can alter the landscape prior to rock glacier formation (Giardino and Vitek, 1988; Humlum, 2000). They may form when a glacier becomes covered in debris and transforms into a rock glacier or alternatively, the more bouldery section of a moraine may be the remains of a re-worked rock glacier (Giardino and Vitek, 1988). It is therefore suggested that rock glaciers are part of a spatial and temporal landscape continuum (Figure 2.11), and are a transitional form, produced by a particular process of formation from an initial stage, to a deposit which would no longer suite the definition of a rock glacier (Giardino and Vitek, 1988).

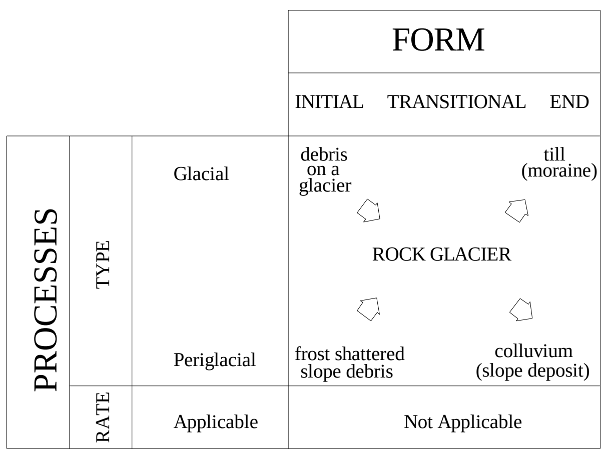

Figure 2.11 The concept of an alpine landscape continuum (after Giardino and Vitek, 1987).

Difficulties sometimes arise in discriminating between pronival ramparts and moraines, particularly when glaciers are likely to have been very small (Harris, 1986; Shakesby and Matthews, 1993) and as a result of the close resemblance between valley-side ramparts and lateral moraine fragments (Washburn, 1979). Until recently, most accounts of pronival ramparts concerned fossil features, which led to the misidentification of true ramparts, questionable examples being claimed (Shakesby, 1997), and subsequent reinterpretations being made (Ballantyne, 1989a; Shakesby and Matthews, 1993; Ballantyne and Harris, 1994; Gordon and Ballantyne, 2006). Lack of data on the characteristics of actively forming pronival ramparts has been a particular problem in distinguishing true ramparts from moraines, landslides and rock glaciers

(Curry *et al.,* 2001). There has been a considerable amount of work undertaken by British workers concerning the identification of diagnostic characteristics that can be used to distinguish fossil ramparts formed at the foot of large snowbeds from small glacial moraines (Ellis-Gruffydd, 1977; Ballantyne and Kirkbride, 1986; Shakesby and Matthews, 1993) (Table 2.8).

Four characteristics have been proposed to distinguish pronival ramparts from cirque moraines in the Brecon Beacons (Lewis, 1966). Firstly it is suggested that the angle of elevation would be lower for cirque moraines than for pronival ramparts, secondly, that a small ridge to backwall distance would occur, thirdly, ridge boulders dip away from the backwall for a pronival rampart, and fourthly, pronival ramparts tend to be parallel to the backwall and are therefore often linear (Lewis, 1996). In contrast, Watson (1966) suggested that deposits could be distinguished based on the lack of glacial erosional features. A small ridge to backwall distance is also regarded as diagnostic of pronival ramparts (Unwin, 1975), as is restricted potential snow accumulation depth, an absence of striated clasts, angular clasts, and the backwall and ridge having the same lithology (Unwin, 1975). Ballantyne and Kirkbride (1986) suggest that pronival ramparts, normally located at the foot of talus slopes, rarely exceed 300 m in length, normally consist of a single ridge or crest and have steep distal slopes. In addition, rampart size increases with distance from the talus foot, and usually consist of openwork deposits with variable infill of fines and clasts, which are more angular and slabbier than on moraines (Ballantyne and Kirkbride, 1986). Restricted potential snow depth accumulation is also regarded as diagnostic of pronival rampart accumulation (Shakesby and Matthews, 1993). For instance, in determining the origin of a deposit at Fan Hir in the Brecon Beacons, it was concluded that the amount of rockwall retreat was relatively high, and which would give a very low snow patch surface angle for debris transport (Shakesby and Matthews, 1993).

Ballantyne and Benn (1994a) provide a simple rule to distinguish between pronival ramparts and moraines, suggesting that ridges located at distances of ca. >30 m to 70 m from a talus slope cannot be true ramparts. It is suggested that beyond this distance, the snowbed becomes sufficiently thick and dense to permit movement, in which case the snowbed has to be regarded as a small glacier (Ballantyne and Benn, 1994a)

Table 2.8 Suggested 'diagnostic' criteria indicating a pronival rampart rather than a moraine origin according to various authors (after Shakesby, 1997).

Rampart Criteria	Lewis (1966)	Watson (1966)	Unwin (1975)	Ballantyne and Kirkbride (1986)	Shakesby and Matthews (1993)	Ballantyne and Benn (1994a)
Site						
• Absence of glacial erosional forms		✔				
• Talus-foot location				✔		
• Large ridge to backwall summit inclination	✔					
• Small ridge to backwall distance	✔		✔			
• Ridge crest to talus-foot distance < *c.* 30-70 m						✔
• Restricted potential snow accumulation depth		✔	✔		✔	✔
Morphology and size						
• Linear plan form	✔					
• Asymmetrical cross-profile			✔ [a]	✔		
• Symmetrical cross-profile			✔ [a]			
• Length < 300 m				✔		
• Single ridge				✔		
• Ridge size increases with distance from talus foot				✔		
Sedimentology						
• Backwall and ridge same lithology			✔	✔		
• Openwork fabric with/without infilling fines				✔		
• Absence of striated clasts			✔		✔	
• Angular clasts			✔	✔ [b]	✔	
• Clasts dip away from backwall	✔					

Notes:
[a] Both alternatives are discussed as possibilities.
[b] 'Slabbiness' is regarded as an additional clast attribute.

(Figure 2.12). This model provides a comparatively simple means of distinguishing relict scarp-foot ramparts from moraines on the basis of a single, easily obtained measurement (Shakesby, 1997). The maximum variable depth at which firn to ice transformation occurs was suggested to be 30 m or 60 m for a temperate glacier (Watson, 1966), with the 30 m value being subsequently accepted by Gray (1982) and Shakesby and Matthews (1993).

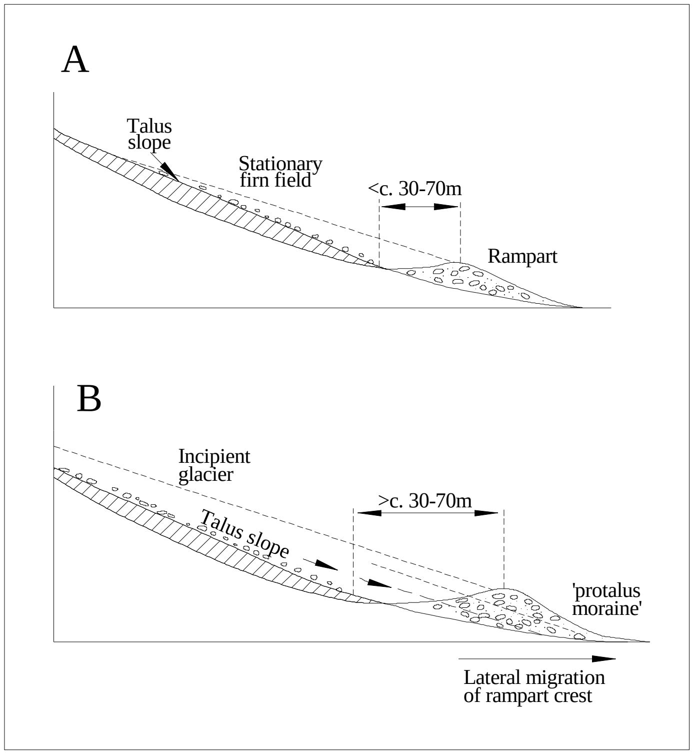

Figure 2.12 Effect of snowbed/firn field thickening on the development of a rampart located close to the junction between the talus foot and the valley floor, according to Ballantyne and Benn (1994a) (after Shakesby, 1997).

The effect of snow-push processes in pronival rampart formation has also recently been proposed (Shakesby *et al.*, 1999). It is suggested that although the pronival ramparts receive much of their sediment from avalanching, subnival processes also appear to take place as a result of the presence of subangular and subrounded clasts, implying snow-push mechanisms (Shakesby *et al.*, 1999). It is therefore necessary to establish whether active snowbeds can produce landforms with the scale and sedimentological characteristics of push moraines (Shakesby *et al.*, 1999).

Diagnostic criteria for distinguishing pronival ramparts from landslides and rock glaciers have also been used, given that ramparts may easily be confused with protalus rock glaciers, as both landforms occupy similar talus-foot locations and are composed of rockwall debris (Blagborough and Breed, 1967; Washburn, 1979). It has also been suggested that some talus-foot rock glaciers may evolve from pronival ramparts (Corte, 1976). Protalus rock glaciers can be distinguished from ramparts on the basis that protalus rock glaciers have a wrinkled appearance as a result of internal flow structures (Smith, 1973; Washburn, 1979). Further typical protalus rock glacier characteristics include crenulated outer margins (Smith, 1973; Sissons, 1980a) and a much greater width than ramparts (Ballantyne and Kirkbride, 1986). However, it is suggested that such diagnostic criteria for distinguishing between pronival ramparts, rock glaciers and landslides is inadequate as the diagnostic criteria is not exclusive to each individual feature (Shakesby *et al.,* 1987). Recent work highlighting the erroneous identification of landforms, describes a possible landslide origin for the Nant Ffrancon 'pronival rampart' in Snowdonia (Curry *et al.*, 2001). This landslide origin is based on the presence of much larger clasts than those usually found in pronival ramparts, the distribution of boulders being restricted to the crestline and backing depression, the relative thickness of the deposit beneath the highest rockwall source area, the resemblance of the slope directly above the deposit to a major rock slope failure, and finally the joint pattern favouring rockwall instability (Curry *et al.*, 2001).

As a result of the fact that various talus-derived landforms exist in close proximity to one another, linkages between these landforms have been suggested. Two opposing views exist (Figures 2.13 and 2.14); the first suggests that a morphological continuum exists, where ramparts, rock glaciers and moraines are separate and independently produced (Johnson, 1983; Shakesby *et al.*, 1987, 1989) (Figure 2.13). The second view considers a developmental continuum, where the talus sheet can be modified progressively from rampart to rock glacier or moraine (Corte, 1976; Ballantyne and Kirkbride, 1986) (Figure 2.14).

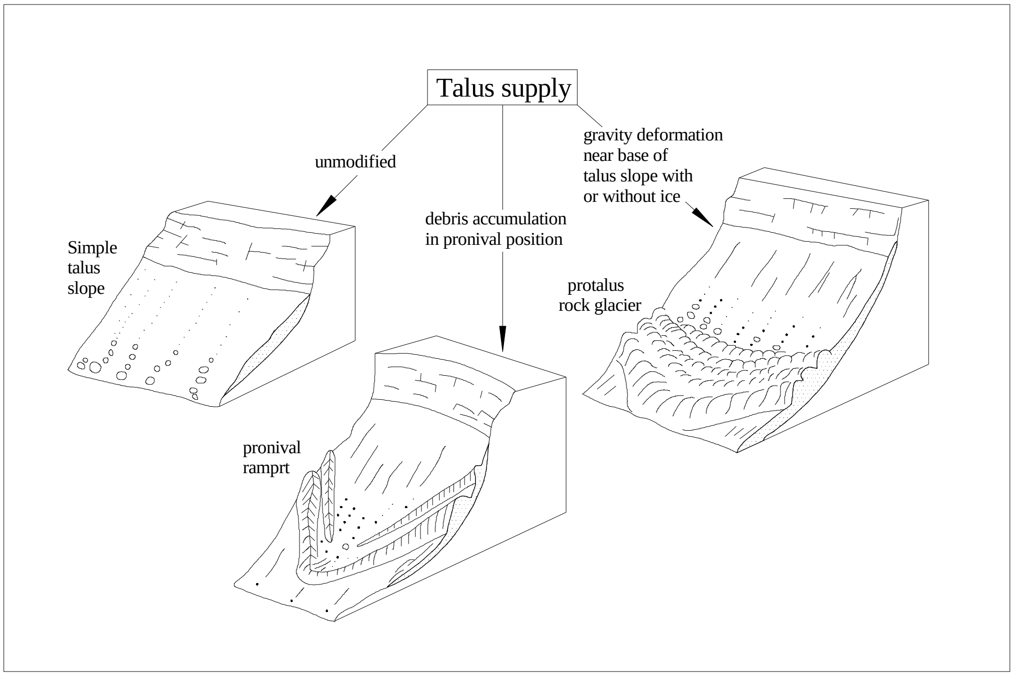

Figure 2.13 Pronival rampart as part of a nondevelopmental morphological continuum of talus-derived landforms (shown in fossil form). Based on Shakesby *et al.* (1987) (after Shakesby, 1997).

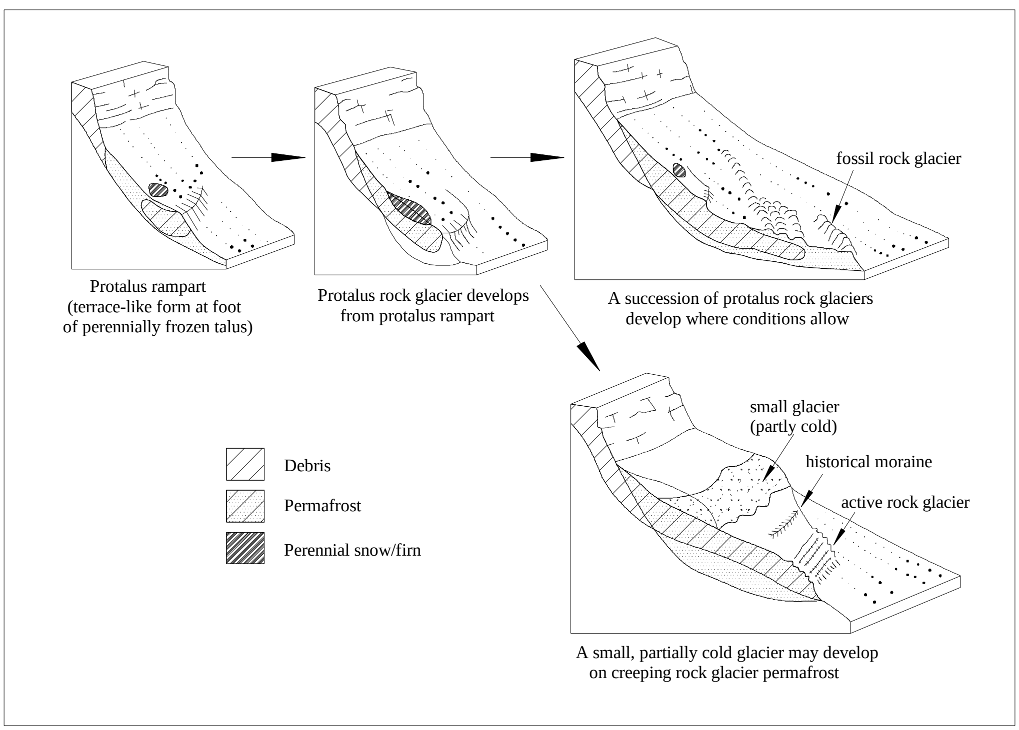

Figure 2.14 Pronival ramparts viewed as part of a linear developmental continuum with rock glacier and glacier formation. Modified from Haeberli (1985) (after Shakesby, 1997).

2.2.2 Problems associated with clast orientation and fabric eigenvalues

Arguments have been presented by Bennett *et al.* (1999), who suggest that clast fabric determinations are of little value in the interpretation of glacigenic diamicts. A similar argument has more recently been presented by Millar (2005), who describes the high variability of clast fabrics within a solifluction landform and suggests that the results cast serious doubt on the utility of fabric analysis for identifying individual processes that occur in the placement of sediments. In contrast to work undertaken by Warren and Croot (1994), Carr and Rose (2003) found few cases where the preferred orientation of grains is parallel to the direction of ice movement. However, Carr and Rose (2003) suggest that the basic assumption in the use of fabrics is that they indicate the orientation of the stress field.

Fabric generation appears to be partially due to clast properties (Millar, 2005) and it has recently been established that clast size can have an effect on fabric strength, and that the variation in fabric strength, relative to clast size can have a significant influence on the interpretation of the depositional history of the sediment (Kjær and Krüger, 1998). When a wide range of clast sizes is used for till-fabric analysis, as in the case of this research, caution should be applied in using eigenvalues as a discriminant tool to interpret the genesis of diamicts (Kjær and Krüger, 1998). It is further suggested that the positive correlation between clast size and fabric strength reflects differences in orientation stability during deposition (Kjær and Krüger, 1998).

Clast shape is also believed to have an effect on fabric development as suggested by Drake (1974), who proposes that pebbles near the common Zingg shape boundary intersection have the appropriate shape to attain a transverse orientation and roll about their a-axis more freely than elongate and flattened shapes. Glenn *et al.* (1957) suggested that prolate pebbles should produce transverse fabrics as these grains tend to roll along their axes, which was further reinforced by Boulton (1970). However, Drake (1974) found that prolate pebbles generally have an a-axis orientation parallel to ice flow, which somewhat contradicts the previous findings. Rod a-axes are strongly aligned in the ice-flow direction and blades less so (Drake, 1974), which is once again contradicted by Boulton (1970), who suggests that oblate (blade-shaped) grains are more likely to remain parallel to the stress-field orientation, whereas prolate (rod shaped) grains are more likely to roll along their a-axes, resulting in a transverse fabric. Work undertaken by Carr and Rose (2003) on thin section microstructures has revealed that the presence of rotation structures is an indication that particles within the samples are rotating in line with Jeffery/Taylor rotation. The particles initially align themselves parallel to the stress field orientation; however over time there is a tendency for grains to align themselves transverse to the stress field orientation (Jeffery, 1922; Taylor, 1923) (Figure 2.15). Thus, samples with particles aligned parallel to ice flow direction would have been affected by a much lower stress than those where grains are aligned transverse to ice flow direction, as it takes a higher applied total stress for particles to move through Taylor rotation (Carr and Rose, 2003). Transverse orientations therefore indicate compressional stress and parallel orientations indicate tensional stress (Boulton, 1970; Carr and Rose, 2003).

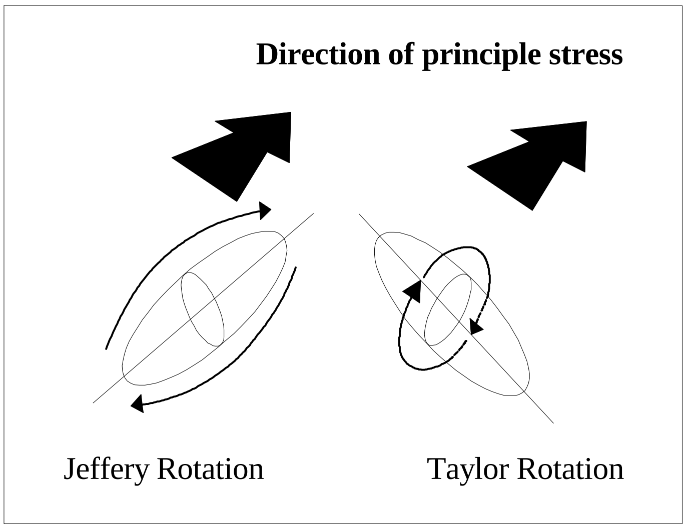

Figure 2.15 The response of individual grains to an applied stress (after Carr and Rose, 2003).

Doubt has recently been cast over whether fabric eigenvalues are truly representative of the facies under investigation. Benn and Ringrose (2001) suggest that there is uncertainty in the way that fabric eigenvalues are subject to statistical variance about the true population values, which may limit the accuracy of results. Benn and Ringrose (2001) further suggest that the variation between samples, which they experienced whilst trying to differentiate till facies from fabric data, may be due to statistical variance, rather than spatial variations in sediment properties associated with physical processes or conditions. Caution should be applied when using fabric eigenvalue plots for interpreting deposits of unknown origin, particularly when data points plot close to the boundary of fabric shape envelopes (Benn and Ringrose, 2001).

In terms of clast orientation within the various deposits, caution must be exercised when determining the implications of clast shape, given that some authors appear to be in disagreement as to which shapes produce which preferred orientations. However, based on the idea that clast orientations represent stress, it can be concluded that tensional stress causes parallel orientations, whilst compressional stress causes the transverse orientations.

2.2.3 Problems associated with particle shape

Clast morphology reflects both the physical properties of the source material and the subsequent modification by erosion, weathering and transport (Benn and Ballantyne, 1994), therefore clasts deposited in different environments commonly exhibit contrasting morphologies (Benn, 2004a). Clast shape is dependant on both process and lithology (Benn and Evans, 1998). In mountain environments for example, rocks such as granite and gabbro tend to have compact, blocky shapes as a result of active transport, in contrast with the more elongate and slabby shapes of periglacially weathered clasts of similar lithologies (Vere and Benn, 1989; Benn and Ballantyne, 1994). Roundness is affected in opposite ways by abrasion, which increases edge-rounding, and fracture, which creates new sharp edges (Benn and Evans, 1998). The balance between these two processes means that angular and well rounded forms tend to be rare in actively transported debris, and most clasts have intermediate roundness characteristics (Benn and Evans, 1998). Lithology appears to play a large part in determining the roundness of material as it exerts a strong influence on the processes which may take place (Hall *et al.*, 2002). Only short distances of active transport are necessary for significant edge-rounding to occur (Drake, 1972; Humlum, 1985; Matthews, 1987), however when other process mechanisms are considered, for example debris flows and debris avalanches, distance travelled will be a major factor in clast rounding (Crandell, 1969; de Scally and Owens, 2005). It is therefore important to consider lithology and distance travelled when taking into account particle shape and making comparisons to various process mechanisms. The basalt found in the high Drakensberg is highly weathered and distance travelled would be no more than a few hundred metres. It is suggested that basalt will weather to rounded clasts particularly in cold climates, where rock temperatures are high and conditions are wet (Sarracino and Prasad, 1988). This means that prior to movement, the basalt may already be rounded as a result of *in situ* weathering (Sumner, 1995).

It is generally agreed that the morphology of clasts containing angular edges is indicative of frost action in the fragmentation of clasts (DeWolf, 1988; Hanvey and Lewis, 1991; Lowe and Walker, 1997; Prick, 2004), and that angular, coarse debris reflects freeze-thaw (Hall *et al.,* 2002). High Mountain environments or high latitude environments usually contain large amounts of angular material, however whether this is exclusively the case has yet to be shown. Recently, it has been suggested that mechanically weathered material may also take on rounded forms (Hall *et al.,* 2002). Lithology may play an important role in determining the shape of a particle. Ballantyne and Harris (1994) describe a rounded tor in the Cairngorm Mountains which has resulted from weathering in a cold environment. A further example of the lithological effects on the shape of particles in cold environments is presented by Hall (1997), who describes both angular and rounded sandstone in Antarctica, which is frost-weathered debris. Although the reasoning for the occurrence of angular clasts within solifluction deposits is no longer accepted, the presence of angular clasts in these deposits cannot be dismissed. Although comparisons are made with various process mechanisms, the roundness of clasts alone will not be used to determine their origin.

2.3 COMPARISONS OF THE TIMING OF THE LGM IN SOUTHERN HEMISPHERE AND AFRICAN LOCATIONS

2.3.1 Introduction

It has been suggested that the sedimentary features may be glacial moraines, as presented in Chapter 1, and these are most likely to have formed during the LGM, when temperatures were significantly colder than at present (Talma *et al.,* 1974; Heaton *et al.,* 1986; Stute and Talma, 1997; Holmgren *et al.,* 2003). The timing of the LGM will therefore be considered for a variety of regions, in order to determine a comparative chronology of glaciation, deglaciation and temperature depreciations. Ethiopia is considered to be an important analogue in this context, given the controversy regarding Quaternary glaciation (Umer *et al.,* 2004; Osmaston and Harrison, 2005; Osmaston *et al.,* 2005), which is similar to that concerning the

Drakensberg. In contrast, evidence from Mount Kenya and Kilimanjaro provide a more reliable chronological history of the timing and climate at the time of the LGM. It is also considered important to provide the timing of the LGM for other countries in the Southern Hemisphere, and in particular those at similar latitudes. Thus, Australia, Tasmania, New Zealand, Chile and Argentina are described, based on their detailed chronological histories. Work has previously focussed on trying to link past climates in the Southern Hemisphere with those of the Northern Hemisphere, especially in New Zealand (e.g. Denton and Hendy, 1994; Ivy-Ochs *et al.*, 1999; Turney *et al.*, 2003). However, it has become increasingly apparent that the Southern Hemisphere signal is dominated by the southern Ocean, Antarctic and tropical signals, rather than the teleconnections of Northern Hemisphere mid/high latitude climate events (Pepper *et al.,* 2004; Shulmeister *et al.*, 2005).

2.3.2 Africa

Although several regions of Africa are known to have been glaciated during the LGM, such glaciation remains an uncertainty for several other regions on the continent, such as the Drakensberg (Figure 2.16). The African mountains have been subject to investigations regarding glaciation for more than a century, however the history of glaciation remains sketchy given the lack of absolute dating (Shanahan and Zreda, 2000; Osmaston and Harrison, 2005). The difficulty in dating deposits is primarily due to the scarcity of datable material and the limited time range of applicable methods (Shanahan and Zreda, 2000). Only high tropical mountains over 4000m a.s.l. were glaciated in Africa during the Quaternary (Osmaston, *et al.*, 2005). East Africa hosts the highest mountains on the continent and traces of former glaciations are known from Mount Kenya, Kilimanjaro and Rwenzori (Rosqvist, 1990).

2.3.2.1 Ethiopia

Mountains in Ethiopia reach altitudes of over 4000 m a.s.l. and it appears that at least three out of the ten peaks were glaciated during the LGM, however evidence is contradictory and little work is substantiated (Umer *et al.*, 2004; Osmaston and Harrison, 2005; Osmaston *et al.,* 2005). The highest peaks reach altitudes between 4353 m a.s.l. and 4543 m a.s.l. and occur in the Simen Mountains (Umer *et al.,* 2004; Osmaston and Harrison, 2005; Osmaston *et al.*, 2005). These are also the driest of the mountains (Umer *et al.*, 2004). There is evidence of small cirques, moraines and

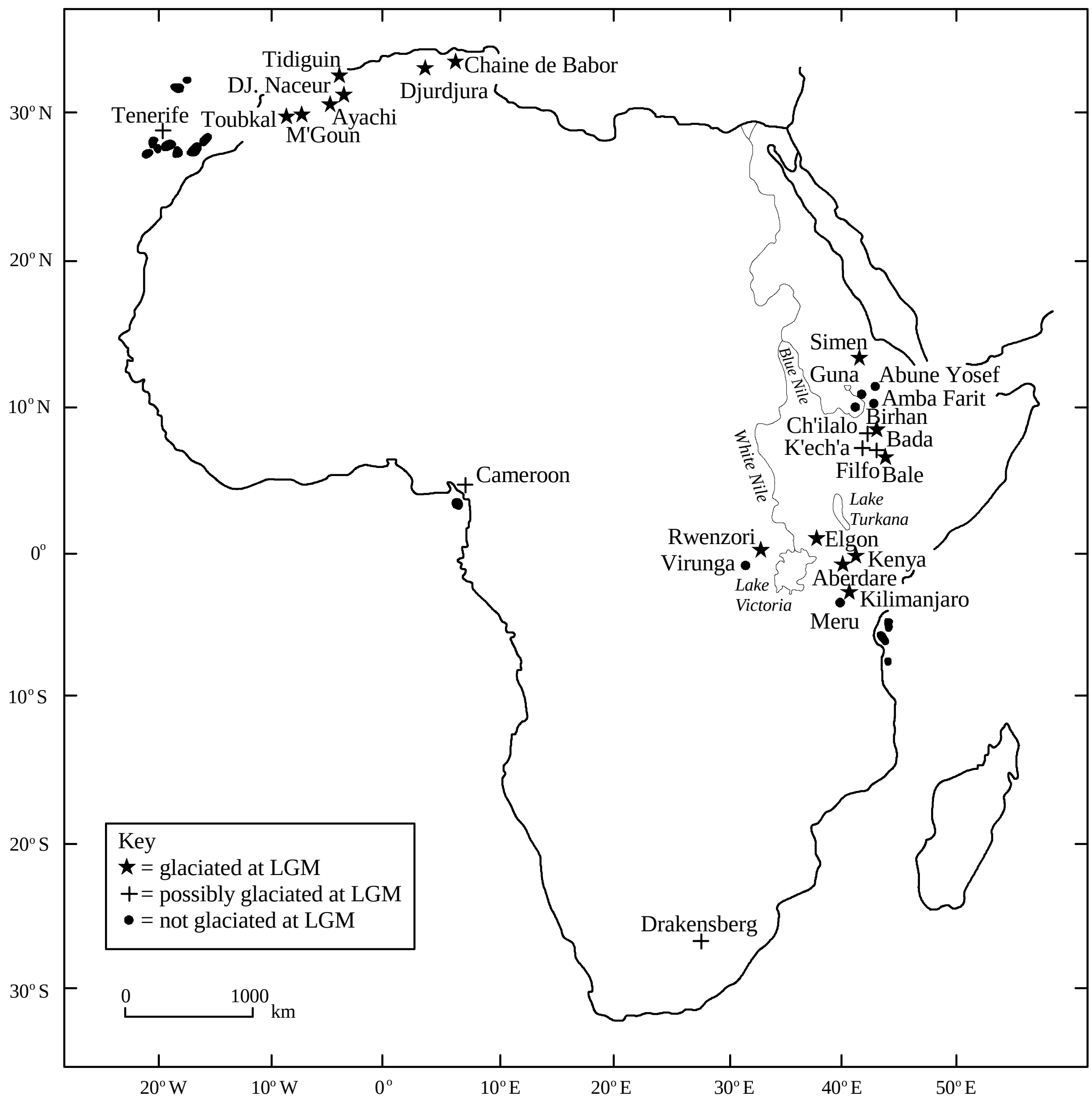

Figure 2.16 The location of sites in Africa with records of former glaciation, and generally assumed to date to the Last Glacial Maximum (after Osmaston and Harrison, 2005).

glacial striations, suggesting the former presence of small glaciers (Osmaston *et al.,* 2005), whilst moraines have been mapped down to 3760 m a.s.l. by Hastenrath (1974) and Hurni (1989). The extent of glaciation in Ethiopia was limited to approximately12 glaciers with a total surface area of approximately 13 km^2 (Umer *et al.,* 2004; Osmaston and Harrison, 2005; Osmaston *et al.,* 2005). The former ELAs in the Simen Mountains were approximately 4100 m a.s.l. on the northern side and 4400 m a.s.l. on the southern side of the mountains (Umer *et al.,* 2004; Osmaston *et al.,* 2005). Evidence of intense periglacial activity below the glaciers suggest that the climate may have been dry and cold at the time the glaciers were present (Osmaston and Harrison, 2005).

The Bada Mountains of Ethiopia have a moister climate and large prominent terminal moraines are present between 3200 m a.s.l. and 3700 m a.s.l., which are believed to have formed by a series of valley glaciers (Potter, 1976; Street, 1979; Umer *et al.,* 2004; Osmaston *et al.,* 2005). Estimated ELAs are 3700 m a.s.l. on the eastern side and 3900 m a.s.l. on the western side of the mountains (Osmaston and Harrison, 2005).

In the Bale Mountains, peaks reach a maximum of 4400 m a.s.l. and it is suggested that these mountains are considerably wetter than the mountains to the north (Umer *et al.,* 2004; Osmaston and Harrison, 2005; Osmaston *et al.,* 2005). This indicates that the area may have been extensively glaciated and Messerli *et al.* (1977) suggest that the high plateau was completely covered by an ice cap of 600 km^2. However, it has since been proposed that this was an overestimation and that the extent of glaciation on the plateau could have been approximately 70 km^2 (Osmaston *et al.,* 2005). The ELA of the former glaciated ice cap and the valley glaciers which extended from it has been estimated around 3700 m a.s.l. (Messerli *et al.,* 1977; Messerli and Winiger, 1992), however it is suggested that the ELA would have been about 4070 m a.s.l. on the southern slope and 4230 m a.s.l. on the other slopes (Osmaston *et al.,* 2005). In the north-east valleys, where valley glaciers were present, an ELA between 3750 m a.s.l. and 3900 m a.s.l. has been proposed (Osmaston *et al.,* 2005). Evidence of very cold but dry conditions around the development of the ice cap comes from boulder slopes thought to be of periglacial origin (Osmaston and Harrison, 2005; Osmaston *et al.,* 2005). Radiocarbon ages indicate that the various sites were free from ice by 14 000

^{14}C yrs BP to 7 500 ^{14}C yrs BP, based on the dating of a core from Garba Gurcha lake, a core from a bog in the Danka valley and a core from a swamp near Badegesa Hill (Osmaston *et al.,* 2005).

2.3.2.2 East Africa

Glaciers exist at present on the three highest mountains of East Africa (Kilimanjaro, Mount Kenya and Rwenzori), which reach altitudes over 5000 m a.s.l. (Hastenrath, 1984; Rosqvist, 1990; Kaser and Osmaston, 2002; Osmaston, 2004; Osmaston and Harrison, 2005). The contemporary glaciers are however small and disappearing rapidly (Hastenrath and Greischar, 1997; Alverson *et al.,* 2001). Mount Elgon and Aberdare have no current glaciers however probable LGM moraines exist (Osmaston, 2004). This literature review will focus on the more pronounced glaciations of Mount Kenya and Kilimanjaro.

2.3.2.2.1 Mount Kenya

Mount Kenya represents one of the principal high mountains in East Africa and reaches an altitude of 5199 m a.s.l. (Vortisch *et al.,* 1987; Mahaney, 2004). Although contemporary temperatures are not precisely known for Mount Kenya, the MAAT at 3000 m a.s.l. is approximately 10°C, whilst at 4000 m a.s.l. it is approximately 3ºC (Mahaney, 1990, 2004). It is thought that temperature depressions of between 5ºC and 9°C occurred during periods of Pleistocene glaciation (Rosqvist, 1990) and averaged approximately 7°C (Coetzee, 1967; Mahaney, 2004). Glacial deposits are present from 4200 m a.s.l. to below 2900 m a.s.l. on Mount Kenya (Shanahan and Zreda, 2000), whilst end moraines deposited during the LGM are located as low as 3800 m a.s.l. (Mahaney, 1989). ELAs for the LGM were between approximately 3660 m a.s.l. and 3990 m a.s.l., based on the assumption that they lie at the mid-altitudes of the lateral moraines (Mahaney, 1990). However, Osmaston and Harrison (2005) suggest that more realistic estimates lie between 4100 m a.s.l. and 4500 m a.s.l.

Seven stages of glaciation have been identified on Mount Kenya (Mahaney, 1990), however only the ones relating the LGM will be discussed here. Two stages represent the LGM; the Liki II and Liki III glaciations (Osmaston, 2004) (Table 2.9). Radiocarbon ages from bog-bottom sediments on Liki II moraine surfaces yield

Table 2.9 The different glaciations for Mount Kenya summarised from Mahaney (1987; 2004), Mahaney *et al.* (1991) and Shanahan and Zreda (2000).

Glaciations	Absolute dating chronology	Cosmogenic dating chronology
Liki II	25 000 – 15 000 yrs BP	28 000 ± 3 000 yrs BP
Liki IIA		14 600 ± 1 200 yrs BP
Liki III	12 500 – 8 500 yrs BP	10 200 ± 500 yrs BP
Liki IIIA		8 600 ± 200 yrs BP

minimum ages of around 15 000 yrs BP (Mahaney, 1987). Unfortunately, it is not possible to date these moraines directly, owing to the lack of organic material in them. However, it is believed that the onset of the Liki II glaciation (LGM equivalent) occurred around 25 000 yrs BP as indicated by buried palaeosols in the Teleki valley (Mahaney, 1987, Mahaney *et al.*, 1991). Moraines at 4200 m a.s.l. have been dated at 12 500 yrs BP and represent the Liki III glaciation (Mahaney *et al.*, 1991). Glaciers during this later period either disappeared completely or retreated into their cirques by the end of the Pleistocene (Mahaney *et al.*, 1991).

Problems in constructing an accurate glacial history for Mount Kenya have arisen due to difficulties in the absolute dating of the deposits; however a new glacial chronology has been developed for East Africa using in situ cosmogenic ^{36}C1 measured from boulders from moraines (Shanahan and Zreda, 2000). Dates obtained from a series of smaller moraines above LGM deposits on Mount Kenya indicate the occurrence of several readvances (Liki IIA and Liki IIIA) (Table 2.9). Dates obtained from the deposits are 14 600 ± 1 200 yrs BP for the Liki IIA substage and 8 600 ± 200 yrs BP for the Liki IIIA substage (Shanahan and Zreda, 2000).

2.3.2.2.2 Kilimanjaro

Kilimanjaro is situated in northern Tanzania on the Kenya-Tanzania border, approximately 370 km south of the equator and is Africa's highest mountain, comprising three peaks (Shira, Kibo and Mawenzi) (Kaser *et al.*, 2004). Of these, Kibo stands the highest at 5895 m a.s.l. and is the only peak to retain glaciers (Hamilton, 1982; Kaser *et al.*, 2004). Monthly mean temperatures vary only slightly around the annual mean of -7.1°C at the summit (Kaser *et al.*, 2004). The present glacier surface on Kilimanjaro is 2.6 km^2, as determined from aerial photographs taken in February 2000 (Thompson *et al.*, 2002). Present day ELAs are thought to be at approximately 5300 m a.s.l. on Kibo, however glaciers are retreating so rapidly that it is not possible to measure the quasi-equilibrium ELA (Osmaston and Harrison, 2005).

Large moraines occur on the south and west sides of Kibo, whilst smaller moraines also exist on the north and east slopes (Hamilton, 1982). A complex of comparatively small moraines is found on eastern Kibo at 5400 m a.s.l. and between 4600 m a.s.l. and 5000 m a.s.l. on the south and west slopes (Meyer, 1900). These moraines occur inside those of the LGM; however there is no chronological control available for these deposits (Shanahan and Zreda, 2000) (Figure 2.17). It is suggested that during the LGM, the summits of Kibo and Mawenzi were completely covered by ice to 4300 m a.s.l. (Humphries, 1972; Osmaston and Harrison, 2005). Below this level, glaciers were more lobe-like, which in turn formed moraine ridges and lateral moraines up to 100 m high and 5 km long between 3200 m a.s.l. and 4600 m a.s.l. (Rosqvist, 1990). It is suggested that most of the obvious glacial features belong to the LGM (Downie, 1964; Hamilton, 1982), which concurs with dated boulders on Mawenzi moraines, which yielded cosmogenic radionucleide ages of 17 300 ± 2900 cal. yrs BP and 20 000 ± cal. yrs BP (Shanahan and Zreda, 2000). The maximum extent of the LGM on Kilimanjaro was at about 17 000 yrs BP to 20 000 yrs BP, with evidence for retreat stages or minor advances around 14 000 yrs BP to 16 000 yrs BP (Osmaston, 2004).

The Little Glaciation was also identified by Downie (1964) and dating of moraines believed to have formed during this stage have yielded dates of 16 000 ± 2000 cal. yrs BP and probably represent a retreat stage (Shanahan and Zreda, 2000). Former ELAs on Kilimanjaro during the LGM are believed to have been at around 3900 m a.s.l. at the lowest point on Mawenzi and 4250 m a.s.l. on the northern slopes (Osmaston and Harrison, 2005). On Kibo, the former ELA was at 5200 m a.s.l. on the northeast and east slopes and 4600 m a.s.l. on the south and west slopes (Rosqvist, 1990; Osmaston and Harrison, 2005). These differences have been attributed to the greater precipitation received on the southern and eastern slopes of Mawenzi, as opposed to the north-western slopes which lie in a precipitation shadow (Osmaston and Harrison, 2005). The differences in the ELAs on Kibo have been attributed to intense solar

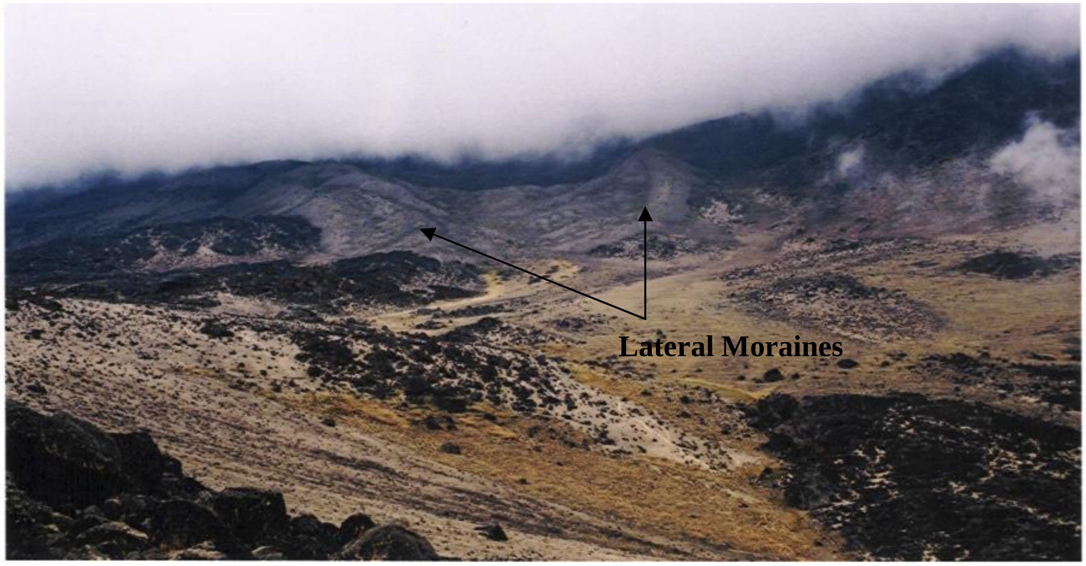

Figure 2.17 Lateral moraines on the south-western side of Kibo at 4800 m a.s.l. representing a Holocene glaciation period (photo by S. Mills).

radiation on the eastern slope in the morning, whilst the western slopes are shaded from intense radiation by afternoon clouds (Osmaston and Harrison, 2005).

2.3.2.2.3 Summary of LGM glacial advances and climate in East Africa

^{36}C1 ages for moraines on Mount Kenya and Kilimanjaro indicate that there were a series of younger glacial advances at 28 000 ± 3000 yrs BP, 20 000 ± 1000 yrs BP, between 15 000 ± 2500 yrs BP and 13 800 ± 2800 yrs BP, 10 400 ka ± 600 yrs BP and possibly at 8 600 ± 500 yrs BP (Shanahan and Zreda, 2000). These advances suggest that towards the end of the last glacial cycle, the climate in these areas was highly variable (Shanahan and Zreda, 2000).

Pollen records indicate that the climate in Africa between approximately 35 000 yrs BP and 15 000 yrs BP was cold and dry (Bonnefille *et al.*, 1990), with the driest period occurring around 21 000 yrs BP (Gasse *et al.*, 1989). Temperatures were lowered by 3ºC to 4°C during this period and a pronounced increase in temperature and precipitation values occurred around 15 000 yrs BP (Bonnefille *et al.*, 1990). However, available pollen sequences for the period 15 000 yrs BP to 12 000 yrs BP show a progression from cold to warmer to colder temperatures during the Liki III substage (Coetzee, 1967; Mahaney, 1985).

2.3.3 New Zealand

New Zealand comprises of South and North Island, both of which have a variety of local climates with contrasting temperatures and rainfall patterns (Salinger, 1984). The Southern Alps, Tasmania and the southern Andes, are the only regions at mid-latitudes in the Southern Hemisphere which were extensively glaciated during the Quaternary (Kiernan, 1990; Augustinus, 1999; Preusser *et al.,* 2005). New Zealand's climate is dominated by the westward movement of weather systems over the Tasman Sea and is sensitive to changes in this movement (McGlone *et al.,* 1993). Present-day ELAs range from approximately 1570 m a.s.l. on Caroline peak in Fiordland to 2140 m a.s.l. on Mount Ella near the northern limit of the main Southern Alps (Lamont *et al.,* 1999). In the central Southern Alps at Franz Josef, ELAs range from l500 m a.s.l. on the western slopes to over 2300 m a.s.l. east of Mount Cook (Chinn and Whitehouse, 1980). Modern glacier systems in western New Zealand respond to anomalies in the regional air flow pattern, with temperature forcing being only a secondary effect (Hooker and Fitzharris, 1999). Enhanced south-westerly air flow during summer and winter reduces ablation and enhances precipitation, whereas enhanced northerly flows and high pressure systems reduce precipitation and increase ablation, thus causing retreat (Shulmeister *et al.,* 2005).

The Otira glaciation represents the last glacial cycle and has been subdivided into three glacial advances known as Kumara-2_1, Kumara-2_2 and Kumara-3 (Suggate, 1965). Temperatures estimated from palaeosnowlines (Porter, 1975; Chinn, 1983) and speleothems (Hendy and Wilson, 1968) indicate a 4ºC to 5°C temperature depression compared with present-day values during this glacial period. The climate was also drier and windier with frequent incursions of polar air masses (McGlone and Topping, 1977; 1983, McGlone *et al.*, 1993; Pillans *et al.*, 1993). The Kumara 2_2 advance began around 25 000 yrs BP (Suggate, 1965; Denton *et al.,* 1999; Preusser *et al.,* 2005) and there was an onset of more favourable climatic conditions around 22 000 yrs BP as indicated by a change in vegetation until 19 200 yrs BP (Harris *et al.,* 1983; Hormes *et al.,* 2003), with the most extreme glacial conditions occurring at 19 000 yrs BP (Hellstrom *et al.,* 1998). In contrast, it has been suggested that a prominent maximum glacial advance occurred during the Kumara 2_2 stage at around 21 750 yrs BP to 20 950 yrs BP (Moar, 1980; Denton *et al.,* 1999). The Kumara 2_2 advance lasted until about 18 000 yrs BP, when a brief interstadial occurred until 17 000 yrs

BP (Chinn, 1983). The final Kumara 2_2 advance lasted until between 16 000 yrs BP and 17 500 yrs BP (Suggate, 1965; Preusser *et al.,* 2005). The Kumara 3 advance occurred from 15 000 yrs BP to 13 000 yrs BP (Gage, 1958), during which time glacier expansion was considerably reduced from the period before 22 000 yrs BP and temperature depressions were about 3ºC colder than at present (Chinn, 1983). Speleothem records indicate a further glacial advance in southern New Zealand from 13 800 yrs BP to 11 700 yrs BP, which coincides with the Younger Dryas Stage in northern Europe (Hellstrom *et al.,* 1998).

There appears to have been some conflict in timing the deglaciation in New Zealand, with dates ranging between 16 000 yrs BP and 17 500 yrs BP (Suggate, 1965; Gage, 1958). More recent work suggests that deglaciation in South Westland (Southern Alps) commenced prior to 18 300 yrs BP, yet vegetation records indicate a renewed climate cooling occurred around 17 000 yrs BP (Vandergoes *et al.,* 2003). Work undertaken in north-west Nelson indicates that ice commenced its retreat no earlier than 20 000 yrs BP and that by 18 000 yrs BP ice wastage and retreat was extensive (Shulmeister *et al.,* 2005), yet several short-lived still stands and minor re-advances occurred during the deglaciation period (Shulmeister *et al.* 2005). Results from the work by Schulmeister *et al.* (2005) adds to the increasing evidence that glaciers in the Southern Hemisphere commenced their recession at about 19 000 yrs BP, with the onset of a major global climatic reversal following the LGM, which culminated with abrupt warming at about 15 000 yrs BP. Glacial re-advances during deglaciation may have been limited to possible small cirque reoccupation of permanent snow patches (Shulmeister *et al.,* 2005).

2.3.4 Australia and Tasmania

There are no glaciers in Australia today and only a small part of mainland Australia was glaciated during the LGM (Barrows *et al.,* 2001; Kiernan *et al.,* 2004), however glaciation in the Tasmanian highlands was widespread (Barrows *et al.,* 2002). The Snowy Mountains are the only area where indisputable Late Pleistocene glaciation took place on the mainland (Barrows *et al.,* 2001). The maximum area of glacial extent in the Kosciuszko Massif in the Snowy Mountains was approximately 15 km^2 during the LGM (Barrows *et al.,* 2001). It has been suggested that deglaciation occurred between 20 000 ^{14}C yrs BP and 15 000 ^{14}C yrs BP based on the dating of organic deposits (Costin, 1972). Terminal moraines, dated in the Snowy Mountains have yielded ages between 17 000 yrs BP and 20 000 yrs BP, consistent with the LGM (Barrows *et al.,* 2001, 2002). More recently, ^{10}Be ages indicate a glacial advance at 19 100 ± 1600 yrs BP and 16 800 ± 1400 yrs BP, suggesting that the LGM was followed by a readvance (Barrows *et al.,* 2001).

During the LGM, two ice caps were present in the central west of Tasmania, but elsewhere glaciers were restricted to cirques (Barrows *et al.,* 2002). It has been suggested that approximately 450 cirques were occupied during the LGM (Peterson and Robinson, 1969; Colhoun *et al.,* 1996), which occurred around 19 000 ^{14}C yrs BP (Colhoun *et al.,* 1996). Dates from recessional moraines range between 15 800 ± 800 yrs BP and 18 000 ± 700 yrs BP and it is suggested that the cirque glaciers probably existed briefly, whilst the larger glaciers probably existed longer (Barrows *et al.,* 2002). Further work from moraines in southwest Tasmania indicates that the last glacial advance occurred at 19 400 ± 600 yrs BP (Kiernan *et al.,* 2004).

2.3.5 South America

The Andean Cordillera extends along the western side of the South American continent and glaciers which are sensitive to climate occur throughout the Andes (Mercer, 1984; McCulloch *et al.*, 2000). Large moraine systems suggest an eventful climatic history (Hastenrath, 1971; Clapperton, 1993), however dating is difficult and it is rare to separate the different glacial advances (Clapperton, 1993).

2.3.5.1 Argentina

The Andes of Mendoza occur between 33°S and 36°S and five Pleistocene drifts have been differentiated by Espizua (1993). The Late Pleistocene drifts have been termed Penitentes, Horcones and Almacenes (Espizua, 2004). A travertine layer overlying Penitentes till has yielded ages of 24 200 ± 2000 yrs BP and 22 800 ± 3100 yrs BP, which are minimum ages for the underlying Penitentes till (Espizua, 2004). A unit representing the non-glacial period between the Penitentes and Horcones was dated using the thermoluminescence method (TL) and yielded an age of 31 000 ± 3100 yrs BP (Espizua, 1999), suggesting that the Penitentes ice advance occurred before the LGM, around 40 000 yrs BP (Espizua, 2004). Pollen and diatom analyses of lacustrine sediments suggest that interglacial climatic conditions existed between 33

000 yr BP and 27 000 yrs BP at 40°S, whilst the climate was cold between 24 500 yrs BP and 15 500 yrs BP (Markgraf *et al.,* 1986; Espizua, 2004).

Non-glacial sediments between the Horcones and Almacenes tills have been dated by TL to 15 000 ± 2100 yrs BP and have been interpreted as representing the non-glacial interval between the Horcones and Almacenes glacial periods (Espizua, 1999). A further TL date from laminated silts and clays overlying Horcones till has yielded an age of 15 000 ± 1500 yrs BP, indicating that the Horcones ice advance represents the final advance of the last glaciation (Espizua, 2004). The Almacenes till is believed to represent a stand-still or readvance that occurred at 14 000 yrs BP or between 11 000 yrs BP and 10 000 yrs BP (Espizua, 2004). Dating of moraines in Argentina east of Lago Buenos Aires has identified five glacial advances between approximately 23 000 yrs BP and 16 000 yrs BP, based on a combination of cosmogenic ages of moraines and ^{14}C ages of varved sediment (Kaplan *et al.,* 2004; Singer *et al.,*2004).

The general consensus from the southern Andes of Argentina is that final deglaciation occurred around 13 500 yrs BP (Mercer, 1982; Marden and Clapperton, 1995; Markgraf *et al.,* 1992; Clapperton, 1997). There is ongoing debate regarding the behaviour of glaciers during the late-glacial period, especially with regards to linking colder periods to the European Younger Dryas Stage (11 000 yrs BP to 10 000 yrs BP) (Wenzens, 1999). It has been suggested that there was neither a decrease in temperature nor increase in snowfall in Argentina during this time period (Mercer, 1976, 1982; Markgraf, 1993; Ashworth and Hoganson, 1993), however evidence has been proposed for a climatic reversal in southern South America during this time period (Heusser, 1993).

2.3.5.2 Argentine Patagonia

Argentine Patagonia extends between 36°S and 55°S and a thick ice sheet exists at present between 46°S and 52°S (Coronato *et al.*, 2004). This ice sheet is divided in two sections at approximately 48°S by the Río Baker depression (Coronato *et al.,* 2004). No absolute dating is available for northern Patagonia, however in the Lake Buenos Aires region at 46°S to 47°S, glaciolacustrine rhythmites have been dated and an age of 15 300 ± 300 yrs BP has been obtained, which provides an upper limit for the last glaciation in this region (Ton-That *et al.*, 1999). Further south, at Lake

Viedma (49° 41'S), well-defined arcs of moraines exist and it has been suggested that these represent three ice advances during the late glacial, younger than 13 000 yrs BP (Wenzens, 1999). At Lake Argentino (50° 10'S), it has been suggested that less extensive advances occurred around 16 000 yrs BP to 12 000 yrs BP and 12 000 yrs BP to 10 000 yrs BP (Clapperton, 1993). It is still unknown however whether the presence of the moraine arcs younger than the LGM correspond to minor glacial advances or to phases of stabilisation during ice recession (Coronato *et al.*, 2004).

2.3.5.3 Chile

Chile can be separated into three main sections; northern Chile (18ºS to 30ºS), central Chile (30ºS to 40ºS) and southern Chile (40ºS to 55ºS) (Harrison, 2004). In northern Chile the contemporary ELA is very high and only summits above 5 500 m a.s.l. to 6000 m a.s.l. have permanent snow and ice (Rabassa and Clapperton, 1990; Harrison, 2004). In central Chile, the ELA falls below 4000 m a.s.l. as a result of increased precipitation, whilst in southern Chile, the ELA falls to 1800 m a.s.l., reflecting even higher precipitation in a maritime climate (Rabassa and Clapperton, 1990; Harrison, 2004).

Northern and central Chile display little evidence for glacial advances during the LGM (Harrison, 2004), and it has been suggested that some summits above 5000 m a.s.l. in northern Chile were probably unglaciated during the LGM (Clapperton, 1993). More recently it has been suggested that precipitation increased by 100% (Harrison, 2004) and that snowline altitudes decreased by 800 m to 1000 m in the northern Cordillera (Klein *et al.*, 1999). Unfortunately the exact age of the LGM is unknown due to poor dating control; however radiocarbon ages suggest that this occurred prior to 20 000 ^{14}C yrs BP (Harrison, 2004). In contrast, in the Andes of northern Chile, the timing of glaciations is better known and Grosjean *et al.* (1998) suggest that glaciers were most advanced between 30 000 yrs BP and 20 000 yrs BP. It is also suggested that a readvance took place between 16 000 yrs BP and 12 000 yrs BP (Grosjean *et al.*, 1998). In central Chile, moraines have been dated to approximately 20 000 yrs BP (Harrison, 2004).

The best dated sequence of glacier fluctuations during the LGM is in the Chilean lakes region (41ºS to 43ºS), where outlet lobes from the north Patagonian Andes advanced into a landscape containing forest and peat bogs (Rabassa and Clapperton, 1990). Three glacial advances took place during the LGM in Chile; namely the Llanquihue I, II and III (Porter, 1981a), however it has been suggested that the Llanquihue I moraines predate the LGM and may be as old as 73 000 yrs BP (Mercer, 1983). The Llanquihue II glacial advance occurred after 30 000 yrs BP (Rabassa and Clapperton, 1990) and end moraines, which indicate the most advanced position, have yielded dates of between 20 000 yrs BP to 19 000 yrs BP (Mercer, 1972, 1976; Porter, 1981a). These dates broadly correlate with the Late Wisconsin advances in eastern North America (Mercer, 1984). It has been suggested that two pulses of glacial readvance took place during Llanquihue III, at approximately 15 000 yrs BP to 14 500 yrs BP and after 13 200 yrs BP (Porter, 1981a). This first readvance is further described by Mercer (1984), who suggests that it took place between 15 700 yrs BP and 13 200 yrs BP.

Deglaciation began close to 19 000 yrs BP (Porter, 1981a) in the Chilean Lakes area, with the possibility of a glacial readvance at around 15 600 yrs BP to 14 200 yrs BP (Heusser, 1993). This is further supported by Denton *et al.* (1999), who identify a last glacial advance at 14 805 yrs BP to 14 550 yrs BP. A comparison of past vegetation types with their present counterparts suggests a temperature cooling of 6ºC to 7°C during the last glacial readvance, with twice the present annual precipitation (Denton *et al.,* 1999). There is less certainty for a possible Younger Dryas climatic reversal in the Chilean lakes region, however Heusser *et al.* (1999) suggest a cooling after approximately 12 000 yrs BP to 10 000 yrs BP, based on an expansion of cold tolerant species and a temperature reduction of 2ºC to 3ºC. Further pollen investigations in Lake Mascardi have revealed younger-dryas advance of a small mountain glacier (Ariztegui *et al.,* 1997). There is still much controversy as to whether a glacial re-advance took place at this time, given that beetle records show no evidence of a Younger Dryas cooling (Hoganson and Ashworth, 1992; Ashworth and Hoganson, 1993). It is suggested that although the pollen record may reflect a Younger Dryas cold reversal, it may only represent a relatively minor depression in temperature (McCulloch *et al.,* 2000).

2.3.6 Summary

The timing of the LGM around the Southern Hemisphere is provided in Table 2.10. There appears to be a unanimous synchronicity regarding the timing of the LGM in the southern hemisphere (ca. 30 000 yrs BP to 15 000 yrs BP) (Suggate, 1965; Mercer, 1972, 1976; Porter, 1981a; Markgraf *et al.*, 1986; Rabassa and Clapperton, 2000; Colhoun *et al.,* 1996; Denton *et al.,* 1999; Shanahan and Zreda, 2000; Barrows *et al.,* 2001, 2002; Espizua, 2004; Kiernan *et al.,* 2004; Osmaston, 2004; Preusser *et al.,* 2005), with maximum cooling occurring between 21 000 yrs BP to 17 000 yrs BP in East Africa (Gasse *et al.*, 1989; Osmaston, 2004), around 19 000 yrs BP in New Zealand (Hellstrom *et al.*, 1998), 22 500 yrs BP in Australia (Colhoun *et al.,* 1996) and between 20 000 yrs BP and 19 000 yrs BP in Chile (Mercer, 1972, 1976; Porter, 1981a). What appears to be more problematic is the identification of glacial advances and their timing around the late glacial period (Wenzens, 1999). East Africa and New Zealand have clear evidence of a later period of glacial advance based on dating of moraines in East Africa and speleothems in New Zealand (Shanahan and Zreda, 2000; Hellstrom *et al.,* 1998), however there is no evidence of such advances in Australia and Tasmania (Barrows *et al.*, 2002) and the debate is ongoing in South America (Wenzens, 1999; Heusser *et al.*, 1999).

Table 2.10 A summary of the timing of the LGM around the Southern Hemisphere.

Ethiopia	Mount Kenya	Kilimanjaro	New Zealand	Australia	Tasmania	Argentina	Chile
	Liki II 28 000 ± 3 000 – 15 000 yrs BP[2,3,4]	Main glaciation 17 000 – 20 000 yrs BP[2,5]	Kumara-2_2 25 000 – 16 000 yrs BP[7,8,9]	LGM between 20 000 – 17 000 yrs BP[12,13]	Late Margret 19 400 ± 600 yrs BP – 18 800 ± 500 yrs BP[14,15]	Horcones 24 500 – 15 500 yrs BP[16,17]	Llanquihue II 30 000 – 19 000 yrs BP[19,20,21,22]
		Little glaciation 16 000 ± 2000 yrs BP[6]	Kumara-3 15 000 – 13 000 yrs BP[10]	Mt. Twynam advance 16 800 ± 1 400 yrs BP[12]			Llanquihue III 15 000 – 14 500 yrs BP[22]
Ice free by 14 000 – 7 500 ^{14}C yrs BP[1]	Liki IIA 14 600 ± 1 200 yrs BP[2]	Younger advance 13 800 ± 2 800 yrs BP[2]	Glacial advance 13 800 – 11 700 yrs BP[11]			Almacenes 14 000 yrs BP or 11 000 – 10 000 yrs BP[16]	Llanquihue III readvance 15 700 – 13 200 yrs BP[22,23]
	Liki III 10 200 ± 500 yrs BP[2]	Younger advance 10 400 ± 600 yrs BP[2]					

[1]Osmaston *et al.* (2005), [2]Shanahan and Zreda (2000), [3]Mahaney (1987), [4]Mahanney (2004), [5]Osmaston (2004), [6]Downie (1964), [7]Suggate (1965), [8]Denton *et al* (1999), [9]Preusser *et al.* (2005), [10]Gage (1958), [11]Hellstrom *et al.* (1998), [12]Barrows *et al.* (2001), [13]Barrows *et al.* (2002), [14]Colhoun *et al.* (1996), [15]Kiernan *et al.* (2004), [16] Espizua (2004), [17] Markgraf *et al.* (1986), [18] Mercer (1983), [19] Rabassa and Clapperton (1990), [20] Mercer (1972), [21] Mercer (1976), [22] Porter (1981a), [23]Mercer (1984).

CHAPTER 3

Environmental and Geomorphic Setting

3.1 GEOLOGY

3.1.1 Background

The continent of Africa formed part of the larger landmass of Gondwana during the late Palaeozoic and early Mesozoic Eras (Figure 3.1 and 3.2). During the Lower Carboniferous period to the Lower Permian period, Gondwana was situated in the South Polar Region, with the South Pole positioned in South Africa, causing widespread glaciation (Schmitz and Rooyani, 1987). Reconstructions of the Southern Hemisphere continents confirm the central position occupied by Africa, which was responsible for the high altitude of southern and eastern Africa before the break-up of Gondwana (Dingle *et al.,* 1983; Partridge, 1997a). The fragmentation of Gondwana took place around 183 Ma ago (Thomas *et al.,* 1993; Duncan *et al.,* 1997) and led to the formation of the present-day continents (Eriksson, 2000). Lesotho is situated in the Karoo Basin, which consists of a variety of sediments deposited during various Eras (Fig 3.3 and 3.4). The Karoo Supergroup was laid down between 300 Ma to approximately 190 Ma ago (Smith *et al.,* 1993). The Karoo formations extend over 600 000 km^2 (Furon, 1963) and they consist of a 9 km thick succession of alternating sandstones and shales (Eriksson, 2000). The Karoo Supergroup includes several groups which are defined on the basis of overall sedimentary characteristics. These are the Dwyka, Ecca, Beaufort, Stormberg and Drakensberg Groups (Catuneanu *et al.,* 2005). Only the Drakensberg Group will be discussed, as this forms the underlying bedrock at all of the study sites.

3.1.2 Drakensberg Group

The Drakensberg Group was formed by Basaltic lavas, which escaped from fissures and reached thicknesses of 1 000 m in the Eastern Cape and over 1 500 m in Lesotho (Furon, 1963; Hooper *et al.,* 1993). Extrusion of these basalts continued from the Late Triassic to Early Cretaceous and is believed to have been associated with the break-up of Gondwana (Eales *et al.,* 1984; Cox, 1988; Bell and Haskins, 1997; Whitmore *et al.,* 1999; Eriksson, 2000). Four major southern African provinces are recognised by

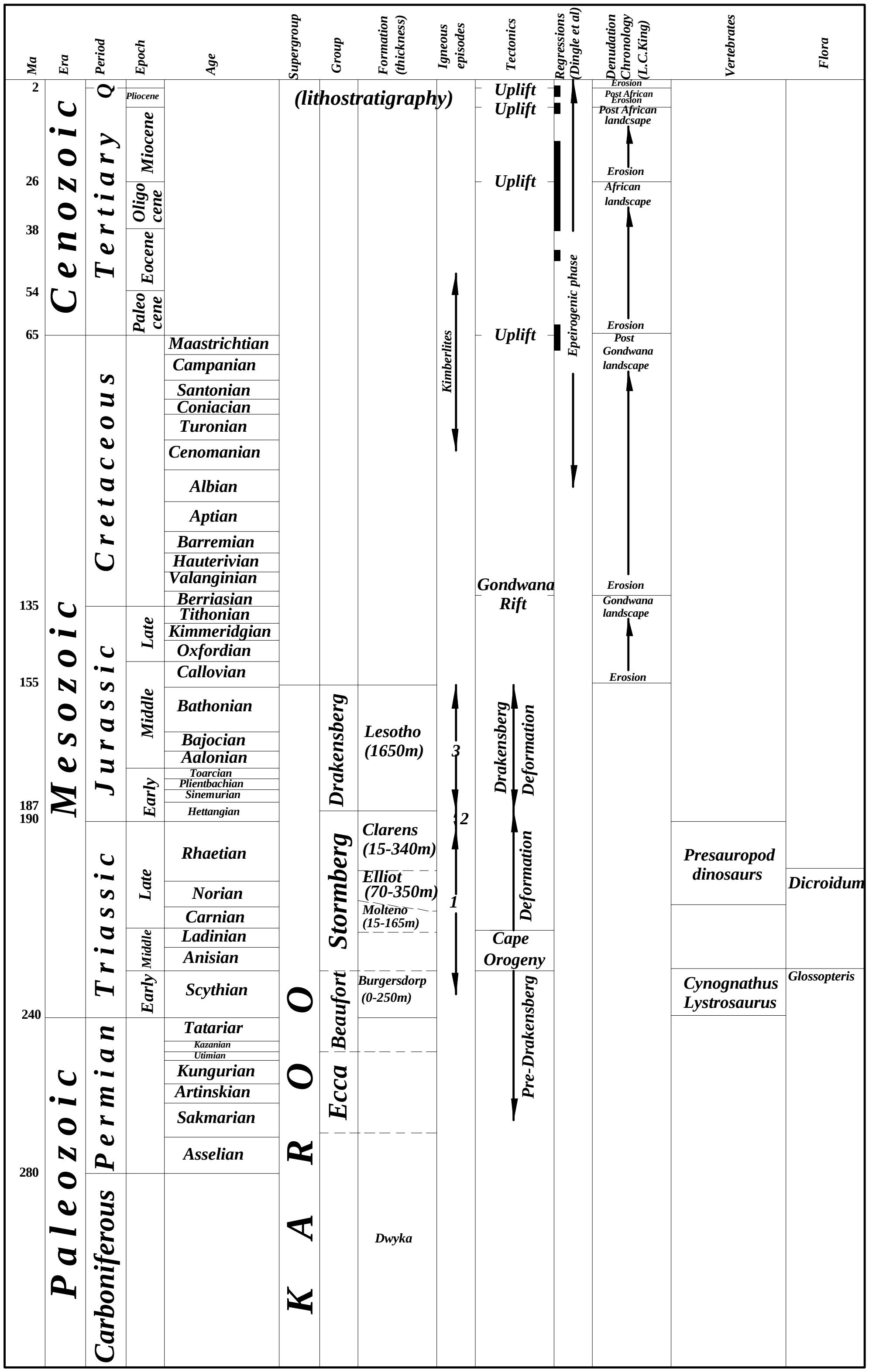

Figure 3.1 Geological Time Scale (after Schmitz and Rooyani, 1987).

Figure 3.2 The configuration of the Southern Hemisphere continents at the time of the break-up of Gondwanaland (after Dingle *et al.,* 1983).

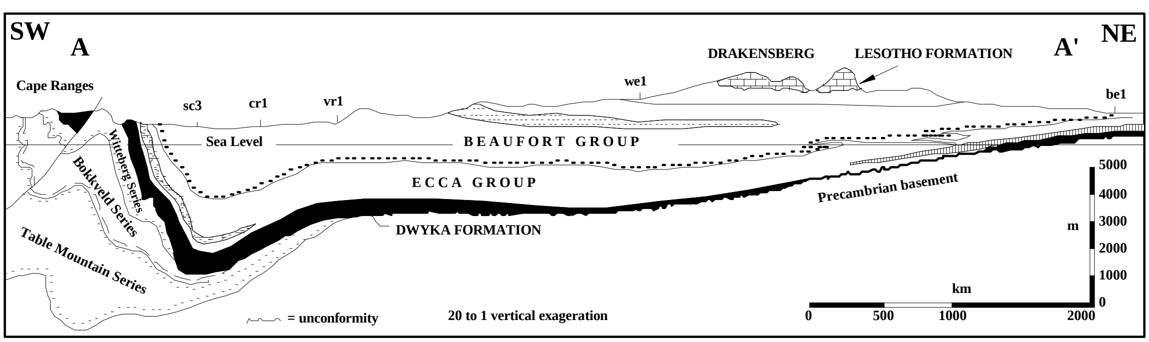

Figure 3.3 Cross section from the Cape ranges through Lesotho to KwaZulu-Natal (after Schmitz and Rooyani, 1987).

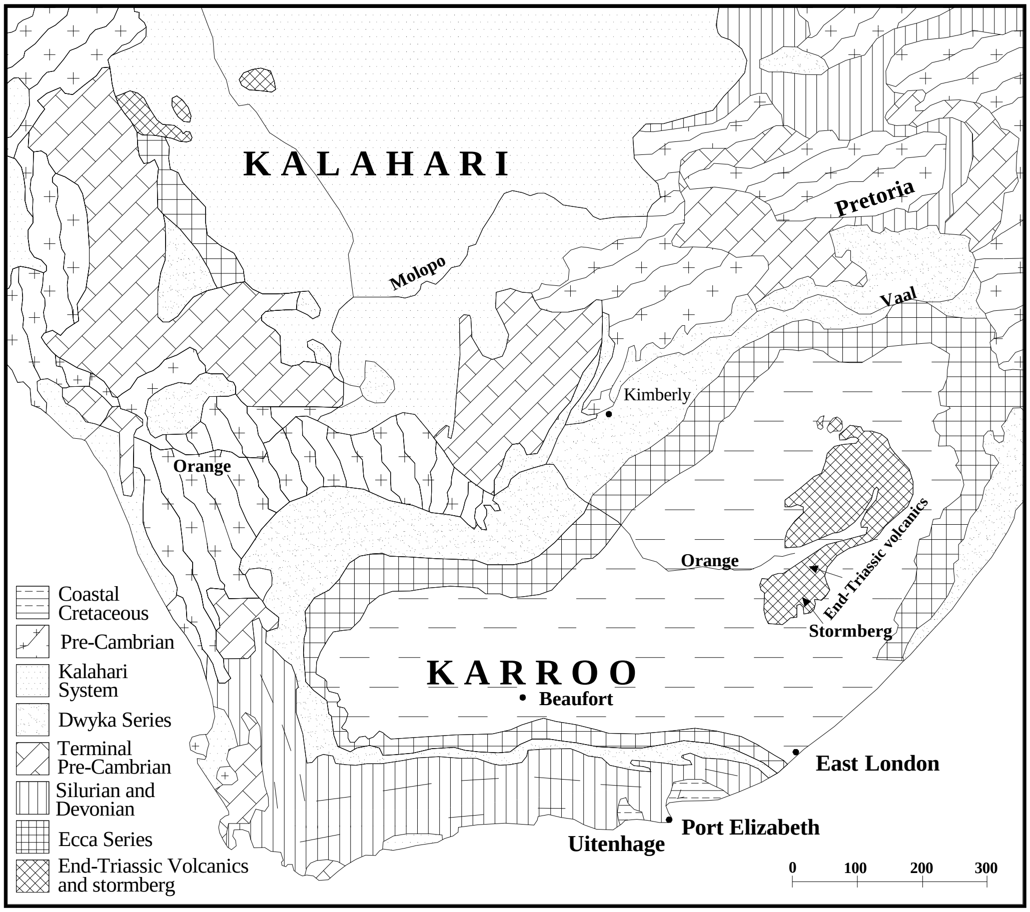

Figure 3.4 Geological sketch map of South Africa (after Furon, 1963).

Duncan *et al.* (1984); holistic lavas, olivine-poor basalts and acid lavas, olivine-rich basalts and silica-rich basalts and latites. Initially, a phase of explosive phraeto-magmatic volcanism deposited pyroclastic breccias and tuffs in the southern and south-eastern parts of the Karoo basin (Lock, 1978). A subsequent period of subdued fissure eruptions followed, which built up thick sequences of basalt flows (Dingle *et al.,* 1983). Dolerite dykes which formed the channels along which the lava was fed to the surface, intersect the Drakensberg Basalts (Van Rooy and Van Schalkwyk, 1993). The theolitic lava flows form the Lesotho basaltic plateau, which is 300 km wide and up to 3500 m a.s.l. (Kosterov and Perrin, 1996).

The Drakensberg volcanics in Lesotho began extruding lava 187 Ma ago and continued intermittently until at least 155 Ma ago (Fitch and Miller, 1971). The flows are horizontally disposed and there is a complete absence of faulting and tilting (Marsh, 1987). In contrast, Brackley *et al.,* (1991) note persistent weaknesses in the basalt in the form of horizontal shear zones and observe that high angled dip-slip faults trend in a north-east to south-west direction and strike-slip faults trend from east-south-east to west-north-west. The lava flows vary in thickness from less than 1 m to up to 50 m (Bell and Haskins, 1997); however are approximately 6 m in thickness (Olivier Shand Lahmeyer MacDonald Consortium, 1986). It is suggested that the flows were laid down in rapid succession, given the lack of highly weathered flow contacts (Bell and Haskins, 1997). The flows are mainly basaltic, containing calcic labradorite, augite, opaque minerals and olivine (Duncan *et al.*, 1983) (Table 3.1).

Table 3.1 Average composition of Lesotho Formation Basalt (after Duncan *et al.*, 1983).

	%		***ppm***
SiO_2	51.50	Cr	283
Al_3O_3	15.69	Sr	192
Fe_2O_3	10.96	Ba	177
CaO	10.69	Zr	94
MgO	7.01	Ni	94
Na_2O	2.17	Y	24
TiO_2	.95	Rb	12
K_2O	.70	Nb	14.9
MnO	.16		
P_2O_5	.16		

Many of the lavas and thicker flows are often coarse grained and tubular, with coalescing pipe amygdales marking the base of nearly every flow (Van Rooy and Van Schalkwyk, 1993). Thin flows contain amygdales throughout, however the thicker ones tend to contain amygdaloidal zones at the top and bottom (Van Rooy and Van Schalkwyk, 1993). The dominant mineralogy of the Lesotho Basalt Formation is plagioclase, which is a sodium/calcium aluminosilicate and is observed within the basalt clasts at the study sites (Figure 3.5). The plagioclase is frequently unaltered; however some may undergo saussuritization (Bell and Haskins, 1997). Next in abundance is pyroxene, which is dominantly iron/magnesium silicate and olivine, which is a magnesium/iron silicate (Binnie and Partners, 1971). Olivine within the Drakensberg basalts undergoes the most extensive alteration and may be replaced by serpentine, iron oxides or clay (Bell and Haskins, 1997). The Drakensberg Basalts also contain up to 25% interstitial glass (Van Rooy and Van Schalkwyk, 1993), which

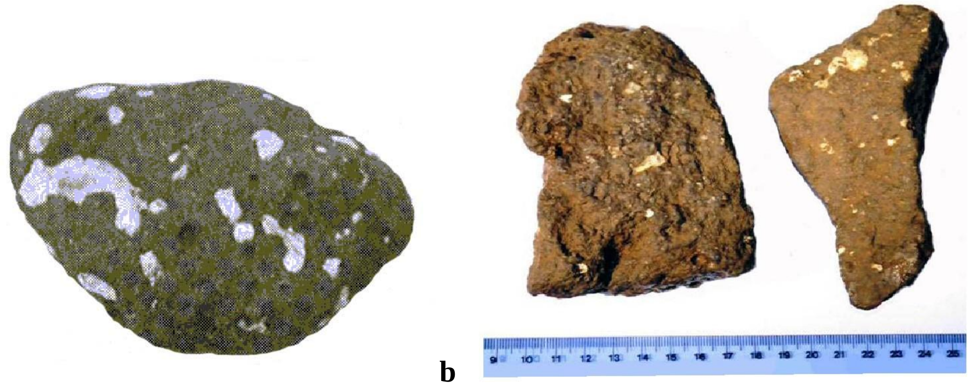

a **b**

Figure 3.5 Basalt clasts. a) Amygdaloidal basalt rich in plagioclase (source: Schmitz and Rooyani, 1987). b) Clasts from the Tsatsa-La-Mangaung deposit.

formed as a result of the rapid cooling of interstitial residual liquid and subsequent solidification (Bell and Haskins, 1997).

The Road up Sani Pass provides an 800 m thick sequence of flood basalts, of which the lower 175 m of the succession have been subdivided into a series of four units (Mitchell *et al.,* 1996). Above 175 m, the basalts are relatively uniform (Mitchell *et al.,* 1996). The units have been named from the base up; the Giants Cup unit, the Agate unit, the Sakeng unit and the Mkhomazana unit, whilst above these lies the Lesotho unit, which is over 600 m thick (Mitchell *et al.,* 1996). This unit extends to the top of Sani Pass and individual flow units range from 0 3 m to 20 m in thickness (Mitchell *et al.,* 1996).

There is little published material on weathering processes in southern Africa and recent work has specifically focussed on biological and cryogenic (freeze-thaw) weathering (Sumner, 2000b). It has been suggested that the basalts weather rapidly on exposure and the depth of weathering of the basalt varies from less than 10 metres on the upper slopes of Lesotho, to more than 25 meters at the valley bottoms (Van Rooy and Van Schalkwyk, 1993; Bell and Haskins, 1997). This higher degree of weathering in the valley bottoms is in part due to the more frequent occurrence of inclined open stress-relief joints, which is caused by the removal of sediment as the river cuts downward, and to increased water seepage at the river level (Van Rooy and Van Schalkwyk, 1993). Some of the lava flows in the Drakensberg have undergone deuteric alteration, which means they may contain disseminated clay spots (Bell and

Haskins, 1997). These, along with olivine basalts, break down rapidly on exposure and are most susceptible to disintegration with cyclic wetting and drying as a result of their readily accessible clay content (Bell and Haskins, 1997). In contrast, highly amygdaloidal basalts are more resistant as a result of their low content of swelling clay (Bell and Haskins, 1997).

3.2 GEOMORPHIC EVOLUTION

Two tectonic phases that overlapped in time were responsible for the formation of the continental margins around South Africa (Gilchrist, 1995). Firstly, rifting between South America and Africa began during Permo-Triassic times, with the main phase occurring during the late Jurassic and early Cretaceous periods (Maslanyj *et al.*, 1992), whilst the separation of Antarctica and Africa occurred during the Jurassic (Dingle *et al.*, 1983). The last flood basalts of the Lesotho Formation were deposited around 155 Ma ago, and since then the area has experienced tectonic activity such as the fragmentation of Gondwana during the early Cretaceous, and differential crustal movements since the middle Cretaceous (Schmitz and Rooyani, 1987; Gilchrist, 1995). The post-Gondwana uplift was a major geological event, which lead to the formation of the Great Escarpment (Partridge and Maud, 1987; Partridge, 1997a) (Figure 3.6). The Great Escarpment encompasses the Lesotho highlands, the eastern margin of the Transvaal Bushveld basin to the north and stretches even further north into eastern Zimbabwe (Eriksson, 2000).

Classical models of landscape evolution include those by Davis (1899), King (1953) and Penk (1953). Davis (1899) considered landscape change in terms of an evolutionary sequence, which responded to an initial endogenic pulse, which in turn lowered the base level of denudation adjacent to a landmass, causing rejuvenation (Gilchrist, 1995). King (1953) also proposed an evolutionary sequence in response to an endogenic pulse, however related landscape evolution to escarpment retreat, whilst Davis (1899) related it to slope decline. Davis (1899) suggested that there is a progressive decrease through time in overall slope angles as the rate of basal downcutting by streams decreases and slopes become mantled with weathered material, which can then be transported along lower gradients (Summerfield, 1991). Penk (1953) on the other hand, considered that landscape morphology was a function of the continuous interaction between tectonics and surface processes (Gilchrist,

Figure 3.6 The Great escarpment photographed at Cathedral Peak in the north-eastern Drakensberg (photo by S. Mills).

1995), whereby the process of slope replacement creates a broadly concave slope profile (Summerfield, 1991). Nixon (1973) suggests that continuous erosion of flat-lying beds (as opposed to cyclic) would result in the typical Lesotho topography and that a combination of erosion cycles and structural origin are the most likely causes for landscape evolution. However, these models are not based on empirical observations, and they do not yield specific quantitative predictions as to how slope form may be expected to change over time (Summerfield, 1991). The classic models generally envisaged more rapid rates of landscape change than are actually observed in the passive setting of southern Africa and it has more recently become apparent that the geomorphic evolution of escarpment systems may be more complex (Gilchrist and Summerfield, 1990; Brown *et al.*, 2000).

Early views are that the Escarpment evolved through parallel retreat from a coastal location (King, 1962; Partridge and Maud, 1987). King (1962) suggested that the escarpment retreat was constant, however Partridge and Maud (1987) suggested that very rapid escarpment retreat occurred in the Early Cretaceous, whilst much slower retreat took place during the Cenozoic. It is suggested that rapid retreat occurred due to the high energy potential provided by the elevated margin created at breakup and to the humid tropical climates during the Cretaceous (Partridge, 1998). In contrast, Brown *et al.* (2002) propose that a drainage divide coincided with the creation of the escarpment at the coast. Van der Beek *et al.* (2002) suggest that the drainage divide existed close to the present position of the escarpment, which may have formed by thickness variations in the pile of Drakensberg basalts. The escarpment became pinned at this divide, and subsequently retreated inland at a rate of 100-200 m/Myr and accelerated denudation of the Drakensberg escarpment occurred from approximately 90 Myr to 70 Myr (Brown *et al.*, 2002; Van der Beek *et al.*, 2002). The presence of a drainage divide close to the present-day escarpment indicates that any relief that was created by rifting and breakup would have been rapidly destroyed by rivers and replaced by an escarpment formed at the pre-existing drainage divide (Van der Beek *et al.*, 2002).

3.3 SOILS

Twenty six mappable soil units have been recognised in Lesotho, belonging to eight major soil types (Carroll and Bascomb, 1967). The summit area soils have been classified principally as Lithosols on lava (Carroll and Bascomb, 1967; Bascomb and Carroll, 1967) (Figure 3.7). The soils are immature, shallow (<45cm) and sometimes absent and are mostly colluvial in origin (Killick, 1976; Sene *et al.*, 1998; Grab *et al.*, 1999; Partridge, 1997a; Sumner, 2003). The thin summit soils are often waterlogged during summer and subject to freeze-thaw processes during winter (Killick, 1994). Deeper soils exist in the wide valley floors where small amounts of alluvial material have contributed to their development; however most of these soils lack a ‘B’ horizon and are frequently underlain by a yellowish-brown cambic horizon at depth (Klug *et al.*, 1989). Soils which only contain an A and C horizon and have developed from weakly weathered bedrock are known as Lithosols (Ellis and Mellor, 1995), which concurs with the Lithosols on Lava ascribed to this area of Lesotho (Carroll and Bascomb, 1967; Bascomb and Carroll, 1967).

Dark silty soils are common in Lesotho as a result of the present climate (Hanvey and Marker, 1994). Oxidation occurs in summer, which results in slow organic accumulation, however the existence of peat deposits suggests past wetter conditions (Hanvey and Marker, 1994; Marker, 1994a). Organic soils have also been identified at higher elevations in Lesotho (above 3000 m a.s.l.), which have been classified as

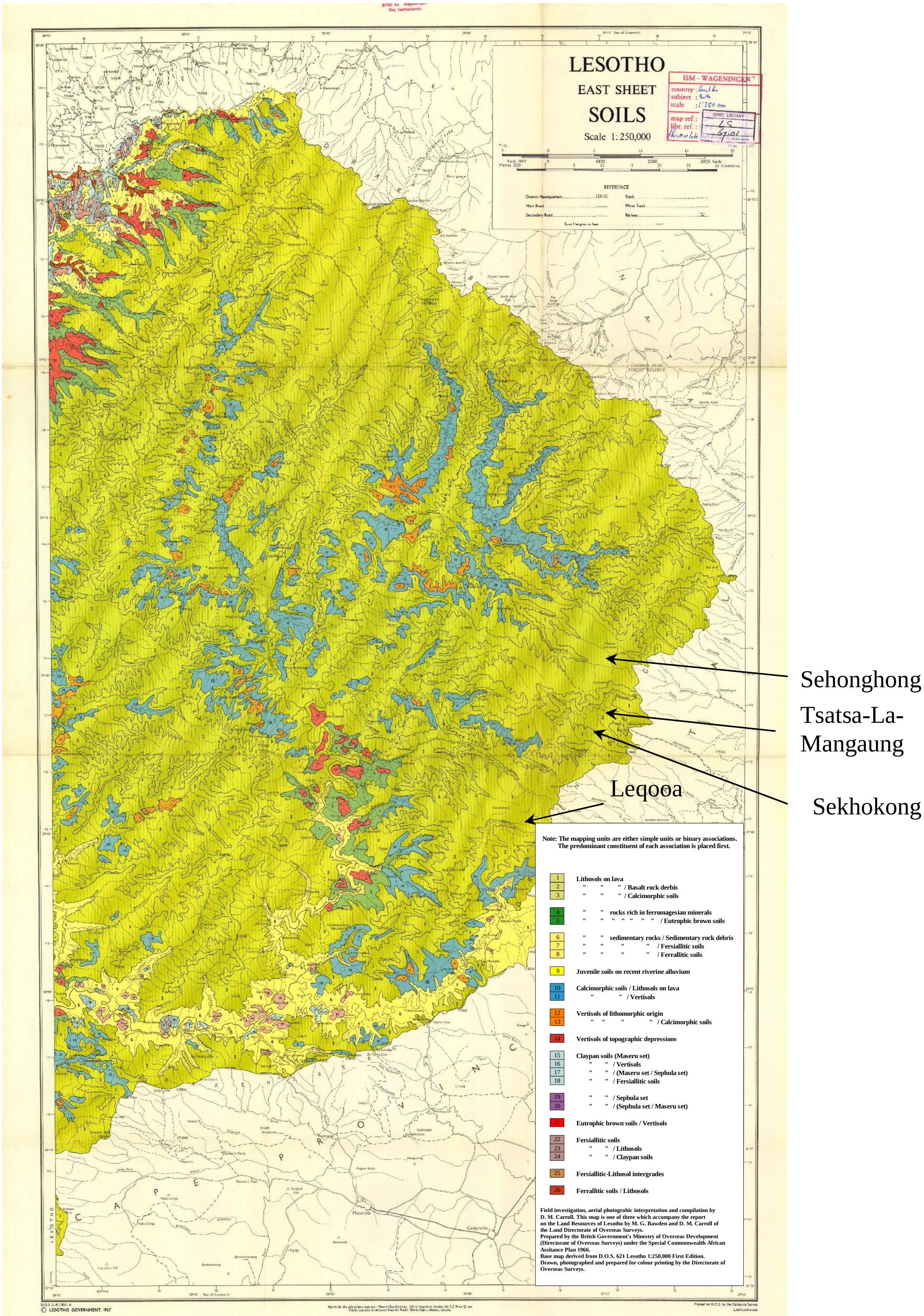

Figure 3.7 Soils map of Lesotho (after Bascomb and Carroll, 1967).

Borosaprists and have formed under a dense grass cover where the mean annual temperature is less than 8ºC, and where the drainage is impeded (Schmitz and Rooyani, 1987). This high level of organic matter can be attributed to the low temperatures, the high level of moisture and the presence of basalt as the parent material (Schmitz and Rooyani, 1987). Temperature and rainfall greatly influence the amount of organic matter found in soils (Jenny, 1941). Generally, the decomposition of organic matter is accelerated in warm climates, whilst colder climates experience a lower rate of decay (Brady, 1990). In addition, soil moisture affects organic matter content, which increases as the effective moisture becomes greater (Brady, 1990).

Soil development is impaired on the steep mountain slopes as a result of greater erosion and low temperatures, which lead to the formation of immature skeletal soils like Moroke and Popa soils (Schmitz and Rooyani, 1987). These soils form from basalt bedrock which is moderately weathered and gives rise to dark coloured, neutral soils (Lundén *et al.,* 1990). Moroke and Popa soils both form part of the wider group of Mollisols (Schmitz and Rooyani, 1987). Mollisols typically contain 2% to 5% organic matter according to tables in soil taxonomy; however grassland soils have higher contents to greater depths (Birkeland, 1999). Most Mollisols develop under grassland vegetation and they are characterised by a dark surface horizon which generally has a granular or crumb structure, resulting from the presence of organic matter (Brady, 1990). The Moroke series consists of a well-drained, shallow, medium textured soil which ranges in thickness from 20 cm to 50 cm and is characteristically dark brown to black (Schmitz and Rooyani, 1987). The Popa series is a well-drained, shallow, medium textured, very dark brown to black loam or sandy loam and is a residual soil formed on mountain slopes, where basalt is predominant (Schmitz and Rooyani, 1987). These immature and discontinuous soils, which occur in the high mountain regions of Lesotho, form a distinct contrast to the African surface, which is characterised by advanced weathering and pedogenesis (Partridge, 1997a).

3.4 CLIMATE

3.4.1 General Atmospheric Circulation

The climate of South Africa is sustained by the position of the subcontinent relative to the major atmospheric circulation features of the Southern Hemisphere, which causes rainfall to be seasonal over most of the southern continent (Dube, 2002) (Figure 3.8).

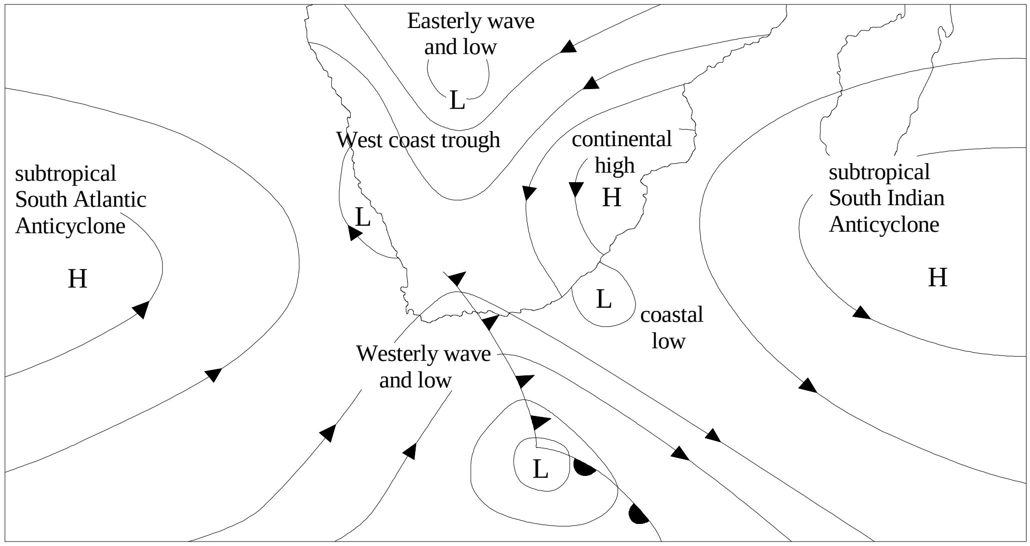

Figure 3.8 Surface air features over southern Africa (after Preston-Whyte and Tyson, 1988).

The mean circulation of the atmosphere is anticyclonic throughout the year over South Africa (Tyson and Preston-Whyte, 2000). South Africa is located almost on the mean position of the subtropical high-pressure belt at 30°S, which undergoes a seasonal displacement of approximately 5° to 6º in the South Atlantic and South Indian Ocean (Tyson *et al.,* 1976; Tyson and Preston-Whyte, 2000). The high-pressure belt moves northwards in winter and southwards in summer and a movement of the mean position of the Indian high-pressure cell westwards accompanies the winter increase in high pressure over South Africa and the surrounding ocean (Tyson *et al.,* 1976) (Figure 3.9). At all times of the year the surface pressure field is characterised by large, semi-permanent high-pressure cells in the subtropics (Tyson *et al.,* 1996; Tyson and Preston-Whyte, 2000). The presence of this subtropical high-pressure cell tends to bring about clear conditions for much of the year, with frost occurring if temperatures drop sufficiently during cloudless nights (Tyson *et al.,* 1976; Vogel, 2000). The position of the South Atlantic high-pressure cell causes strong temperature inversions along the coast, which frequently occur in summer and rise above the level of the escarpment to produce thunderstorms (Tyson *et al.,* 1976).

Ridging anticyclones are responsible for the major rainfall producing systems in South Africa and account for 16% to 25% of the rainfall variance over the region (Preston-Whyte and Tyson, 1988). These cold fronts are a product of the meeting of the warm air from the north-east of the country and the cold sub-polar air from the

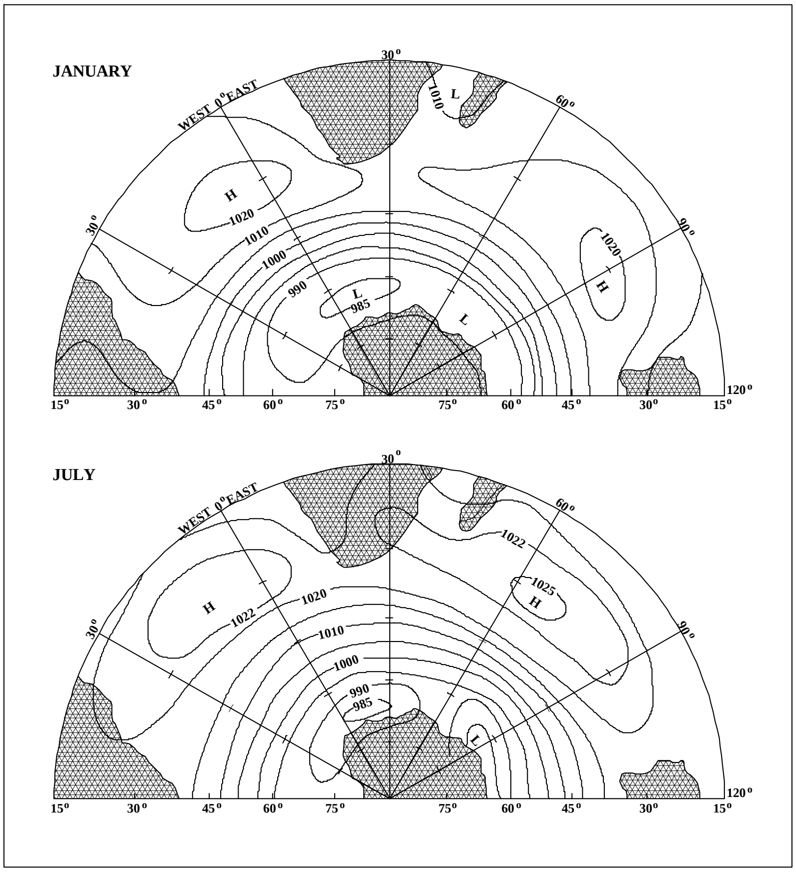

Figure 3.9 Mean January and July sea-level pressure maps (mb) of the Southern Hemisphere for longitude 60°W to 120°E and south of latitude 15°S (after Tyson *et al.,* 1976).

south-west of the country (Vogel, 2000). Warm fronts seldom occur in southern Africa, however cold fronts frequently cross the coastal areas and may occasionally penetrate inland (Vogel, 2000).

3.4.2 Temperature

It is difficult to provide precise temperature data for the Drakensberg as a result of the lack of temperature recording stations (Tyson *et al.,* 1976) and there has been failure to establish patterns of temperature change at altitudes over 1700 m a.s.l. in Lesotho (Grab, 1997b). The Drakensberg escarpment causes important temperature irregularities as a result of topographic variation and hence reduces the MAAT (Schulze, 1997). Temperatures at high altitudes in Lesotho are characterised by cool to mild summers and cold winters (Tyson *et al.,* 1976; Grab, 1994c) and the mean annual temperature for the higher peaks is believed to be around 7ºC (Schulze, 1979).

On average, the first frosts will occur on the Lesotho plateau in mid to late April and end in October, with 183 frost days per year (Tyson *et al.*, 1976). More recently, it has been suggested that some areas experience frost on 200 to 225 days per year (Schulze, 1997; Sene *et al.*, 1998).

There are many local variations in temperature caused by topography (Tyson *et al.*, 1976). Valleys tend to trap heat during the day and loose more heat at night than air over plains, as a result of valleys holding a smaller mass of air than the plains (Tyson *et al.*, 1976). Thus, it can be expected that the temperatures in the Drakensberg valleys are more extreme than over flat areas or at higher elevations (Tyson *et al.*, 1976).

3.4.2.1 Air temperature variations

A terrestrial lapse rate of 8°C/km has been suggested for Lesotho (Ambrose, 1976), however present findings show a mean annual lapse rate of 6.2°C/km (Grab, 1997b), which is closer to the accepted terrestrial lapse rate of 5.5°C/km (Meyer, 1992). The mean annual lapse rate from the montane to mid-alpine zone is only 3.9°C/km but reaches a very high value of 19.4°C/km in a belt between the mid and upper sub-alpine zones. It then drops to 3°C/km towards the alpine zone (Grab, 1997b). Although it is difficult to account for the differences in lapse rates, they may arise due to variations in wind frequency (Grab, 1997b). Further work suggests that cold fronts have a considerable impact on lapse rates, especially before and after the passing of the cold front, where lapse rates may reach 10.2°C/km (Grab and Simpson, 2000).

3.4.3 Precipitation

The Drakensberg escarpment is situated in the summer rainfall region receiving maximum precipitation (Vogel, 2000). The zone of maximum precipitation along the main escarpment is estimated to be between 2287 m a.s.l. to 2927 m a.s.l., but decreases rapidly towards the western interior (Killick, 1963). Rains in Lesotho vary from long frontal and orographic drizzle to hard convective downpours (Wilken, 1978) and are markedly influenced by local topography (Tyson, 1986). Most of the rain falls between October and March during spring and summer (Killick, 1976; Sene *et al.*, 1998), and typically accounts for 80% of the average annual rainfall (Calles and Kulander, 1996; Sene *et al.*, 1998), whilst less than 10% falls between May and August (Tyson *et al.*, 1976). Summer thunderstorms are the primary precipitation producing systems over the escarpment (Sene *et al.*, 1998) and may produce rainfall intensities in excess of 10 mm per hour in more than 7% of all storms (Tyson and Preston-Whyte, 2000). It has been suggested that the mean annual frequency of storms in the Drakensberg is approximately 80 events (Griffiths, 1972), however Schulze (1965) suggests that these storms occur on approximately 100 days per annum during mid to late afternoon. There are two categories of storms which occur over the Drakensberg escarpment; those that move to the northeast and develop along large-scale squall-lines, and those that develop as a result of local slope convection along the escarpment (Tyson *et al.*, 1976). Light orographic rain can also occur at any time on the eastern escarpment when moist maritime air comes from the east (Sene *et al.*, 1998). The escarpment produces a rain shadow to the western interior, where a marked decrease in precipitation occurs (Schulze, 1979) (Figure 3.10). In addition, a study undertaken by Sene *et al.* (1998) indicates that greater rainfall occurs on the eastward facing slopes than on other nearby slopes at a similar elevation.

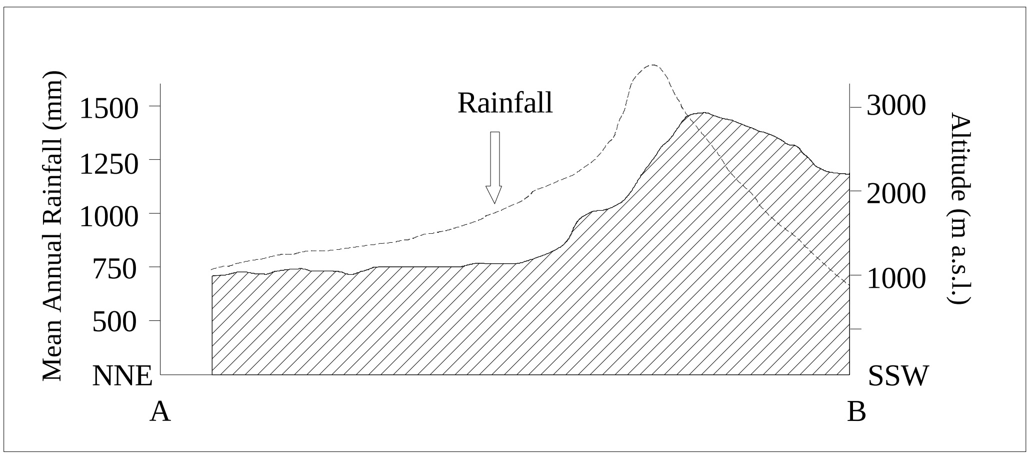

Figure 3.10 Rainfall: altitude relationship along A (Bergville) to B (Mothelsessane), Lesotho (after Schulze, 1979).

Cold front events are relatively frequent over the eastern regions of southern Africa, occurring approximately 43 times annually (Grab and Simpson, 2000). They occasionally bring snowfalls during winter and snow is common in the highest regions in the north-eastern highlands, occurring on average five to ten times during the months of June and July (Sene *et al.*, 1998). This is similar to the frequency of 8.3 snowfalls per annum, proposed by Schulze (1997), of which 5.2 may be expected from May to August. Snow may lie for up to two months on the south-facing slopes during winter (Killick, 1976). Light to moderate snowfalls occasionally occur throughout the year, however are primarily confined to months between April and September (Grab, 1994c). Contemporary cold front events tend to deliver snow only to the high Drakensberg escarpment and any snowfalls decline rapidly westwards (Grab and Simpson, 2000). The suggested increase in the frequency of cold fronts in autumn and spring during the LGM (as described in Chapter 1), would have resulted in heavier snowfalls, which would have increased the snow cover at higher altitudes and in turn significantly altered the albedo (Grab and Simpson, 2000).

3.4.4 Winds

Gradient winds in winter, south of 20º, are dominated by the permanent high over the south Atlantic and Indian Ocean, and by the annual fluctuations of the Intertropical Convergence Zone (ITCZ) (Linacre and Geerts, 1997). Trade winds bring warm moist air along the east coast during summer (Linacre and Geerts, 1997). Diurnal wind variations over the Drakensberg escarpment at Sani Pass have been described by Preston-Whyte (1971). North-westerly winds were recorded at night, whilst south-easterly winds were recorded by day. The north-westerly winds were described as upper winds which conform to pressure gradients of the general circulation over South Africa and were channelled near the surface due to the north-west to south-east alignment of the Sani valley, whereas the south-easterly winds were attributed to a local valley wind (Preston-Whyte, 1971). In contrast, airflow over the southern Drakensberg escarpment is described by Freiman *et al.* (1998) and indicates no real variation between summer and winter. Dominant winds are mostly northerly, with a secondary peak of north-north-westerly winds (Freiman *et al.*, 1998). This is similar to findings by Sene *et al.* (1998), who suggest that prevailing winds in winter are from the north and west, whilst they are from the north and east in summer. Winds blowing from the north and north-west may reach speeds exceeding 30 m s^{-1} (Freiman *et al.* 1998). Freiman *et al.* (1998) identify two major flow types; namely lee eddies and jets, where air descends towards the coast over the Drakensberg and low-velocity flow off the southern African plateau and up the mountain slopes.

The local winds occur in response to solar heating of the ground by day and infrared cooling at night (Tyson *et al.*, 1976). During the day the warm air moves up the slopes and at night air moves downslope by katabatic flow, filling the hollows with cold air

(Tyson *et al.*, 1976; Freiman *et al.* 1998). Accumulated cool air within valleys tends to drain down-valley in *mountain winds*, whereas up-valley airflow occurs in *valley-winds* (Tyson *et al.*, 1976).

3.4.5 Palaeoclimate

Continuous, high series, reliably dated proxy data are still rare in southern Africa, making it difficult to test regional palaeoclimates (Tyson, 1999). Oxygen isotope records for an ocean sediment core taken off the KwaZulu-Natal coast show that climate oscillations for the region are similar to those for elsewhere in the world during Late Pleistocene times (Prell *et al.*, 1979). Glacial and Interglacial conditions occurred with a quasi-periodicity of approximately 100 000 years, as a result of Milankovitch forcing caused by changes in the eccentricity of the earth's orbit (Prell *et al.,* 1979).

Milankovitch forcing of climate change is evident in South Africa during the past 200 000 yrs through both the 100 000 year and 23 000 year effect (Partridge *et al.,* 1997; Tyson and Partridge, 2000; Tyson and Preston-Whyte, 2000). Perihelion currently occurs in early January in the Southern Hemisphere, whilst aphelion occurs in early July, which causes Southern Hemisphere summers and winters to be more severe than their northern counterparts (Tyson, 1999; Tyson and Partridge, 2000; Tyson and Preston-Whyte, 2000) (Figure 3.11). The opposite is true after 11 500 years, and the cycle then reverts back after a further 11 500 years (Tyson, 1999; Tyson and Partridge, 2000; Tyson and Preston-Whyte, 2000). When perihelion occurs during the mid-southern Hemisphere summer (at present), wetter conditions prevail as the temperature gradient between equator and South Pole strengthens, yet when aphelion occurs in the mid-southern Hemisphere summer, drier conditions prevail as the temperature gradient between equator and South Pole weakens (Tyson, 1999; Tyson and Partridge, 2000; Tyson and Preston-Whyte, 2000). The precessional low which occurred at the beginning of the Holocene is associated with reduced incoming solar radiation and dry conditions south of the equator, whilst north of the equator wetter conditions prevailed as a result of a northward shift in the ITCZ (Partridge and Scott, 2000; Tyson and Partridge, 2000).

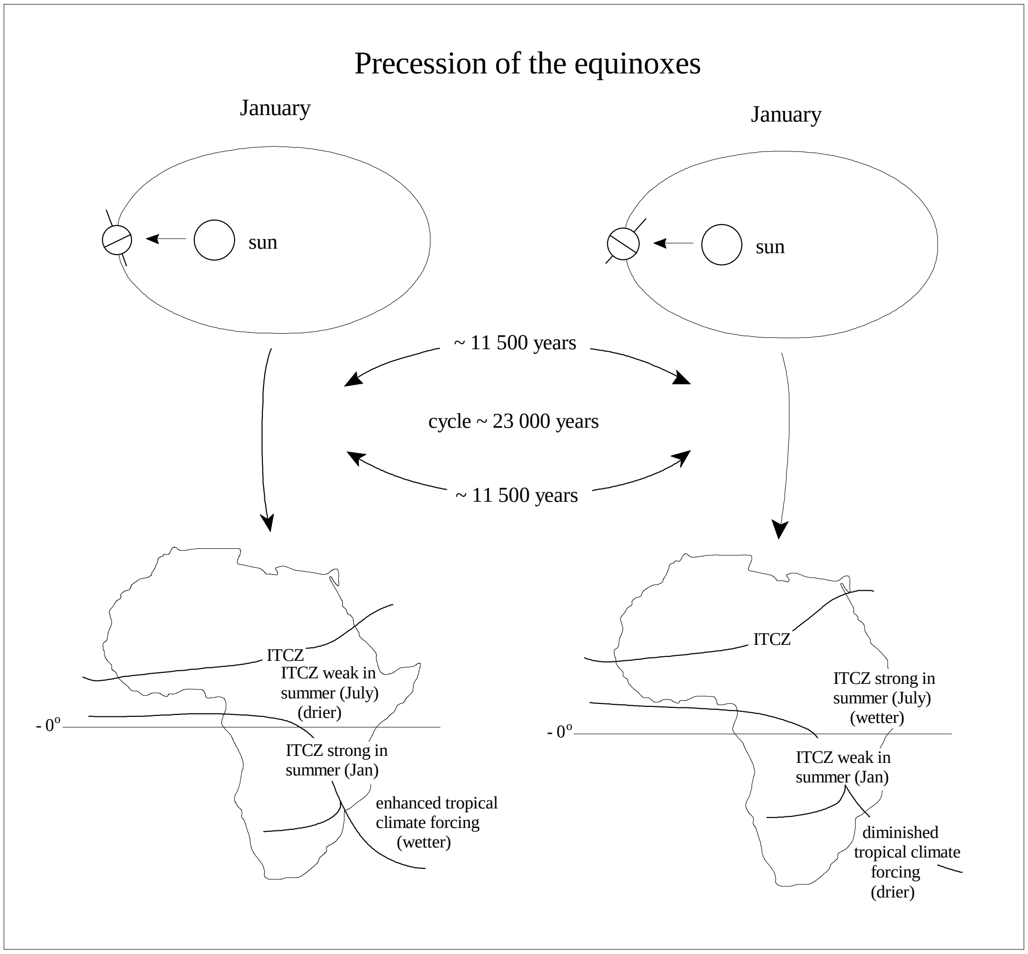

Figure 3.11 The forcing of climatic change over Africa as a result of the 23 000 year cycle of the precession of the equinoxes (after Tyson and Preston-Whyte, 2000).

Early proxy records from a stalagmite from the central interior indicated a Glacial Maximum temperature of 8°C to 9.5°C lower than at present (Talma *et al.*, 1974). Records of dissolved $\delta^{18}O$ and N_2 from the Uitenhage artesian aquifer, southern Cape (Heaton *et al.*, 1986) and records of dissolved Ne, Ar, Kr and Xe in the Stampriet artesian aquifer in south-eastern Namibia (Stute and Talma, 1997) indicate a maximum cooling during the LGM of 5°C to 6ºC. Further proxy data are found from an $\delta^{18}O$ record from a stalagmite from the Cango Cave in the southern Cape, which reveals that coldest terrestrial conditions were observed in the southern coastal region of South Africa at around 18 000 yrs BP, when temperatures were lowered by about 5°C (Talma and Vogel, 1992). Stalagmite evidence in the Makapansgat Valley indicates a 5.7°C temperature lowering during the Late Pleistocene (Holmgren *et al.*, 2003), which compares well with estimates of 5° to 6ºC (Heaton *et al.*, 1986; Talma and Vogel, 1992; Stute and Talma, 1998). The stalagmite also indicates drier conditions, lower temperatures and sparser grass cover at around 23 000 yrs BP to 21 000 yrs BP, 19 500 yrs BP to 17 500 yrs BP and 15 000 yrs BP to 13 500 yrs BP (Holmgren *et al.*, 2003) (Table 3.2).

Table 3.2 The climatic reconstruction for southern Africa with time.

Stage	Timescale
Cold Stage	23 000 – 21 000 yrs BP[1]
Warm Stage	21 000 – 19 500 yrs BP[1]
Cold Stage	19 500 – 17 500 yrs BP[1], 18 000 yrs BP[2]
Warm Stage	17 500 – 15 000 yrs BP[3], 15 000 yrs BP[4,5,6]
Cold Stage	15 000 – 13 500 yrs BP[1,3]
Warm Stage	13 500 yrs BP[3]

[1](Holmgren *et al.*, 2003), [2](Talma and Vogel, 1992), [3](Scott, 1999), [4]Partridge *et al.*, 1990), [5](Partridge, 1993), [6](Partridge, 1997b).

Widespread evidence is available to demonstrate that rapid warming took place after 15 000 yrs BP in southern Africa (Partridge *et al.*, 1990; Partridge, 1993, 1997b), however evidence presented by Holmgren *et al.* (2003) suggests a phase of renewed cooling at around 15 000 yrs BP. This is also reinforced from a pollen derived temperature index from nearby Wonderkrater (Scott, 1999), which shows rapid warming after a cold event at 17 500 yrs BP, a return to colder conditions around 15 000 yrs BP and renewed warming after about 13 550 yrs BP. Maximum cooling occurred at 17 500 yrs BP and the Wonderkrater sequence indicates a 1000 m drop in vegetation zones, which supports the 5°C to 6°C depression (Scott, 1982). The return to colder conditions from 15 000 yrs BP to 13 500 yrs BP in the stalagmite record appears to be a local reflection to the Antarctic Cold Reversal recorded in ice cores from Antarctica (Holmgren *et al.*, 2003).

Palaeoprecipitation variations are more widespread than temperature records, and the best evidence comes from palynological and lake-level studies (Partridge *et al.*, 1999). Precipitation indices based on data from a number of palynological sites reveal that over most of southern Africa, precipitation during the LGM ranged from approximately 40 % to 70% of the present mean (Scott, 1999) (Figure 3.12). Postglacial warming was accompanied by increased wetness, almost everywhere after16 000 yrs BP (Partridge, 1997b). Sediment taken from the Tswaing Crater indicates that rainfall was approximately 25% lower than at present in this area (Partridge 1997b; Tyson and Partridge, 2000). Rainfall appears to have been lower over the entire subcontinent of South Africa between 21 000 yrs BP to 18 000 yrs BP, with the smallest drop in precipitation experienced over the eastern regions of South Africa (Partridge *et al.*, 1999; Tyson and Preston-Whyte, 2000).

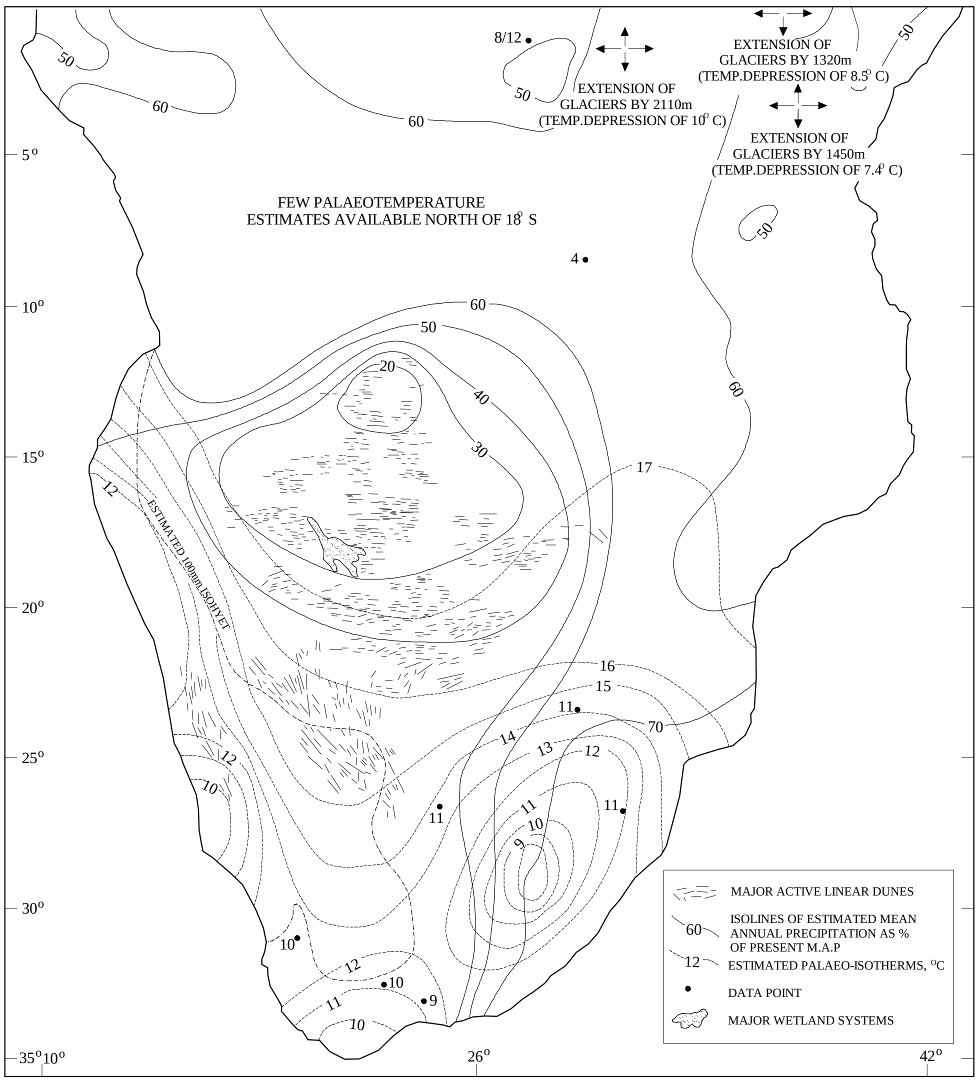

Figure 3.12 Palaeoclimatic reconstruction for Africa south of the equator at the Last Glacial Maximum (*c*. 21-18 kyr) (after Partridge, 1997b).

It has been suggested that the summer rainfall region of southern Africa was drier during the LGM based on lower $\delta^{18}O$ values from stalagmites in the Makapansgat valley (Holmgren *et al.,* 2003). It has however been suggested that during drier periods, although annual rainfall is less than during wetter periods, thunderstorms and hail increase in frequency and the rainfall amount in single rainfall events may also be increased (Holmgren *et al.,* 2003). There is evidence from the Makapansgat valley that wetter conditions accompanied warming between 17 500 yrs BP and 15 000 yrs BP, which concurs with similar trends in the Southern Hemisphere polar and tropical ice-core records (Thompson *et al.,* 1995; Steig *et al.,* 2000; Holmgren *et al.,* 2003). It has also been proposed that the intensity of anticyclonic circulation was significantly greater during the LGM and that there was a shift to a greater proportion of winter rainfall (Tyson, 1999; Partridge *et al.,* 1999; Tyson and Partridge, 2000).

3.5 VEGETATION

Lesotho is a grassland country with an almost complete absence of natural tree growth (Nixon, 1973). Three types of vegetation dominate the Kingdom of Lesotho, namely the Alti Mountain Grassland, Afro Mountain Grassland and Cold Highveld Grassland (Low and Rebelo, 1996) (Figure 3.13). The Alti Mountain Grassland is the dominant vegetation type at the study sites and occurs at an altitude of between 2 500 m a.s.l. and 3 480 m a. s. l. It consists mainly of tussock grasses, ericoid dwarf shrubs and creeping or mat-forming plants (Van Zinderen Bakker and Werger, 1974; Granger and Bredenkamp, 1996).

The climax community on the summit of the Drakensberg is *Erica-Helichrysum* Alpine Heathland which consists of dwarf and low shrubs, which are 15 cm to 60 cm high. The *Erica dominans* heathland is the most extensive of the heathland communities (Killick, 1976). It is a dwarf or low shrub, 5 cm to 45 cm high and occurs on lower levels of the summit, forming dense communities interspersed with alpine grasses, and is usually located above 3200 m a.s.l. (Killick, 1976) (Figure 3.14).

More recently the Grassland area of the Drakensberg has been renamed '*The Drakensberg Alpine Centre*' (DAC). The DAC covers 40 000 km^2 (Carbutt and

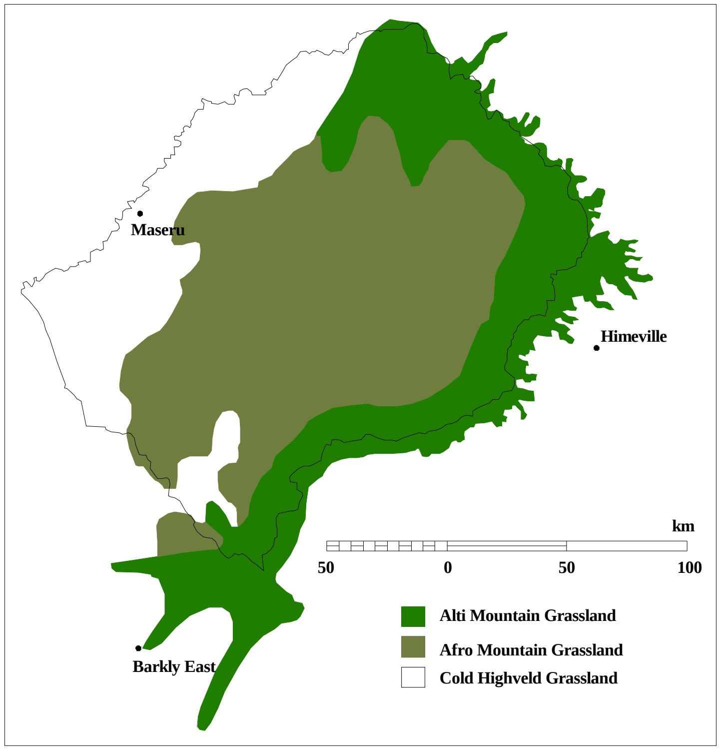

Figure 3.13 Vegetation types of Lesotho. Source: The Vegetation of South Africa, Lesotho and Swaziland (1: 2000 000 map) (after Low and Rebelo, 1996).

Figure 3.14 An example of the *Erica-Helichrysum* vegetation in the Drakensberg at 3160 m a.s.l. (photo by S. Mills).

Edwards, 2006) and encompasses the high plateau of Lesotho and the western boundary of KwaZulu Natal and the Eastern Cape Drakensberg (Carbutt and Edwards, 2004). It is regarded as being the only true alpine region in southern Africa (Linder, 1990) and ranks as having the fourth richest regional flora in southern Africa, based on the estimated 2618 species identified by Carbutt and Edwards (2004).

3.6 SUMMARY

There appears to be no variation in the geology at the study sites, where basalt makes up the bedrock. This basalt tends to weather rapidly (Van Rooy and Van Schalkwyk, 1993; Bell and Haskins, 1997); however the basalt at the various sites appears to be amygdaloidal and therefore rich in plagioclase, suggesting that this type of basalt is more resistant to weathering than olivine rich basalt (Bell and Haskins, 1997). The study sites fall within the summer rainfall region of southern Africa and are characterised by relatively cool temperatures. There appears to be unanimous agreement concerning the palaeotemperatures for southern Africa during the LGM, with average temperature reductions in the range of 5°C to 6°C (Talma and Vogel, 1992; Stute and Talma, 1997; Holmgren *et al.,* 2003), and suggestions that the climate was drier during this time period (Scott, 1999; Partridge, 1997b; Tyson and Partridge, 2000; Holmgren *et al.,* 2003). The present-day vegetation at the study sites consists of Alti Mountain Grassland with a climax community of alpine heathland; however it has been suggested that during the LGM the Lesotho highlands were occupied by steppe vegetation (Partridge *et al.,* 1999).

CHAPTER 4

Methodology

4.1 INTRODUCTION

This chapter presents the procedures adopted for sedimentological analysis, morphological mapping, palaeoclimatological reconstruction, glacial reconstruction and hillshade modelling work at the research sites. Four sites were chosen and six depositional features sampled in order to undertake meaningful research and obtain quantitative results (Figure 1.4). The Tsatsa-La-Mangaung site was initially chosen for its accessibility, whilst the Sekhokong and Leqooa Valley sites were chosen due to their varied depositional morphologies (Sekhokong) and the relative proximity of individual deposits to each other (Leqooa Valley). The Sehonghong River site was chosen in order to provide a comparison between the linear deposits at the Tsatsa-La-Mangaung, Sekhokong and Leqooa Valley sites and the colluvial mantles found on both the north- and south-facing aspects of the Sehonghong valley.

4.2 FIELDWORK

4.2.1 Sedimentological Analysis

4.2.1.1 Field Procedure

Sampling localities were selected at the upper, mid and lower crest positions along the Tsatsa-La-Mangaung, Sekhokong and Leqooa deposits, where trenches were dug through the crest of the features. These sampling localities were chosen in order to evaluate sedimentological differences between the upper, middle and lower positions of the deposits. The trenches were dug to depths ranging from 1.45 m to 1.9 m, beyond which it became impossible to excavate boulders. Loose material was cleared, in order to expose the undisturbed sediment.

At the Sehonghong River site, two sampling localities were selected along the south-facing exposure and one sampling locality along the north-facing exposure. The sampling localities were chosen according to their accessibility for sampling as the exposures reached 12 m in height and were extremely unstable in places. The north-facing exposure was chosen in order to make comparisons with the two south-facing exposures. The faces were cleared as best as possible, however this was often difficult in the case of the two south-facing exposures due to slumping of material.

Fieldwork was undertaken at 40 cm intervals at the Tsatsa-La-Mangaung, Sekhokong and Leqooa Valley sites, and in each visible stratigraphic unit at the Sehonghong Site. Texture, sorting, colour, induration, shape and clast fabric were recorded and samples were collected for particle size analysis and radiocarbon dating in the laboratory. The soil profile data collected for the trenches were reproduced as logs for each individual trench using a modified graphic data chart after Krüger and Kjær (1999) (Figure 4.1).

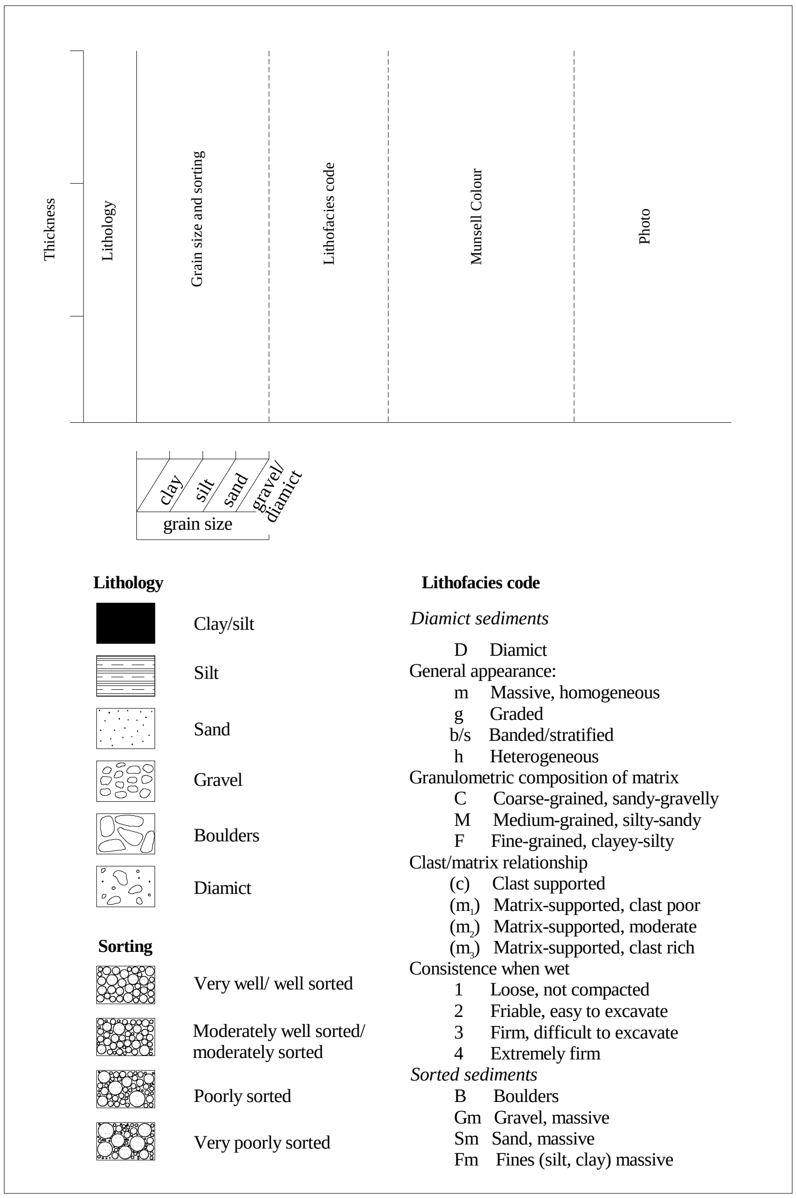

Figure 4.1 Data chart for field description of diamicts and associated sediments (modified from Krüger and Kjær, 1999).

4.2.1.2 Texture

Texture was measured in the field using a chart produced by Chilingar (1982) (Fig. 4.2). Soil texture describes the proportions of sand, silt and clay particles in the soil and this field analysis was used to complement particle size analysis results.

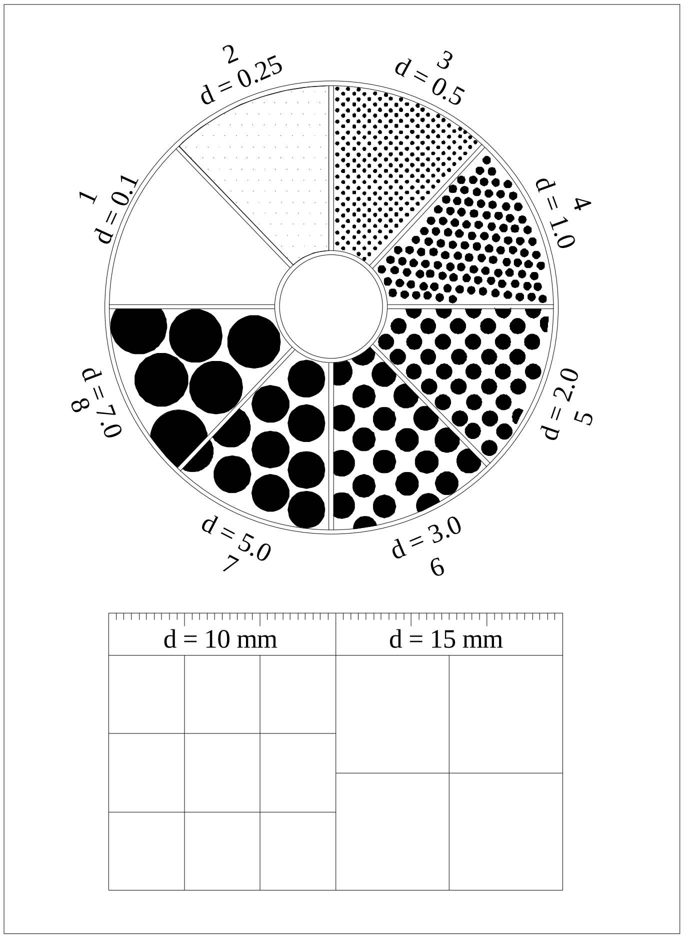

Fig. 4.2 Diagram for determining texture (after Chilingar, 1982).

4.2.1.3 Sorting

Sorting of the sediment was estimated using standard images such as the ones by Hubbard and Glasser (2005) (Figure 4.3). This method is used to demonstrate any downward sorting of the sediment which relates to particular depositional environments. This was used to complement statistical sorting calculations described in a later section. This method was chosen for its practical field value, whereby the images were inserted in a field book and compared to each sampling site.

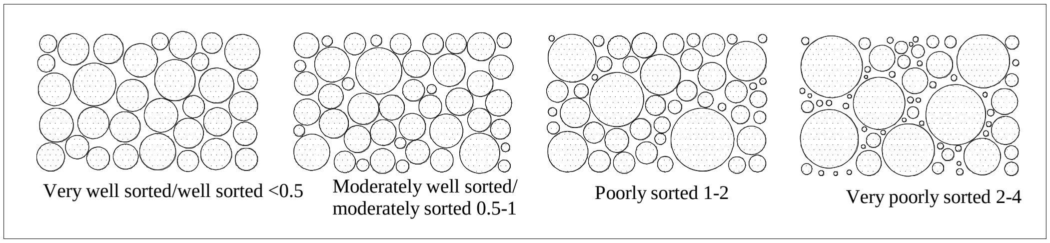

Fig. 4.3 Sorting images (after Hubbard and Glasser, 2005).

4.2.1.4 Colour

Sediment colour was determined using the Munsell colour system. Colour is a useful indicator of the processes operating in the soil profile and is controlled by the amount of organic matter and the state of any iron present (Graham, 1988).

4.2.1.5 Induration

Induration was recorded, which provides an indication of the degree to which material has been weathered. This is determined by assigning a class of hardness to the material and was achieved using the outline in Graham (1988) (Table 4.1).

Table 4.1 Qualitative scheme for induration (hardness) (after Graham, 1988).

Terminology	Description
Unconsolidated	Loose
Very friable	Crumbles easily between fingers
Friable	Rubbing with fingers frees numerous grains. Gentle blow with hammer disintegrates sample
Hard	Grains can be separated from sample with a steel probe. Breaks easily when hit with hammer
Very hard	Grains are difficult to separate with a steel probe. Difficult to break with a hammer
Extremely hard	Sharp hammer blow required. Sample breaks across most grains

4.2.1.6 Clast Fabric

Clast fabrics were assessed in the field with n = 50 per sampling locality (Dowdeswell and Sharp, 1986; Benn, 2004a; Hubbard and Glasser, 2005), based on the presence of a distinctive a-axis (a-b ratios of > 3:2) (Rose, 1974; Dowdeswell and Sharp, 1986). The clasts measured between 2 cm and 20 cm in order to try and limit variability, as fabric characteristics may vary with clast size for a variety of reasons

(Benn, 1994b; Kjaer and Krüger, 1998). Clasts were also sampled from as small an area as possible, to avoid variability associated with subtle facies changes (Benn, 2004a). The individual clast orientations were adjusted to True North, based on the magnetic declination on the South Africa 1:50 000 Sheet (1986) for Sani Pass, Sani Pass West, Manamaneng and Giants Castle.

4.2.1.7 Particle Shape

The a, b and c axes of 50 clasts excavated from each trench were measured using vernier callipers for those particles with an a-axis of less than 15 cm and a tape measure for those with an a-axis greater than 15 cm. These measurements permit the calculation of grain shape (form, sphericity and roundness) in the laboratory. Roundness was assessed in the field by comparing the clasts to a set of standard images (Figure 4.4). Particle shape is potentially important when determining the geomorphic processes which may have produced the features (Benn and Ballantyne, 1993), however problems may arise as a result of the need for subjective assessment. This may be in identifying the location of the three orthogonal axes or with the use of comparative images (Barrett, 1980).

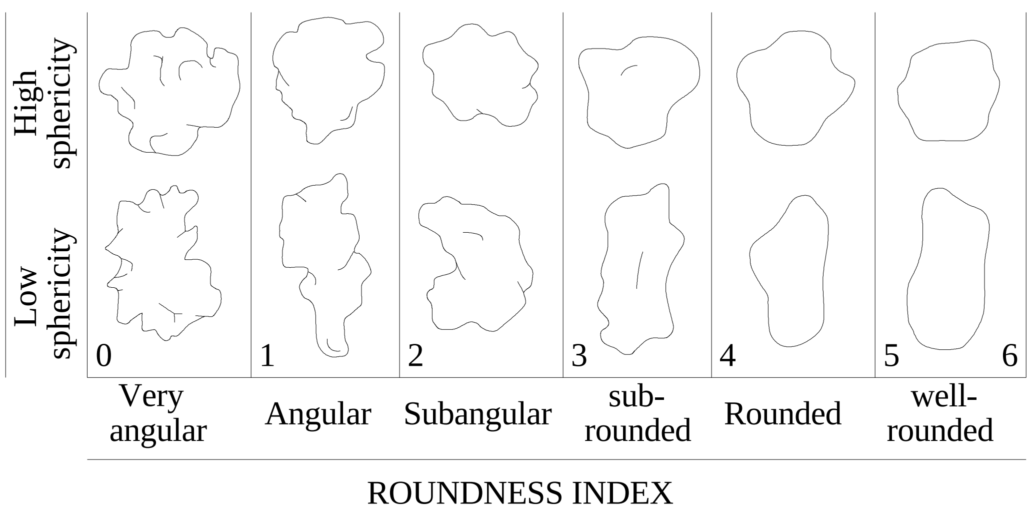

Figure 4.4 Visual images for the determination of roundness of clasts (modified from Powers, 1953; after Benn, 2004b).

4.2.1.8 Radiocarbon Dating

A sample of approximately 4 kg of sediment was collected from each trench at the Tsatsa-La-Mangaung site and one sample from each deposit for the Sekhokong and Leqooa Valley sites for radiocarbon dating. The face of the exposure was cleaned and samples were collected at the maximum depth of each trench, and in the case of the Sekhokong and Leqooa sites, in the deepest trench. This was in order to obtain the most accurate date for the time of deposition and reduce the risk of contamination from root penetration, and deposition of organic compounds of different origins and activities (Goudie, 1981). The samples were then submitted to the Quaternary Dating Research Unit in Pretoria where soil organic matter was extracted for dating. The samples were placed in an oven at 70° overnight in 1% HCL in order to remove any $CaCO_3$. The samples were then washed with distilled water until they attained PH4 and sent off to Groningen for Accelerator Mass Spectrometry (AMS) analysis. AMS is a technique for isotopic analysis, where atoms extracted from a sample are ionized, accelerated to high energies, separated according to their momentum, charge and energy and then individually counted as having correct atomic number and mass (Tuniz, *et al.*, 1998). AMS enables the use of very small samples of carbon-bearing substances (Watchman and Twidale, 2002). Radiocarbon ages for the Sehonghong Site were provided by Prof. Stefan Grab.

The radiocarbon dates are reported in conventional radiocarbon years (i.e. using a half-life of 5568 for ^{14}C. Ages are corrected for variations in isotope fractionation and are given in years BP (i.e. before AD1950). The ages were then calibrated for the southern Hemisphere at the Council of Scientific and Industrial Research (CSIR) in South Africa, using the Pretoria programme (Talma and Vogel, 1993, updated 2000). This calibration procedure uses a simplified approach to the calibration of radiocarbon dates by using splines through the tree-ring data as calibration curves, and thus eliminating a large part of the statistical scatter of the data points (Talma and Vogel, 1993). The ages are given in years BC and the 1 and 2 sigma values are interpreted as the 68% and 95% confidence intervals (Talma and Vogel, 1993). In order to obtain the age in yrs BP (i.e. before AD1950), 1950 was added to the BC ages.

4.2.2 Mapping

A topographic survey of the Tsatsa-La-Mangaung area was undertaken in order to produce a topographic map of the main depositional ridge using a Total Station 550 and further surveying equipment (Supplied by the Department of Mining and Engineering, University of Witwatersrand). Three 'station points' were selected, from where good views of the deposit were obtained. The Total Station 550 was set up at each of the stations and the vertical and horizontal angles recorded to the other stations in order to obtain a closed traverse for maximum accuracy. Survey points were recorded by measuring angles and distances to a prism, held by a field assistant. A Global Positioning System (GPS) was used in order to obtain coordinates for the stations, which then enabled the map to be linked to the South African coordinate system. These coordinates were in Latitude and Longitude and were converted to X, Y, Z coordinates in an Excel package. Once the data had been collected, the coordinates and the angle readings to the stations were placed into the starnet statistical package, in order to calculate X, Y and Z coordinates for each of the stations and for the survey points. Starnet uses the Chi Square test in order to produce a confidence interval of 95% for the traverse and the detailed points within it. The topographic map was created using AutoCAD 2000, which is a computer aided design software package and contours were added.

The Sekhokong and Sehonghong sites were mapped using a Garmin Summit hand-held GPS system. It was not feasible to undertake a more detailed survey, given the difficult access to the sites. The hand-held GPS enables a horizontal position accuracy of 5 m to 10 m depending on the amount of satellites received. The deposits were mapped when there were the maximum numbers of satellites available (usually at least six). The points recorded by the GPS were converted into X, Y and Z coordinates in order to plot them in the same manner as those for the Tsatsa-La-Mangaung deposit. The Leqooa Valley deposits were mapped with assistance from Nicolas Mulder and Helen Every, using a hand-held GPS to obtain coordinates and levels for the site and a compass, electronic tape measure and abney level. The direction and distance values were plotted in AutoCAD and differences in level calculated to obtain coordinates and levels for each point. The deposits were then drawn and contours added, similar to those for the Tsatsa-La-Mangaung, Sekhokong and Sehonghong sites.

4.2.3 Thin section collection

4.2.3.1 Rationale

Micromorphology is the description and interpretation of sediment features that are not visible to the naked eye (Stoops, 2003). Micromorphological assessments have proved useful for the interpretation of sediments, either alone or in conjunction with macro-scale techniques (Van der Meer, 1993; Carr, 1998). This technique was applied to the sediments at the various sites in order to help ascertain possible past transportational and depositional processes.

4.2.3.2 Sampling Strategy

Sampling positions where the thin sections were collected depended mostly on the presence of boulders, which restricted the number of thin section samples to three per trench at Tsatsa-La-Mangaung, three per site at the Sekhokong site and two per site at the Leqooa Valley. Fewer samples were collected at the Sekhokong and Leqooa sites as it was thought unnecessary and time consuming to collect more, especially given that the analysis of the Tsatsa-La-Mangaung thin sections revealed little variation between samples. It was initially decided that one sample would be collected per trench at the Sekhokong and Leqooa Valley sites, however once in the field this was impossible due to the nature of the material in some of the trenches. This meant that sometimes two samples were collected in the same trench. Samples were only collected at Sites 1 and 2 of the Sehonghong Site as the material at Site 3 was exceptionally compact as a result of the lack of any rain for several weeks.

4.2.3.3 Sample Collection

The samples were collected according to the methods outlined in Murphy (1986) and Lee and Kemp (1992), using Kubiena tins (Figure 4.5). The sampling area was identified and the face cleaned. One lid from the Kubiena tin was removed, placed on the cleaned face and inserted. Due to the nature of the bouldery material, it was also necessary to cut around the outside of the tin with a pointer trowel whilst guiding the tin into the material. Once the tin was full, the lid was labelled with the sample number, site, orientation and depth.

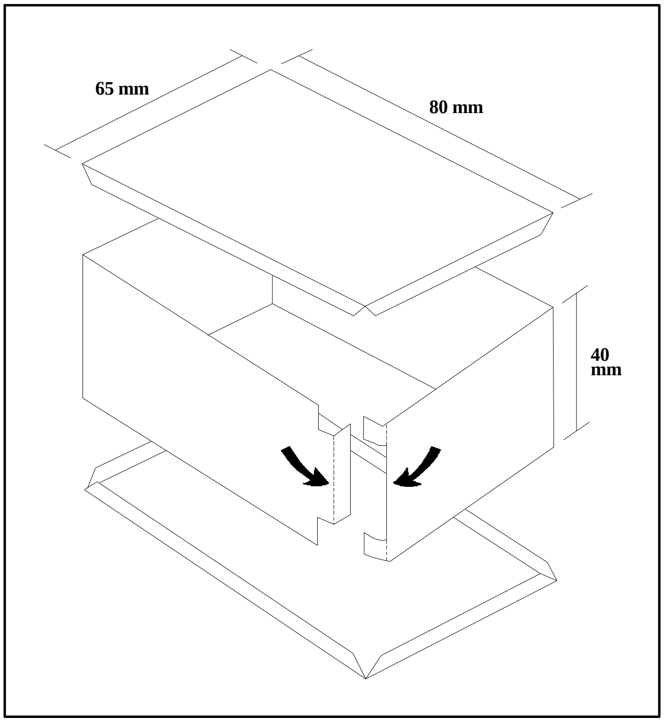

Figure 4.5 Kubiena Tin (after Lee and Kemp, 1992).

Material around the perimeter of the tin was subsequently cut away and the tin removed by inserting the pointer trowel behind the sample, whilst ensuring that an excess of material was left on the open side of the tin. This excess was then carefully removed to the level of the tin and the face covered by the other lid. Where protruding stones made it impossible to replace the lid, the sample was wrapped in cotton wool and polythene bags without the lid, as suggested by Murphy (1986). The samples were then secured with parcel tape and wrapped in aluminium foil and placed in polythene bags to preserve the original moisture content of the samples.

4.3 Laboratory Work

4.3.1 Particle size analysis

4.3.1.1 Rationale

Particle size analysis provides a standard description of the sediment, and is important in understanding both contemporary and historical processes in the physical environment. It reflects the most subtle variations in average grain size or in the range of sizes of clasts, which may thus indicate important changes in the sedimentary environment (Lowe and Walker, 1997). The size of particles may contain information about the source material, the processes of erosion, transport and deposition that have produced the deposit, however only if used in combination with other kinds of evidence (Hoey, 2004).

4.3.1.2 Laboratory Procedure

Samples were collected from each trench at 40 cm intervals and placed into clean, labelled sample bags for transport back to the laboratory. Because of the large amounts of clasts within the deposits, bulk samples of approximately 1.5 kg were collected (McManus, 1988). The samples were prepared according to the methodology outlined by Bascomb and Bullock (1982) and Gale and Hoare (1991). The sample weight for sieving was chosen by following the maximum sieve loadings recommended in BS 1377:1975 (c.f. Gale and Hoare, 1991) (Table 4.2). Sieving was undertaken at ¼ phi intervals (Table 4.3), according to the methodology outlined by Graham (1988). The <63 μm samples were transported to Royal Holloway University of London where a Sedigraph 5100 was used to analyse the finer fractions of the samples.

Table 4.2 List of maximum permissible sieving loadings, after BS 1377: 1975 (after Gale and Hoare, 1991).

BS sieve mesh (mm)	***Maximum* weight (kg)**	**Sieve diameter (mm)**
20	2.0	300
14	1.5	300
10	1.0	300
6.3	0.75	300
5	0.5	300
3.35	0.3	200
2.0	0.200	200
1.18	0.100	200
0.600	0.075	200
0.425	0.075	200
0.300	0.050	200
0.212	0.050	200
0.150	0.040	200
0.063	0.025	200

Table 4.3 Phi-unit to millimetre/micrometer conversion table and the size ranges of the particle-size categories and subcategories in the scheme of Udden (1914) and Wentworth (1922) (after Gale and Hoare, 1991).

Phi-unit (ϕ)	Millimetres (mm)	Micrometres (μ)	Particle-size category	Particle-size subcategory
			gravel	granule
-1.00	2.000			
-0.75	1.682			
-0.50	1.414			very coarse
-0.25	1.189			sand
0.00	1.000			
0.25	0.841			
0.50	0.707			coarse
0.75	0.595			sand
1.00	0.500		sand	
1.25	0.420			
1.50	0.354			medium
1.75	0.297			sand
2.00	0.250			
2.25	0.210			
2.50	0.177			fine
2.75	0.149			sand
3.00	0.125			
3.25	0.105			
3.50		88.388		very fine
3.75		74.325		sand
4.00		62.500		
4.25		52.556		
4.50		44.194		coarse
4.75		37.163		silt
5.00		31.250		
5.25		26.278		
5.50		22.097		medium
5.75		18.581		silt
6.00		15.625	silt	
6.25		13.139		
6.50		11.049		fine
6.75		9.291		silt
7.00		7.813		
7.25		6.570		
7.50		5.524		very fine
7.75		4.645		silt
8.00		3.906		
8.25		3.285		
8.50		2.762		coarse
8.75		2.323		clay
9.00		1.953		
9.25		1.642		
9.50		1.381		medium
9.75		1.161	clay	clay
10.00		0.977		
10.25		0.821		
10.50		0.691		fine
10.75		0.581		clay
11.00		0.488		

4.3.1.3 Data Representation

The Sedigraph computer package was used in association with an Excel spreadsheet to combine the >63 μm and <63 μm data sets. The results were calculated and displayed as percentage weights. Cumulative percentage particle size graphs and percentage sand, silt and clay bar graphs were generated for each phi unit. Graphic mean, mode, bimodality, inclusive graphic standard deviation, inclusive graphic skewness and graphic kurtosis (Folk and Ward, 1957) were also calculated in order to attempt to relate these results to particular environments and processes.

Graphic Mean (M_z) (phi units) (Folk and Ward, 1957):

$$\boldsymbol{M_z = (\phi 16 + \phi 50 + \phi 84) / 3}$$

ϕn is the particle size in phi units at which *n%* by mass of the distribution is coarser.

The Mode of a distribution is the value of the variable that appears most frequently (Burt and Barber, 1996). This is extremely useful for skewed distributions where the mean is not very useful.

Where distributions have two modes, the bimodality index (B^*) may be employed (Hoey, 2004).

Bimodality Index (B^*) (Sambrook Smith *et al.*, 1997):

$$\boldsymbol{B^* = [\phi_2 - \phi_1] (F_2 / F_1)}$$

Subscript 1 refers to the primary mode and subscript 2 to the secondary mode. F_1 and F_2 refer to the proportions of sediment in the two modes, where a mode is defined as the four contiguous ¼ phi units containing the largest proportion of sediment (Hoey, 2004). Where a distribution has a value of B^* in excess of 1.5-2.0, then it can be described as bimodal. Values of <1.5 are unimodal and values within the 1.5-2.0 range are transitional (Hoey, 2004).

Inclusive Graphic Standard Deviation (σ_I) (phi units) (Folk and Ward, 1957):

$$\sigma_I = [(\phi 84 - \phi 16) / 4] + [(\phi 95 - \phi 5) / 6.6]$$

Inclusive Graphic Skewness (SK_I) (phi units) (Folk and Ward, 1957):

$$SK_I = \frac{\phi 16 + \phi 84 - (2\phi 50)}{2(\phi 84 - \phi 16)} + \frac{\phi 5 + \phi 95 - (2\phi 50)}{2(\phi 95 - \phi 5)}$$

Graphic Kurtosis (K_G) (phi units) (Folk and Ward, 1957):

$$K_G = (\phi 95 - \phi 5) / [2.44 (\phi 75 - \phi 25)]$$

4.3.2 Thin Section Manufacturing

4.3.2.1 Laboratory Procedure

Thin section manufacturing was undertaken according to the methodology outlined in Lee and Kemp (1992).

4.3.2.2 Analytical procedure

Each thin section was individually analysed under a petrographic microscope, according to the outline for analysis and description of soil and regolith thin sections by Stoops (2003). Fabric analysis deals with the organisation of a soil, which is expressed by the spatial arrangements of the soil constituents, their shape, size and frequency (Bullock *et al.*, 1985). This involved looking for orientation patterns, size of particles, their sorting, shape and sphericity, and colour.

Soil microstructure relates to the relationship between the solid and the pores. The description of aggregates, voids and microstructures involves looking at peds, the shape and size of voids and their abundance. Mineral constituents were also identified and measured. Groundmass forms the base material of the soil in thin section and reflects the lithology, homogeneity and the degree of weathering of the parent material (Stoops, 2003). The description of the groundmass involved the coarse/fine (c/f) related distribution. Pedofeatures are distinct fabric units present in soil materials that are different in concentration of one or more components or in internal fabric to adjacent material (Stoops, 2003). Clay coatings and passage features are examples of pedofeatures. These were described in terms of coatings, the type of material that made up the coatings and their internal fabric. Infillings (voids filled or partly filled by soil material) (Bullock *et al.,* 1985), were also described in terms of their type. Crystals were described and classified.

4.3.3 Particle Shape

4.3.3.1 Rationale

Clast shape measurement is a valuable method for assessing the conditions under which sediments are deposited (Howard, 1992), as stated previously in section 4.2.1.7.

4.3.3.2 Particle Form

Form is the relative length of the three major orthogonal axes of a particle. Data for the a, b and c axes were plotted on shape triangles, following the method of Sneed and Folk (1958) and Benn and Ballantyne (1993). These triangles were reproduced using the TRI-PLOT spreadsheet of Graham and Midgley (2000). The a, b and c axis of each clast was entered into the table and the appropriate plotting parameters selected. The Sneed and Folk classes and the C_{40} line were selected to plot particle shape. The oblate-prolate isolines were also selected for a second shape diagram. In addition, the oblate-prolate index was calculated.

Oblate-prolate Index (OP) (Dobkins and Folk, 1970):

$$\mathbf{OP = \{10\{[(a - b) / (a - c)] - 0.5\}\} / (c / a)}$$

Where *a* is *a*-axis length, *b* is *b*-axis length and *c* is *c*-axis length (Gale & Hoare, 1991).

OP values range from -: to + :. A perfect blade has a value of 0. (A perfect blade is one where the length of the *b*-axis is exactly half the lengths of the *a*- and *c*- axes). Discs have negative values, rods positive values and a perfect sphere (where the *a*-, *b*- and *c* axes are equal in length) has a value of –5 (Gale and Hoare, 1991).

4.3.3.3 Particle Sphericity

Sphericity measures how nearly equal in length the three major axes of a particle are. The maximum projection sphericity isolines were added to the shape diagrams in TRI-PLOT. The Folk (1955) and the Sneed and Folk (1958) Xp index was also used to calculate maximum projection sphericity.

$$\boldsymbol{\psi_p = \sqrt[3]{(c^2 / ab)}}$$

Where *a*, *b* and *c* are defined above.

Values of χ_p range from 0 to 1, with a sphere having a value of 1. The more discoid a particle, the more χ_p tends towards 0 (Gale and Hoare, 1991).

4.3.3.4 Particle Roundness

Clast visual roundness which was recorded in the field was plotted as histograms, showing the percentage of the sample that falls in each of the six roundness classes (Hubbard and Glasser, 2005) (Figure 4.4).

4.4 STATISTICAL ANALYSIS

4.4.1 Clast orientation test of significance

The chi-square test was used to test the significance of clast orientation distributions against randomness (Curry, 1956). This method tests the significance of the differences between a distribution and a model of randomness, where the formula is:

$$\mathbf{X^2 = \Sigma\, [\, (\mathit{f_o} - \mathit{f_e})^2 / \mathit{f_e}\,]}$$

Where X^2 = chi-square, f_o = the observed frequency in each group, f_e = the expected frequency in each group if the distribution is random. The probability value is obtained from standard statistics tables knowing X^2 and the number of degrees of freedom, which is the number of groups minus 1 (Curray, 1956).

4.4.2 Clast Fabric

Marks' (1973) eigen value method was used to evaluate pebble fabric mathematically. This method was used because it is three-dimensional and therefore accounts for both pebble orientation and dip, as opposed to two-dimensional methods such as rose diagrams which consider only pebble orientation. The eigen value method has also been used in previous studies of pebble fabrics for a variety of environments (e.g. Lawson, 1979; Dowdeswell and Sharp, 1986). This technique treats individual observations of pebble orientation and dip as unit vectors. Three-dimensional vector analysis is used to extract the eigenvectors and eigenvalues of a 3 x 3 matrix.

Eigenvectors (V_1, V_2 and V_3) and normalised eigenvalues (S_1, S_2 and S_3) of the matrix are then computed. Eigenvector V_1 refers to the direction of maximum clustering and V_3 to that of minimum clustering. The eigenvalues summarize fabric strength or the degree of clustering. Eigenvalue S_1 measures the strength of clustering about the mean axis V_1, whereas S_3 represents fabric strengths about the axis of minimum clustering (V_3).

4.4.3 T-test for particle shape

Statistical analysis has been successfully used to test the statistical differences in particle characteristics between fan pairs in order to distinguish between depositional processes (de Scally and Owens, 2005). The significance between trenches and between deposits in each variable (oblate-prolate index, maximum projection sphericity and visual roundness) was tested using the t-test. The t-test is the most commonly used method to evaluate the differences in means between two groups (STATISTICA, 2003). The results for each variable were inserted into an excel spreadsheet and a two sample mean comparison was performed. By comparing the degrees of freedom to the distribution of t (two tailed) table it was possible to evaluate whether the two samples were statistically significant (<0.05%).

4.5 PAST CLIMATE

4.5.1 Palaeoclimatic extrapolations

Palaeoclimatic extrapolations are difficult to make for the Drakensberg region, given the absence of contemporary climate data sets. Nevertheless, it was possible to record hourly air temperatures from data loggers at two sites from 2000 to 2006. These data loggers were set up at Sani Top (2878 m a.s.l.) and Nhlangeni pass (at 2650, 2900 and 3200 m a.s.l) near the Sehonghong Valley (Figure 1.4). Mean summer temperatures

(December, January and February) for the Sani Valley were determined as suggested by several authors (Sutherland, 1984; Ohmura *et al.*, 1992; Carr, 2001). It was then possible to extrapolate the mean summer temperature for each site, assuming an average global environmental lapse rate of 0.55°C/100 m (Meyer, 1992). Unfortunately it was not possible to obtain temperature records for areas near the Sekhokong or Leqooa Valley as a result of theft of the data loggers. Thus, extrapolations had to be made from the Sani Top data records.

The extrapolated palaeotemperatures were then plotted onto a diagram by Ohmura *et al.* (1992), who produced a best-fit climate curve for the Equilibrium Line Altitudes (ELA) of 70 glaciers. These glaciers have known mass balance values and it was found that the climate at the equilibrium line could be described by using the temperature of the three summer months (December, January and February in the Southern Hemisphere), annual precipitation and the sum of global and long-wave radiation (Ohmura *et al.*, 1992). In general, if the precipitation-temperature (P-T) condition of a site falls within the zone of the points of the 70 glaciers, such a location has a good chance of being on the ELA. The site is likely to be found in the accumulation area if the P-T condition falls above the zone of the points and in the ablation area if it falls below the zone of the points (Ohmura *et al.*, 1992). The Ohmura diagram offers the opportunity to make deductions on the likely climatic changes required for glaciation at the Drakensberg study sites.

4.5.2 Reconstruction of former glaciers

4.5.2.1 Palaeoglacier outline

In order to reconstruct the limit of a former glacier, several factors need to be taken into account. These include the position of moraines, confining scarps and topography. The lower portions of the palaeoglaciers were defined by the lateral moraines (Sutherland, 1984). The upper portions were defined according to Gray (1982), who placed the upper margins of former glaciers in north Wales approximately 30 m below confining scarps, which was established as the likely depth of snow to ice transformation (Carr, 2001). The outer margins were determined based on topographical constraints. One of the most significant problems with the glacier reconstruction work discussed above is related to the lack of features which delimit the upper margins of the glaciers. Alternative upper margins would inevitably alter the shape of the palaeoglaciers and influence the location of the ELA and the mass balance characteristics (Carr and Coleman, 2006). The outlines of glaciers in cirque areas are, however, usually fixed by bedrock topography (Sailer *et al.,* 1999). It is suggested that based on the topographic controls at these sites, the upper margins of the palaeoglaciers could not have been substantially different to those presented, and that the upper portions of cirque glaciers presented by Gray (1982), is appropriate for the current reconstruction work.

Once the outline for the palaeoglaciers was established, ice surface contours were reconstructed based on contemporary glaciers which display a distinct contour pattern, with contours becoming increasingly convex below and concave above the ELA, whilst remaining almost straight at the approximate mean altitude of the glacier (Porter, 1975; Gray, 1982; Carr, 2001; Carrivick and Brewer, 2004). This method is rather subjective and alternative contour plots may have been plotted in alternative locations by a different operator. The position of contours inevitably affects glacier depth and area between contours, which in turn affects the mass balance characteristics of the palaeoglaciers (Nye, 1952). Ice surface contours were reconstructed at 20 m intervals at the Tsatsa-La-Mangaung site and at 25 m contour intervals at the Sekhokong and Leqooa Valley sites. Once the glacier contours are determined, it is possible to create the long surface profile of the glacier.

4.5.2.2 ELA calculation

Glacier equilibrium lines represent the lowest boundary of the climatic glacierization, and the climate that prevails at the glacier equilibrium line is considered to be just sufficient to maintain the existence of glaciers (Ohmura *et al.,* 1992). The Equilibrium line separates the zone of accumulation and ablation of a glacier where annual accumulation and ablation are equal, and is determined by local and regional climate and topography (Benn and Evans, 1998). It is particularly connected with annual total precipitation and summer temperature in the free atmosphere and is sensitive to any disruption in either of these two variables (Ohmura *et al.,* 1992). For mid- and high-latitude glaciers, traditional definitions of the ELA refer to altitude, where $b_n = 0$, where b_n is the net balance at the end of the ablation season (Paterson, 1994). The altitude of the ELA varies according to snow accumulation, shading and various other factors (Benn *et al.,* 2005). Variations in the ELA on a particular glacier can be used as an indicator of climate fluctuations (Kuhn, 1981). Thus fluctuations in the ELA provide an important indication of the glacier response to climate change and permit the reconstruction of past climates (Benn and Evans, 1998).

A variety of methods are available to reconstruct former ELAs, the most precise of which are based on the three-dimensional form of the glacier surface, combined with assumed mass balance-altitude relationships (Benn and Evans, 1998). In calculating past ELAs using these methods, a steady-state condition is assumed and glacial-geologic data such as lateral and terminal moraines, erratics and trimlines are used to determine the glaciers extent and topography (Porter, 1981b, 2001; Sutherland, 1984). The steady-state ELA can then be estimated by the accumulation area ratio method (AAR), which is based on the assumption that the accumulation area of the glacier occupies some fixed proportion of the total glacier area (Porter, 1975; Torsnes *et al.*, 1993) (Figure 4.6).

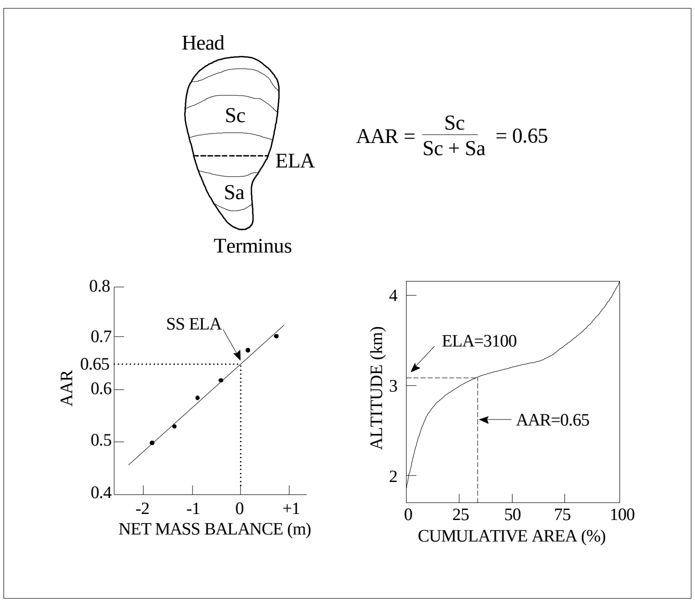

Figure 4.6 Accumulation-area ratio (AAR) method whereby Sc = accumulation area and Sa = ablation area. Empirical studies suggest a steady-state (SS) when the mass balance = 0. (after Porter, 2001).

The AAR will differ for various types of glaciers, and usually lies between 0.5 and 0.8 for mid- and high-latitude glaciers (Meier and Post, 1962; Hawkins, 1985), with typical values around 0.55 to 0.65 (Porter, 1975, 2001). Those glaciers with debris covered snouts will have lower AARs (<0.4) as a result of the effect of debris on ablation (Kulkarni, 1992), whilst glaciers in the tropics have higher AARs (0.8), as a result of steeper ablation gradients (Kaser and Osmaston, 2002).

The area of the glacier between each contour was calculated using the TurboCAD software package, in order to give a total area of the glacier. The Accumulation-area ratio (AAR) method, with an AAR of 0.6 was used (Porter, 1975, 2001). ELA is set as the altitude of the surface contour that lies below 0.6 (60%) of the total area. The area-weighted mean altitude of glaciers (MEG or AWMA) was also used to calculate the ELA of the former glaciers (Sissons and Sutherland, 1976; Sutherland, 1984). This method is best suited to regular-shaped glaciers whose area and altitude distributions do not have a wide range of variation (Porter, 1981b; Nesje, 1992). This method takes into account altitude and glacier area (total glacier area / (height * area of each contour interval)). Sources of error in the AAR method include the fact that topographic reconstructions of former glaciers tend to be subjective as there is usually little control for altitudinal constraints of the glaciers former margins above the ELA (Porter, 2001).

A further problem with the AAR and MEG methods is that they take little account of variations in glacier shape, particularly the distribution of glacier area over its altitudinal range or hypsometry (Furbish and Andrews, 1984; Benn and Gemmell, 1997). In response to this, Furbish and Andrews (1984) developed the balance ratio method, which takes into account both glacier hypsometry and the shape of the mass balance curve. This method is based on the fact that the total annual accumulation above the ELA must exactly balance the total annual ablation below the ELA for equilibrium conditions (Furbish and Andrew, 1984) (Figure 4.7). This method is time-consuming to apply, therefore Benn and Gemmell (1997) have developed a fully computerised procedure, making application of the balance ratio method very quick and easy to use. This new method has been termed the Accumulation-area balance ratio (AABR) or balance ratio (BR) method (Benn *et al.*, 2005). This method simply requires the user to input the glacier area for each contour interval, with a value of

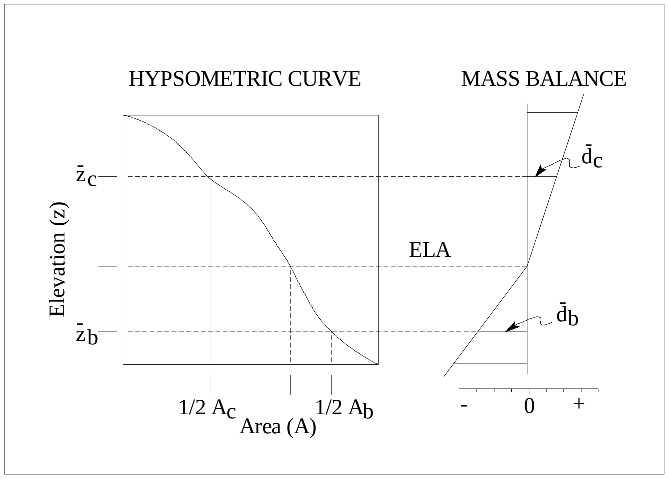

Figure 4.7 Graphical representation of the components of the balance ratio method of calculating glacier ELA's. ½ A_b and ½ A_c denote the mid-area values of the ablation area and accumulation area respectively, and Z_b and Z_c are the associated altitudes, measured relative to the ELA. At these altitudes, the net ablation (d_b) and net accumulation (d_c) are taken to be equal to the mean values for the ablation and accumulation areas (after Benn and Gemmell, 1997).

zero in the altitude bands where there is no ice, into the spreadsheet which is downloadable from the internet (Benn and Gemmell, 1997). The mass balance gradients (b_{nb} and b_{nc}) for the ablation area and accumulation area must then be determined. The value of b_{nc} was set to 1 as suggested by Benn and Gemmell (1997), whilst the value of b_{nb} was set to 0.6 (as in the case of the AAR method). However, this AABR method is also prone to errors and may overestimate the ELA by a small amount (Osmaston, 2005). In order to determine the most accurate ELA for the palaeoglaciers, an average was taken of the AAR, AWMA and AABR methods.

4.5.2.3 Ablation gradient

Ablation is the result of heat supplied to the ice or snow surface and comes from either radiation or directly from the air through convection and condensation (Schytt, 1967). Commonly, the maximum ablation occurs at the glacier snout, which is its lowest point in elevation and where air temperatures are highest, whilst the minimum ablation occurs in the upper part of the glacier. The opposite is true for accumulation (Bennett and Glasser, 1996; Nesje and Dahl, 2000). If an equilibrium condition is considered, there is a relationship between accumulation = ablation at the ELA. This is considered to be the ablation gradient (Andrews, 1972). A large gradient would be in the region of 10 mm m^{-1}, which implies rapid ice movement through the equilibrium line, to replenish ice loss and maintain the steady state (Andrews, 1972).

The precipitation value (accumulation) was converted to an ablation gradient on the basis of empirical data derived from modern glaciers (Andrews, 1972) (Figure 4.8). The data by Andrews (1972) were found to be statistically significant ($p<0.05$), suggesting that this is a valid approach for deriving glacier ablation gradients (Carr, 2001). However it only uses 13 observations, which is a very small dataset from which to infer ablation gradient for palaeoglaciers (Carr and Coleman, 2006). Although Carr and Coleman (2006) present further datasets from which to infer ablation, they suggest the need for further publications of net accumulation and net ablation in areas other than for European glaciers. The calculation of the ablation gradient enables the calculation of mass balance estimates. The amount of ablation for every metre lost was calculated for every contour interval and converted into metres. The ablation in metres for each contour interval was then multiplied by the area for each contour interval to give ablation in m^3 and added to give a total ablation and therefore accumulation value for the glacier. The total ablation and accumulation values are in water equivalent units and in order to calculate the total mass flux of the ice that must pass through the glacier ELA each year, this value was divided by 0.918 (density of ice).

4.5.2.4 Glacier mass balance calculations

Glacier balance velocity at ELA:

Total Mass Flux / glacier cross sectional area at ELA

Basal shear stress was measured using the equation:

$$t_b = p\ g\ h \sin \alpha$$

(Paterson, 1994)

Where p is the specific gravity of ice (910 kg m^{-3}), g is the acceleration due to gravity which is a standard number (9.81 m s^{-2}), h is the ice thickness at the ELA and α is the

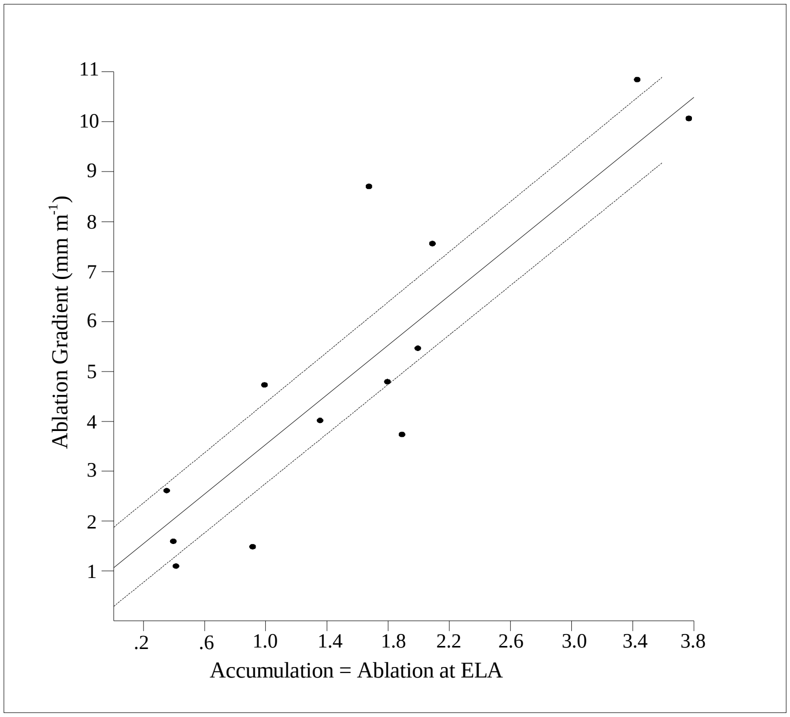

Figure 4.8 Diagram relating accumulation to the ablation gradient of thirteen glaciers (after Andrews, 1972).

surface slope. The answer obtained is in Pascals and is then divided by 100 000 to give the answer in bars. The theoretical value of t_b should range from 0.15 to 1.5 bar (Paterson, 1994).

Glacier movement can be broken down into components of ice deformation and basal slip (Murray and Locke, 1989). Ice deformation may be calculated by integrating Glens flow law of ice (Glen, 1952).

Ice deformation:

$$\mathbf{V} = \frac{\mathbf{2\,A}\,\boldsymbol{t_b\,H}}{\boldsymbol{n}}$$

(Murray and Locke, 1989)

Where A is a temperature dependant constant of 0.167 (Paterson, 1994), t_b is the shear stress (bars), H is the glacier thickness (m) and n is a constant of flow law (3). The result is given in velocity (ma^{-1}). The other component of glacier flow is basal slip. This has been measured to account for 10% to 90% of total velocity (Andrews, 1972; Paterson, 1994). Having worked out the glacier balance velocity, it is possible to calculate the percentage of the total balance velocity. This percentage gives the amount of ice deformation and the remaining percentage gives basal flow. If basal flow is greater than 95% then it is not likely to be a glacier (Carr, 2001).

4.5.3 Hillshade modelling

The position of the sun in the sky at the study sites at solar noon was calculated for the two solstices and equinoxes assuming a 1º change in solar altitude for every 1º change in latitude (Pidwirny, 2006). Therefore, at approximately 29º30"S, the suns altitude at noon is 84º during the summer solstice, 60º during the equinoxes and 37º during the winter solstice. Length of day at 29º30"S was determined from Table 4.4 and it was then possible to determine the angle of the sun in the sky at various times of the day (Figure 4.9). The effect of topography on each site was determined by the hill crest and the surrounding topography. The azimuth (angular direction of the sun) was also determined by the length of day and was measured from north in clockwise degrees from 0º to 360°.

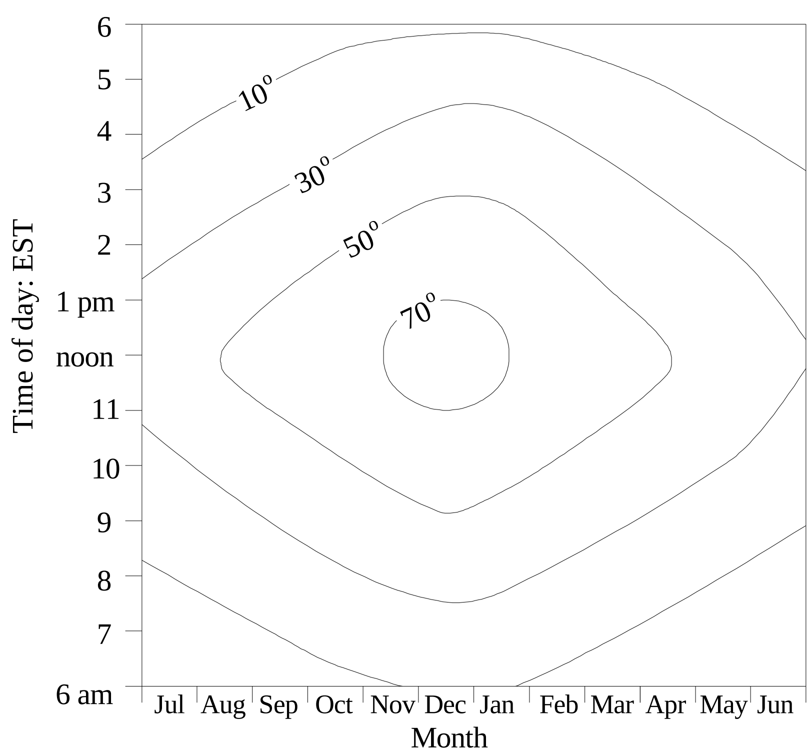

Figure 4.9 The solar elevation at various times of day in various months at 29º30"S.

Table 4.4 Effect of latitude and season on the fortnightly mean day length (after Linacre and Geerts, 1997).

Lat	*Hours of daylight in the Northern Hemisphere*																							
	January		*February*		*March*		*April*		*May*		*June*		*July*		*August*		*September*		*October*		*November*		*December*	
70º	0.5	2.2	4.5	7.0	9.8	12.7	15.5	18.0	20.3	22.4	24.0	24.0	24.0	22.4	20.2	17.8	15.1	12.2	9.5	6.9	4.5	2.3	0.3	0.0
60º	6.3	7.3	8.5	9.9	11.0	12.5	13.8	15.0	16.5	17.7	18.6	18.8	18.5	17.5	16.4	15.0	13.6	12.2	10.9	9.5	8.2	7.0	6.2	5.9
50º	8.3	8.9	9.7	10.6	11.3	12.4	13.3	14.2	15.0	15.8	16.2	16.4	16.2	15.6	14.9	14.1	13.2	12.2	11.3	10.3	9.4	8.7	8.3	8.1
40º	9.5	9.9	10.4	11.0	11.5	12.3	13.0	13.6	14.2	14.6	14.9	15.0	14.9	14.5	14.1	13.5	12.8	12.1	11.5	10.9	10.3	9.8	9.5	9.3
30º	10.3	10.6	10.9	11.4	11.7	12.2	12.7	13.1	13.5	13.8	14.0	14.1	14.4	13.8	13.4	13.0	12.6	12.1	11.7	11.3	10.8	10.5	10.3	10.2
20º	11.0	11.2	11.4	11.7	11.9	12.2	12.5	12.7	13.0	13.2	13.3	13.3	13.3	13.1	12.9	12.7	12.4	12.1	11.9	11.6	11.3	11.1	11.0	10.9
10º	11.6	11.7	11.8	11.9	12.0	12.1	12.3	12.4	12.5	12.6	12.7	12.7	12.7	12.6	12.5	12.4	12.3	12.1	12.0	11.8	11.7	11.6	11.6	11.5
0º	12.1	12.1	12.1	12.1	12.1	12.1	12.1	12.1	12.1	12.1	12.1	12.1	12.1	12.1	12.1	12.1	12.1	12.1	12.1	12.1	12.1	12.1	12.1	12.1
	July		*August*		*September*		*October*		*November*		*December*		*January*		*February*		*March*		*April*		*May*		*June*	
Lat	*Hours of daylight in the Southern Hemisphere*																							